

Electromagnetic and weak form factors of nucleon and
charged quasielastic scatterings of neutrino
(antineutrino) and nucleon

Bing An Li

Department of Physics and Astronomy, University of Kentucky

Lexington, Kentucky, 40506, USA

Contents

1	Introduction	5
2	Relativistic quark model	7
3	Wave functions of nucleon and Δ	8
4	Transit matrix elements and the effective currents	26
5	EM form factors of baryons	27
6	Relationship Between $f_1(x_1, x_2, x_3)$ and $f_2(x_1, x_2, x_3)$	32
7	EM form factors of proton and neutron	37
7.1	Magnetic form factors of nucleon	39
7.2	Charge form factor of neutron and the ratio of the EM form factors of proton	40
7.3	Magnetic moments of $\frac{1}{2}^+$ baryons	51
7.4	Electric and magnetic radii of nucleon	57
7.5	Electromagnetic form factors of hyperons	58
8	EM transition of $p \rightarrow \Delta(1236)$	60
8.1	Photoproduction of Δ resonance	61
8.2	$\Delta \rightarrow N + \gamma$ decay	65

8.3	The electromagnetic form factors of $p \rightarrow \Delta^+(1236)$	66
9	The axial-vector and pseudoscalar form factors of baryons	75
9.1	Weak matrix elements of $\frac{1}{2}^+$ baryons	77
9.2	Axial-vector form factor of nucleon	79
9.3	Pseudoscalar form factor of $n \rightarrow p$	84
9.4	Semileptonic decays of baryons	86
10	Charged quasielastic reactions of neutrino and nucleon	89
10.1	$\Delta S = 0$ scatterings of neutrino (antineutrino) and nucleon	89
10.2	$\Delta S = 1$ quasielastic reactions of neutrino and nucleon	93
11	$\nu_\mu + p \rightarrow \Delta^{++} + \mu^-$ scattering	99
11.1	Form factors of $p \rightarrow \Delta^{++}$	101
11.2	Cross section	105
11.3	Density matrix	106
12	σ term of nucleon	106
13	Antiquark components of nucleon	112
14	Summary	113

Abstract

The study of electromagnetic and weak form factors of nucleon (charged quasielastic scatterings of neutrino (antineutrino) and nucleon) done in 70's and published in Chinese journals is reviewed. In the approach of the study antiquark components are introduced to the wave functions of nucleon and the study shows that the antiquark components of nucleon play an essential role in the EM and weak form factors of nucleon. The SU(6) symmetric wave functions of baryons in the rest frame (s-wave in the rest frame) have been constructed. In these wave functions there are both quark and antiquark components. Using Lorentz transformations these wave functions are boosted to moving frame. In terms of effective Lagrangian these wave functions are used to study the EM and weak form factors of nucleon and $p \rightarrow \Delta$. The ratio $\mu_p G_E^p/G_M^p$, G_E^n , G_M^n , G_M^* , $E1+$ and $S1+$ of $p \rightarrow \Delta$ are predicted. The axial-vector form factors of nucleon is predicted to be $G_A(q^2)/G_A(0) = F_1^p(q^2)$, where the F_1^p is the first Dirac form factor of proton. This prediction agrees with data very well. The pseudoscalar form factor of nucleon is predicted. The model predicts there are three axial-form factors for $p \rightarrow \Delta$ and two of them play dominant roles. The cross sections of $\nu_\mu + n \rightarrow p + \mu^-$ $\bar{\nu}_\mu + p \rightarrow n + \mu^+$, $\Delta S = 1$ quasielastic neutrino scatterings, and $\nu_\mu + p \rightarrow \Delta^{++} + \mu^-$ are predicted. Theoretical results are in agreement with data. The study shows that antiquark components of baryons play an essential role in understanding nucleon structure.

1 Introduction

The structure and properties of hadrons are always important topics of strong interaction, QCD. Photon and neutrino are always used to explore the structure of hadrons. The measurements and theoretical studies of the electromagnetic (EM) and weak form factors of nucleon last for very long time and are still very active. Recently, Jlab Hall A Collaboration has reported the measurements of the ratio of the electric and magnetic form factors of the proton $\mu_p G_E^p/G_M^p$ by using the recoil polarization technique[1]. The measurement of this ratio by Jlab Hall C collaboration has been extended to $q^2 = 8.5 \text{ GeV}^2$ [2]. The ratio $\mu_p G_E^p/G_M^p$ measured by the recoil polarization technique [1,2] shows a systematic decrease as q^2 increases. These experimental results lead to many theoretical study on the shape of nucleon. On the other hand, the experimental measurements [3] in the range of $q^2 < 1 \text{ GeV}^2$ show that this ratio is pretty flat [3] around one. The understanding of this ratio from lower q^2 to high q^2 is a challenge. Besides this ratio the experimental data of the charge and magnetic form factors of neutron and the transit form factors of $p \rightarrow \Delta$ are very significant for understanding the structure of nucleon. Especially, the measurements of the electric quadruple $E1+$ and $S1+$ of $p \rightarrow \Delta$ are strongly related to the structure of nucleon. On the other hand the axial-vector form factor $G_A(q^2)$ of nucleon and the transit axial-vector form factors of $p \rightarrow \Delta$ play important role in understanding the structure of nucleon. A reasonable model of nucleon is needed to understand all these physical quantities.

In 70's we have done systematic study on electromagnetic structure of nucleon and $p \rightarrow \Delta$ and axial-vector form factors of $\nu + N \rightarrow N' + \mu$, $\nu + N \rightarrow Hyperon + \mu$, and $\nu + N \rightarrow \Delta + \mu$ scatterings in a relativistic quark model. These investigations are published in a Chinese journal [4,5,6,7]. In the approach of Refs. [4,5,6,7] the wave functions of baryons are assumed to be SU(6) symmetric in the rest frame of the baryon and are boosted to moving frame by Lorentz transformation. In the rest frame the nucleon of 56-plet is in s-wave and spherical.

The approach used in Refs. [4,5,6,7] is interesting and the predictions of these form factors made by these study many years ago are still compatible with current more accurate data in the range of $q^2 < 5 \text{ GeV}^2$. A review of these study with new fit are presented in this paper. It is not the intention of this paper to review all the development of these topics.

The behavior of $\mu_p G_E^p / G_M^p$ found by experiments [1,2,3] has been studied and predicted by a relativistic quark model in 1975 [4,5]. The charge form factor and the magnetic form factor of the neutron, the transit magnetic form factor, and the the electric quadrupole $E1+$ and Coulomb multiple $S1+$ of $p \rightarrow \Delta$ have been predicted by the same model [4,5]. In 1977 this model has been applied to study semileptonic decays of baryons, $\nu + n \rightarrow \mu^- + p$, $\bar{\nu} + p \rightarrow \mu^+ + n$, and $\nu + p \rightarrow \mu^- + \Delta^{++}$ [6,7]. The axial-vector form factor $G_A(q^2)$ of nucleon, the pseudoscalar form factor of nucleon, and the three axial-form factors of $p \rightarrow \Delta$ have been predicted. Theoretical predictions of the $G_A(q^2)$, the decay rates of the semileptonic decays of baryons, the scatterings of $\nu + n \rightarrow \mu^- + p$, $\bar{\nu} + p \rightarrow \mu^+ + n$, and $\nu + p \rightarrow \mu^- + \Delta^{++}$

agree with data pretty well. The calculation of the σ term of nucleon is new. All these study [4,5,6,7] on the EM and weak form factors of nucleon show that the antiquark components of nucleon play an essential role in the structure of nucleon. In the last two sections both the σ term of proton and the contribution of the antiquark spinors to the density of antiquark of proton are calculated.

After the contents shown above there is Appendix in which the wave functions of low-lying excited baryons [4] are presented. The references are presented too.

2 Relativistic quark model

In 1964 Gell-Mann and Zweig [8] proposed the quark model of hadrons. In 1964 Greenberg [9] proposed the quantum number of color and the paraquark model. In 1965 Han and Nambu applied the new quantum number, color, to quarks of integer charges to solve the problem of statistics of quarks [10]. In 1966 H. Y. Zhu et al. published a paper [11] of a relativistic quark model (straton model named in their papers). In 1966 Y. Y. Liu [12] proposed that the quarks are a triplet of colors to solve the problem of statistics and fractional charges of quarks.

Following Ref. [11], the EM and weak form factors of baryons are studied in Refs. [4,5,6,7] in 70's. The wave function of a baryon is composed of: color part, flavor part, the spin part,

and the part of space and time. A baryon is color singlet and the remaining parts of the wave functions are totally symmetric. The flavor part is determined by SU(3) symmetry. In Ref. [11] the spin part of the wave functions of baryons are constructed by the spinors of quarks only. They are Bargmann-Wigner wave functions. Lorentz transformation is used to boost these wave functions to moving frame. In Ref. [4] a new set of wave functions of baryons are constructed by assuming the SU(6) symmetry in the rest frame of baryon. In these wave functions there are both quark and antiquark components. They are not Bargmann-Wigner wave functions. Effective currents of electromagnetic and weak interactions are used to calculate transit matrix elements. The picture of single quark transition has been applied to study the electromagnetic and weak processes of hadrons. These wave functions are different from the ones used in Ref. [11].

3 Wave functions of nucleon and Δ

There are three parts in the calculations of the form factors of baryons: wave functions, effective Lagrangian, and the matrix elements. A review of new set of wave functions of baryons constructed in Ref. [4] is presented in this section. In Ref. [4] the general expressions of the wave functions of the $\frac{1}{2}^+$ and the $\frac{3}{2}^+$ baryons are constructed by requesting that the wave functions satisfy the SU(6) symmetry in the rest frame.

Baryons are bound states of quarks in nonperturbative QCD. Instead solving nonperturbative QCD, symmetry is applied in this study. It is well known that the SU(6) symmetry [13] works well for low lying hadrons. The $\frac{1}{2}^+$ and $\frac{3}{2}^+$ baryons are $\underline{56}$ -plet of the SU(6) group. The predictions of some of the properties of baryons by SU(6) symmetry are in good agreement with data. It is known that kinetic term violates SU(6) symmetry. In this study the wave functions of the baryons are required to satisfy the SU(6) symmetry in the rest frame of the baryons only and are boosted to moving frame by Lorentz transformation.

The transition matrix elements of EM and weak interactions between baryons are expressed as

$$\langle B' | j_\mu(0) | B \rangle = \int dx'_1 dx'_2 dx'_3 dx_1 dx_2 dx_3 \bar{B}'(x'_3, x'_2, x'_1) G_\mu(x'_3, x'_2, x'_1, x_1, x_2, x_3) B(x_1, x_2, x_3), \quad (1)$$

where j_μ is either the electromagnetic or weak current of quarks, which will be shown below, G_μ is the kernel of the matrix element and will be discussed. In Eq. (1) the wave functions of baryon have indices: color, flavor, and spin and they are Bethe - Salpeter amplitudes. For example, the wave function of a $\frac{1}{2}^+$ baryon is defined as

$$B_{\alpha i, \beta j, \gamma k}^{i' j' k'}(x_1, x_2, x_3)_{l, \lambda}^m = \langle 0 | T \{ \psi_{\alpha i}^{i'}(x_1) \psi_{\beta j}^{j'}(x_2) \psi_{\gamma k}^{k'}(x_3) \} | B(p)_\lambda \rangle, \\ \bar{B}_{ijk}^{i' j' k'}(x_1, x_2, x_3)_{l, \lambda}^m = \langle B(p)_\lambda | T \{ \bar{\psi}_{\alpha i}^{i'}(x_1) \bar{\psi}_{\beta j}^{j'}(x_2) \bar{\psi}_{\gamma k}^{k'}(x_3) \} | 0 \rangle, \quad (2)$$

where $\psi(x)$ is a quark field, $i' j' k'$ are color indices, $i j k$ are flavor indices. For a $\frac{1}{2}^+$ baryon

the flavor state of the baryon is represented by $\begin{pmatrix} m \\ l \end{pmatrix}$ (*see Appendix*) .

Baryon is color singlet and the wave function of color is

$$\frac{1}{\sqrt{6}}\epsilon_{i'j'k'},$$

Therefore the remaining part of the wave function, the indices $x_1\alpha i$, $x_2\beta j$, $x_3\gamma k$ are total symmetric. The baryons of SU(6) 56-plet have positive parity. These wave functions must be Lorentz covariant. According to $SU(3)$ symmetry, $\frac{1}{2}^+$ baryons are octet and the flavor part of the wave function takes following forms

$$\epsilon_{ijm}\delta_{kl}, \quad \epsilon_{jkm}\delta_{il}, \quad \epsilon_{kim}\delta_{jl}. \quad (3)$$

They satisfies the identity.

$$\epsilon_{ijm}\delta_{kl} + \epsilon_{jkm}\delta_{il} + \epsilon_{kim}\delta_{jl} = 0. \quad (4)$$

Besides the color part the rest part of the wave function of a baryon must be total symmetric.

The wave function of $\frac{1}{2}^+$ baryon is expressed as

$$\begin{aligned} B_{\alpha\beta\gamma,ijk}(x,y)_{l,\lambda}^m &= \frac{1}{6\sqrt{2}}\epsilon_{i'j'k'}\{(\epsilon_{ijm}\delta_{kl} + \epsilon_{ikm}\delta_{jl})\Gamma_{\alpha\beta,\gamma}^{\frac{1}{2}}(x,y)_\lambda \\ &+ (\epsilon_{jkm}\delta_{il} + \epsilon_{ikm}\delta_{jl})\Gamma_{\beta\gamma,\alpha}^{\frac{1}{2}}(x,y)_\lambda\}, \end{aligned} \quad (5)$$

where x and y are relative coordinates, $x = x_1 - x_2$ and $y = \frac{1}{2}(x_1 + x_2) - x_3$, and $\Gamma_{\alpha\beta,\gamma}^{\frac{1}{2}}(x,y)_\lambda$ is antisymmetric in (x_1, α) ; (x_2, β) and $\Gamma_{\beta\gamma,\alpha}^{\frac{1}{2}}(x,y)_\lambda$ is antisymmetric in (x_2, β) ; (x_3, γ) . There

is $\Gamma_{\gamma\alpha,\beta}^{\frac{1}{2}}(x, y)_\lambda$ which is antisymmetric in $(x_3, \gamma); (x_1, \alpha)$. These three Γ functions must satisfy the identity

$$\Gamma_{\alpha\beta,\gamma}^{\frac{1}{2}}(x, y)_\lambda + \Gamma_{\beta\gamma,\alpha}^{\frac{1}{2}}(x, y)_\lambda + \Gamma_{\gamma\alpha,\beta}^{\frac{1}{2}}(x, y)_\lambda = 0. \quad (6)$$

These three Γ functions have the O_2 mixing symmetry, where O_2 is the projection operator of permutation group of three indices (see Appendix). The wave function of $\frac{1}{2}^+$ baryon (5) is totally antisymmetric.

$\frac{3}{2}^+$ baryons are SU(3) decuplet whose flavor wave functions are

$$d_{ijk}^{lmn} \quad (7)$$

where lmn are the flavor wave function of the $\frac{3}{2}$ baryon and ijk are the flavor indices of the three quarks and they are totally symmetric respectively, the values of d_{ijk}^{lmn} are presented in the Appendix. The general expression of the wave functions of $\frac{3}{2}^+$ baryons are written as

$$B_{\alpha\beta\gamma,ijk}^{lmn}(x, y)_\lambda = \frac{1}{6\sqrt{2}} \epsilon_{i'j'k'} d_{ijk}^{lmn} \Gamma_{\alpha\beta\gamma}^{\frac{3}{2}}(x, y)_\lambda, \quad (8)$$

where the $\Gamma_{\alpha\beta\gamma}^{\frac{3}{2}}(x, y)_\lambda$ function are totally symmetric in $(x_1\alpha), (x_2\beta), (x_3\gamma)$.

The Γ functions of Eqs. (5,8) can be determined. Besides the symmetric properties mentioned above, these functions must satisfy following properties:

1. they are Lorentz covariant,
2. $\Gamma_{\alpha\beta,\gamma}^{\frac{1}{2}}(x, y)_\lambda$, $\Gamma_{\beta\gamma,\alpha}^{\frac{1}{2}}(x, y)_\lambda$, and $\Gamma_{\gamma\alpha,\beta}^{\frac{1}{2}}(x, y)_\lambda$ are spin- $\frac{1}{2}$ and their parity are positive,

3. $\Gamma_{\alpha\beta\gamma}^{\frac{3}{2}}(x, y)_\lambda$ is spin - $\frac{3}{2}$ and positive parity,
4. according to the SU(6), the $\frac{1}{2}^+$ and $\frac{3}{2}^+$ baryons are 56-plet and they are s-wave states in the rest frame.

Using these properties, the general expressions of these Γ functions in the rest frame can be constructed and they are boosted to moving frame by Lorentz transformation. In the rest frame of the baryon the Γ function of Eqs.(5,8) can be written as

$$\Gamma_{\alpha\beta\gamma}(x, y)_\lambda = \sum_c C_{\frac{1}{2}c, l\lambda-c}^{J\lambda} \{A_{\alpha\beta}(x, y)D_{\gamma\gamma'}(x, y)\}_{l\lambda-c} u_{c, \gamma'}, \quad (9)$$

where $C_{\frac{1}{2}c, l\lambda-c}^{J\lambda}$ is the Clebsch-Gordan coefficient (C - G coefficient), $\{A_{\alpha\beta}(x, y)D_{\gamma\gamma'}(x, y)\}_{l\lambda-c}$ has angular momentum l and the third component is $\lambda - c$. The Lorentz transformations of matrices A and D are

$$\begin{aligned} (AC)' &= \Lambda(AC)\Lambda^{-1}, \\ D' &= \Lambda D \Lambda^{-1}, \end{aligned} \quad (10)$$

where Λ is the Lorentz transformation, C is the operator of charge conjugate, AC and D are linear combinations of γ matrices, $u_{c, \gamma'}$ is the spinor in the rest frame, the indices c is the helicity and the γ' is the Lorentz index.

In the rest frame we can use following γ matrices

$$Scalar : I, \gamma_0,$$

$$Pseudoscalar : \quad \gamma_5, \gamma_0\gamma_5,$$

$$Vector : \quad \gamma_j, \gamma_0\gamma_j,$$

$$Axial - vector : \quad \gamma_j\gamma_5, \gamma_0\gamma_j\gamma_5$$

and x_j and y_j ($j = 1, 2, 3$) to construct the general Γ functions (5,8). Because

$$\gamma_0 u_{c,\gamma'} = u_{c,\gamma'}$$

in the $D_{\gamma\gamma'}$ of Eq. (9) there is no γ_0 matrix. The Γ function can be constructed as

$$\begin{aligned} \Gamma_{\alpha\beta\gamma}(x, y)_\lambda = & \{ (f_1 + f_2\gamma_0 + f_3\vec{x} \cdot \vec{\gamma} + f_4\vec{y} \cdot \gamma + f_5x_i\sigma_{i4} + f_6y_i\sigma_{i4} \\ & + f_7x_iy_j\sigma_{ij} + f_8x_iy_j\gamma_k\epsilon_{ijk}\gamma_5)\gamma_5 C \}_{\alpha\beta} \\ & \{ 1 + f_9\vec{x} \cdot \gamma + f_{10}\vec{y} \cdot \gamma + f_{11}x_iy_j\sigma_{ij} \}_{\gamma\gamma'} u_{\lambda,\gamma'} \\ & + \{ (g_1 + g_2\gamma_0 + g_3\vec{x} \cdot \vec{\gamma} + g_4\vec{y} \cdot \gamma + g_5x_i\sigma_{i4} + g_6y_i\sigma_{i4}) \\ & + g_7x_iy_j\sigma_{ij} + g_8x_iy_j\gamma_k\epsilon_{ijk}\gamma_5 \} C \}_{\alpha\beta} \\ & \{ (1 + g_9\vec{x} \cdot \gamma + g_{10}\vec{y} \cdot \gamma + g_{11}x_iy_j\sigma_{ij})\gamma_5 \}_{\gamma\gamma'} u_{\lambda,\gamma'} \\ & + \{ (h_1\gamma_k + h_2\gamma_0\gamma_k + h_3x_i\sigma_{ik} + h_4y_i\sigma_{ik} + h_5x_i\gamma_j\epsilon_{ijk}\gamma_5 \\ & + h_6y_i\gamma_j\epsilon_{ijk}\gamma_5 + h_7x_iy_j\epsilon_{ijk}\gamma_5 + h_8x_iy_j\epsilon_{ijk}\gamma_0\gamma_5) C \}_{\alpha\beta} \\ & \{ (\gamma_k + h_9x_i\sigma_{ik} + h_{10}y_i\sigma_{ik})\gamma_5 \}_{\gamma\gamma'} u_{\lambda,\gamma'} \\ & + \{ (k_1\gamma_k + k_2\gamma_0\gamma_k + k_3x_i\sigma_{ik} + k_4y_i\sigma_{ik} + k_5x_i\gamma_j\epsilon_{ijk}\gamma_5 \\ & + k_6y_i\gamma_j\epsilon_{ijk}\gamma_5 + k_7x_iy_j\epsilon_{ijk}\gamma_5 + k_8x_iy_j\epsilon_{ijk}\gamma_0\gamma_5) \gamma_5 C \}_{\alpha\beta} \end{aligned}$$

$$\{\gamma_k + k_9 x_i \sigma_{ik} + k_{10} y_i \sigma_{ik}\}_{\gamma\gamma' u_{\lambda,\gamma'}}, \quad (11)$$

where $f_1 \dots f_{11}, g_1 \dots g_{11}, h_1 \dots h_{10}, k_1 \dots k_{10}$ are Lorentz invariant functions of x, y, p . Applying the projection operators Y_s, O_2 (Appendix) to the indices $(\alpha x_1), (\beta x_2), (\gamma x_3)$ respectively we can obtain

$$\begin{aligned} \Gamma_{\alpha\beta,\gamma}^{\frac{1}{2}}(x, y)_\lambda &= O_2 \Gamma_{\alpha\beta\gamma}(x, y)_\lambda, \\ \Gamma_{\alpha\beta\gamma}^{\frac{3}{2}}(x, y)_\lambda &= Y_s \Gamma_{\alpha\beta\gamma}(x, y)_\lambda, \end{aligned} \quad (12)$$

where Y_s is the total symmetric projector. The same way $\Gamma_{\beta\gamma,\alpha}^{\frac{1}{2}}(x, y)_\lambda$ of Eq. (5) is obtained too.

In the rest frame the wave functions of the $\frac{1}{2}^+$ and the $\frac{3}{2}^+$ baryons are the bases of the 56-plet of SU(6) symmetry. The generators of the SU(6) group, $\lambda_a \sigma_l, \lambda_a$, and σ_l , can transform one base to another, where λ_a are the generators of the SU(3) group (flavor) and σ_l are the SU(2) generators (spin). Using these operators, the wave functions of the $\frac{1}{2}^+$ and the $\frac{3}{2}^+$ baryons can be transformed from one to another and the relationships between these two wave functions can be found. Under an infinitesimal SU(6) transformation, for example $\lambda_a \sigma_l$ there are

$$\begin{aligned} B'_{\alpha\beta\gamma,ijk}(x, y)_{\lambda U} &= B_{\alpha\beta\gamma,ijk}(x, y)_{\lambda U} \\ &+ i\epsilon_l^a (\lambda_a \sigma_l)_{i,\alpha\alpha'}^{i'} B_{\alpha'\beta\gamma,i'jk}(x, y)_{\lambda U} \\ &+ i\epsilon_l^a (\lambda_a \sigma_l)_{j,\beta\beta'}^{j'} B_{\alpha\beta'\gamma,ij'k}(x, y)_{\lambda U} \end{aligned}$$

$$+i\epsilon_l^a(\lambda_a\sigma_l)_{k,\gamma\gamma'}^{k'}B_{\alpha\beta\gamma',ijk'}(x,y)_{\lambda U}, \quad (13)$$

where U stands for the flavor state (SU(3)), $B'_{\alpha\beta\gamma,ijk}(x,y)_{\lambda U}$ is the wave function of the baryon after the infinitesimal SU(6) transformation, ϵ_l^a is the infinitesimal parameter of the transformation, the color part of the wave function has been omitted. Similar transformations under λ_a or σ_l can be found respectively. The wave functions of $\frac{1}{2}^+$ and $\frac{3}{2}^+$ (5,8) already satisfy the SU(3) symmetry. Because of the requirement of SU(6) symmetry under an infinitesimal transformation of SU(2) (spin) no baryon states with angular momentum higher than $\frac{3}{2}$ can be generated. Without losing generality we take proton as an example, $i = 1, j = 1, k = 2, a = 2, U = \binom{3}{1}$ and

$$\lambda_2 = \begin{pmatrix} 0 & 1 & 0 \\ 0 & 0 & 0 \\ 0 & 0 & 0 \end{pmatrix}.$$

Using Eq. (13), under an infinitesimal SU(2) (spin) transformation we obtain

$$\begin{aligned} B'_{\alpha\beta\gamma,112}(x,y)_{\lambda U} &= B_{\alpha\beta\gamma,112}(x,y) + i\epsilon_l^2\sigma_{l,\alpha\alpha'}\{\Gamma_{\alpha'\beta,\gamma}^{\frac{1}{2}}(x,y)_\lambda + \Gamma_{\beta\gamma,\alpha'}^{\frac{1}{2}}(x,y)_\lambda\} \\ &\quad + i\epsilon_l^2\sigma_{l,\beta\beta'}\{\Gamma_{\alpha\beta',\gamma}^{\frac{1}{2}}(x,y)_\lambda - \Gamma_{\gamma\alpha,\beta'}^{\frac{1}{2}}(x,y)_\lambda\}. \end{aligned} \quad (14)$$

For $\frac{3}{2}^+$ baryon we take $\Delta^0, U = (122)$, as an example

$$B'_{\alpha\beta\gamma,122}(x,y)_{\lambda U} = B_{\alpha\beta\gamma,122}(x,y)_{\lambda U}$$

$$+\frac{i}{\sqrt{3}}\epsilon_l^2\sigma_{l,\alpha\alpha'}\Gamma_{\alpha'\beta\gamma}^{\frac{3}{2}}(x,y)_\lambda+\frac{i}{\sqrt{3}}\epsilon_l^2\sigma_{l,\beta\beta'}\Gamma_{\alpha\beta'\gamma}^{\frac{3}{2}}(x,y)_\lambda. \quad (15)$$

To satisfy SU(6) symmetry only $\frac{1}{2}^+$ and $\frac{3}{2}^+$ states are allowed on the right-hand sides of Eqs. (14,15) and no states with angular momenta higher than $\frac{3}{2}$.

The spin operator σ_l makes transformations between the $\Gamma_{\alpha\beta\gamma}^{\frac{3}{2}}(x,y)_\lambda$ of the decuplet baryons and the $\Gamma_{\alpha\beta,\gamma}^{\frac{1}{2}}(x,y)_\lambda, \Gamma_{\beta\gamma,\alpha}^{\frac{1}{2}}(x,y)_\lambda, \Gamma_{\gamma\alpha,\beta}^{\frac{1}{2}}(x,y)_\lambda$ of the octet baryons.

The transformation of the space-spin wave function of the $\frac{1}{2}^+$ baryons (11) is studied. In the expression of $\Gamma_{\alpha\beta\gamma}(x,y)_\lambda$ (11) there are scalar terms like

$$\vec{x} \cdot \gamma, \quad \vec{y} \cdot \gamma, \quad x_i y_j \sigma_{ij}, \quad etc.....$$

Applying the spin operator σ_i to these terms, p-waves will be generated. For example,

$$\sigma_i \vec{x} \cdot \gamma = \{x_i + \sigma_{ij} x_j\} \gamma_0 \gamma_5. \quad (16)$$

The term x_i is a vector and p-wave. The couplings of these p-waves with other states will produce states whose angular momentum are higher than $\frac{3}{2}$ which do not belong to 56-plet and SU(6) symmetry is broken. Therefore, to keep SU(6) symmetry in the rest frame the terms related to p-waves in Eq. (11) must be erased. This is consistent with that because of the SU(6) symmetry the internal kinetic motions of the quarks of the baryons of the 56-plet are ignored and they are in s-waves only.

The general Γ function of $\frac{1}{2}^+$ baryon in s-wave is obtained from Eq. (11)

$$\Gamma_{\alpha\beta,\gamma}^{\frac{1}{2}}(x,y)_\lambda = \{(f_1 + f_2 \gamma_0) \gamma_5 C\}_{\alpha\beta} u_{\lambda,\gamma} + \{(g_1 + g_2 \gamma_0) C\}_{\alpha\beta} \{\gamma_5 u_\lambda\}_\gamma$$

$$+\{(h_1 + h_2\gamma_0)\gamma_k C\}_{\alpha\beta}\{\gamma_k\gamma_5 u_\lambda\}_\gamma + \{(k_1 + k_2\gamma_0)\gamma_k\gamma_5 C\}_{\alpha\beta}\{\gamma_k u_\lambda\}_\gamma, \quad (17)$$

where $f_1, f_2, g_1, g_2, h_1, h_2, k_1, k_2$ are totally symmetric Lorentz scalar functions of x_1, x_2, x_3 .

Except the color wave function, the remaining wave functions (5) of $\frac{1}{2}^+$ baryons are totally symmetric and as mentioned above that the $\Gamma_{\alpha\beta,\gamma}^{\frac{1}{2}}$ satisfies

$$O_2\Gamma_{\alpha\beta,\gamma}^{\frac{1}{2}}(x, y) = \Gamma_{\alpha\beta,\gamma}^{\frac{1}{2}}(x, y). \quad (18)$$

From Eq. (18) we obtain

$$g_2 = h_1 = h_2 = k_2 = 0,$$

$$f_1 - f_2 - g_1 - 3k_1 = 0. \quad (19)$$

Similarly, the Γ function of $\frac{3}{2}^+$ baryon in s-wave is constructed as

$$\Gamma_{\alpha\beta\gamma}(x, y)_\lambda = \{(f'_1 + f'_2\gamma_0)\gamma_k C\}_{\alpha\beta}\psi_{k,\gamma}^\lambda + \{(g'_1 + g'_2\gamma_0)\gamma_k\gamma_5 C\}_{\alpha\beta}\{\gamma_5\psi_k^\lambda\}_\gamma, \quad (20)$$

where f'_1, f'_2, g'_1, g'_2 are totally symmetric Lorentz scalar functions of x_1, x_2, x_3 , ψ_k^λ is the Rarita-Schwinger spinor. $\Gamma_{\alpha\beta\gamma}(x, y)$ must be totally symmetric and satisfies

$$O_1\Gamma_{\alpha\beta\gamma}(x, y) = 0. \quad (21)$$

Eq.(21) leads to

$$g'_1 = 0, \quad g'_2 = f'_2 - f'_1. \quad (22)$$

The operators σ_l of SU(6) can do the transformation between the Γ functions of spin- $\frac{1}{2}$ and spin- $\frac{3}{2}$ baryons. For $\frac{1}{2}^+$ baryon it is obtained

$$\begin{aligned} (\sigma_l)_{\alpha'\alpha} \Gamma_{\alpha'\beta,\gamma}^{\frac{1}{2}}(x, y)_\lambda &= -i\{(f_1 + f_2\gamma_0)\gamma_l C\}_{\alpha\beta} u_{\lambda,\gamma} + ig_1\{\gamma_l\gamma_0\gamma_5 C\}_{\alpha\beta}(\gamma_5 u_\lambda)_\gamma \\ &+ ik_1\{\delta_{kl}\gamma_0 C + i\gamma_0\sigma_{lk} C\}_{\alpha\beta}(\gamma_k u_\lambda)_\gamma. \end{aligned} \quad (23)$$

The RHS of eq.(23) can be divided into spin $\frac{1}{2}$ and $\frac{3}{2}$ two parts. The spin $\frac{3}{2}$ part is written as

$$\{(f_2 + f_1\gamma_0)\gamma_k C\}_{\alpha\beta} \psi_{k,\gamma}^\lambda + g_1(\gamma_0\gamma_k C)_{\alpha\beta}(\gamma_5\psi_k^\lambda)_\gamma - ik_1(\gamma_0\sigma_{kl} C)_{\alpha\beta}(\gamma_l\psi_k^\lambda)_\gamma. \quad (24)$$

The indices $\alpha\beta\gamma$ of Eq.(24) must be totally symmetric. $(\gamma_0\sigma_{kl} C)_{\alpha\beta}$ is antisymmetric in $\alpha\beta$.

Therefore,

$$k_1 = 0. \quad (25)$$

The totally symmetric requirement leads to

$$g_1 = f_1 - f_2. \quad (26)$$

Substituting Eqs.(25,26) into Eq.(24) and comparing with Eq.(20), we obtain

$$f'_1 = f_2, \quad f'_2 = f_1, \quad g'_2 = f_1 - f_2. \quad (27)$$

Using all Eqs.(25,26,27), the spin $\frac{1}{2}$ part of Eq.(20) can be written as

$$\sum_{\lambda, r_3} C_{1\lambda\frac{1}{2}r_3}^{\frac{1}{2}c} \{[(f_2 + f_1\gamma_0)\gamma_l C]_{\alpha\beta} e_l^\lambda u_{r_3} + (f_1 - f_2)(\gamma_0\gamma_l\gamma_5 C)_{\alpha\beta} e_l^\lambda(\gamma_5 u_{r_3})_r\}, \quad (28)$$

where e_t^λ is the polarization vector. It can be proved that Eq.(28) is the same as the expression(17) which satisfies Eqs.(18,19). Taking $c = \frac{1}{2}$ and using the four spinors, the expression(28) can be rewritten as

$$\begin{aligned}
& 2\sqrt{2} \sum_{r_1 r_2 r_3} C_{1\lambda\frac{1}{2}r_3}^{\frac{1}{2}\frac{1}{2}} C_{\frac{1}{2}r_1\frac{1}{2}r_2}^{1\lambda} \{f_+ u_{r_1,\alpha} u_{r_2,\beta} u_{r_3,\gamma} - f_- \epsilon_{r_1 r'_1} \epsilon_{r_2 r'_2} v_{r'_1,\alpha} v_{r'_2,\beta} u_{r_3,\gamma}\} \\
& - f_- (\epsilon_{r_1 r'_1} v_{r'_1,\alpha} u_{r_2,\beta} + \epsilon_{r_2 r'_2} u_{r_1,\alpha} v_{r'_2,\beta}) \epsilon_{r_3 r'_3} v_{r'_3,\gamma} \} \\
& = -\frac{i}{\sqrt{3}} \{[(f_1 + f_2 \gamma_0) \gamma_5 C]_{\beta\gamma} u_{\frac{1}{2},\alpha} \\
& + [(f_1 + f_2 \gamma_0) \gamma_5 C]_{\alpha\gamma} u_{\frac{1}{2},\beta} + (f_1 - f_2) C_{\alpha\gamma} (\gamma_5 u_{\frac{1}{2}})_\beta \}, \tag{29}
\end{aligned}$$

where

$$\begin{aligned}
& f_+ = \frac{1}{2}(f_1 + f_2), \quad f_- = \frac{1}{2}(f_1 - f_2), \\
& \epsilon_{\frac{1}{2},-\frac{1}{2}} = 1, \quad \epsilon_{-\frac{1}{2},\frac{1}{2}} = -1, \quad \epsilon_{r_1,r_2} = -\epsilon_{r_2,r_1}, \\
& u_{\frac{1}{2}} = \begin{pmatrix} 1 \\ 0 \\ 0 \\ 0 \end{pmatrix}, \quad u_{-\frac{1}{2}} = \begin{pmatrix} 0 \\ 1 \\ 0 \\ 0 \end{pmatrix}, \quad v_{\frac{1}{2}} = \begin{pmatrix} 0 \\ 0 \\ 0 \\ -i \end{pmatrix}, \quad v_{-\frac{1}{2}} = \begin{pmatrix} 0 \\ 0 \\ i \\ 0 \end{pmatrix}. \tag{30}
\end{aligned}$$

Multiplying Eq.(29) by corresponding SU(3) wave function

$$\epsilon_{ikm} \delta_{jl} + \epsilon_{jkm} \delta_{il}$$

and symmetrizing the indices (α i), (β j), (γ k), the wave function of $\frac{1}{2}^+$ baryon (5) is indeed obtained. It is important to notice that all the four spinors (30) are in s-wave. Because of

the requirement of SU(6) symmetry in the rest frame of the nucleon the kinetic terms of these spinors or internal motions of quarks are ignored. After ignoring the kinetic terms, the u_{\pm} are the spinors of quarks and the v_{\pm} are the spinors of antiquarks.

It is worth to point out that if a spin operator σ_l acts on the index γ of $\Gamma_{\alpha\beta,\gamma}^{\frac{1}{2}}$ it doesn't change the the spin of the baryon and only changes the third component.

Using C-G coefficients, following two expressions are obtained after a σ_l acts on the $\Gamma_{\alpha\beta\gamma}^{\frac{3}{2}}(x, y)_{\lambda}$ of $\frac{3}{2}$ baryon

1.

$$\sum_{\lambda_1, \lambda_2} C_{\frac{3}{2}\lambda_1, 1\lambda_2}^{\frac{1}{2}\lambda} e_l^{\lambda_2} (\sigma_l)_{\gamma\gamma'} \Gamma_{\alpha\beta\gamma'}^{\frac{3}{2}}(x, y)_{\lambda} = \frac{2\sqrt{2}}{3} i \{ \Gamma_{\alpha\gamma, \beta}^{\frac{1}{2}}(x, y)_{\lambda} + \Gamma_{\beta\gamma, \alpha}^{\frac{1}{2}}(x, y)_{\lambda} \}. \quad (31)$$

α and β are symmetric. Multiplying Eq.(31) by $\epsilon_{ikm}\delta_{jl} + \epsilon_{jkl}\delta_{il}$ and symmetrizing the indices $\alpha i, \beta j, \gamma k$, the wave function of $\frac{1}{2}^+$ baryon is obtained.

2.

$$\sum_{\lambda_1, \lambda_2} C_{\frac{3}{2}\lambda_1, 1\lambda_2}^{\frac{3}{2}\lambda} e_l^{\lambda_2} (\sigma_l)_{\gamma\gamma'} \Gamma_{\alpha\beta\gamma'}^{\frac{3}{2}}(x, y)_{\lambda_1} = -\sqrt{\frac{5}{3}} \Gamma_{\alpha\beta\gamma}^{\frac{3}{2}}(x, y)_{\lambda}, \quad (32)$$

where $\Gamma_{\alpha\beta\gamma}^{\frac{3}{2}}(x, y)_{\lambda}$ is the wave function of $\frac{3}{2}$ baryon.

Eqs.(31,32) show that the spin operators make the transformations between the $\frac{1}{2}^+$ and $\frac{3}{2}^+$ wave functions of baryons only. Therefore, the $\frac{1}{2}^+$ and $\frac{3}{2}^+$ wave functions of baryons satisfy the SU(6) symmetry.

Finally, the wave functions of $\frac{1}{2}^+$ and $\frac{3}{2}^+$ baryons, which satisfy SU(6) symmetry in the rest frame are written as

$$\begin{aligned}
B_{\alpha\beta\gamma,ijk}(x,y)_{l,\lambda}^m &= \frac{1}{6\sqrt{2}}\epsilon_{i'j'k'}\{(\epsilon_{ijm}\delta_{kl} + \epsilon_{ikm}\delta_{jl})\Gamma_{\alpha\beta,\gamma}^{\frac{1}{2}}(x,y)_\lambda \\
&\quad + (\epsilon_{jkm}\delta_{il} + \epsilon_{ikm}\delta_{jl})\Gamma_{\beta\gamma,\alpha}^{\frac{1}{2}}(x,y)_\lambda\}, \\
B_{\alpha\beta\gamma,ijk}^{lmn}(x,y)_\lambda &= \frac{1}{6\sqrt{2}}\epsilon_{i'j'k'}d_{ijk}^{lmn}\Gamma_{\alpha\beta\gamma}^{\frac{3}{2}}(x,y)_\lambda,
\end{aligned} \tag{33}$$

where

$$\begin{aligned}
\Gamma_{\alpha\beta,\gamma}^{\frac{1}{2}}(x,y)_\lambda &= \{(f_1 + f_2\gamma_0)\gamma_5 C\}_{\alpha\beta}u_{\lambda,\gamma} + (f_1 - f_2)C_{\alpha\beta}\{\gamma_5 u_\lambda\}_\gamma, \\
\Gamma_{\alpha\beta\gamma}^{\frac{3}{2}}(x,y)_\lambda &= \{(f_2 + f_1\gamma_0)\gamma_k C\}_{\alpha\beta}\psi_{k,\gamma}^\lambda + (f_1 - f_2)(\gamma_0\gamma_k\gamma_5 C)_{\alpha\beta}\{\gamma_5\psi_k^\lambda\}_\gamma.
\end{aligned} \tag{34}$$

Eqs. (33,34) show that the SU(6) symmetry leads to that the general expressions of the wave functions of $\frac{1}{2}^+$ and $\frac{3}{2}^+$ baryons contain $f_1(x,y)$ and $f_2(x,y)$ two functions only, which are Lorentz invariant and symmetric in x_1, x_2, x_3 . In these two functions there are only s-waves in the rest frame. Therefore, according to SU(6) symmetry in the rest frame, the $\frac{1}{2}^+$ and the $\frac{3}{2}^+$ baryons are spherical.

Using Lorentz transformation, the Γ functions (33,34) are boosted to moving frame and expressed as

$$\begin{aligned}
\Gamma_{\alpha\beta,\gamma}^{\frac{1}{2}}(x,y,p)_\lambda &= \{(f_1(x,y) + f_2(x,y)\frac{-i}{m}\gamma \cdot p)\gamma_5 C\}_{\alpha\beta}u(p)_{\lambda,\gamma} \\
&\quad + \{f_1(x,y) - f_2(x,y)\}C_{\alpha\beta}\{\gamma_5 u(p)_\lambda\}_\gamma,
\end{aligned}$$

$$\begin{aligned}
\Gamma_{\alpha\beta\gamma}^{\frac{3}{2}}(x, y, p)_\lambda &= \{(f_2(x, y) + f_1(x, y)\frac{-i}{m}\gamma \cdot p)\gamma_\mu C\}_{\alpha\beta}\psi_\mu^\lambda(p)_\gamma \\
&+ \{f_1(x, y) - f_2(x, y)\}\frac{-i}{m}(\gamma \cdot p\gamma_\mu\gamma_5 C)_{\alpha\beta}\{\gamma_5\psi_\mu^\lambda(p)\}_\gamma.
\end{aligned} \tag{35}$$

If taking

$$f_1(x, y) = f_2(x, y) = f(x, y),$$

Eq. (34) becomes

$$\begin{aligned}
\Gamma_{\alpha\beta,\gamma}^{\frac{1}{2}}(x, y)_\lambda &= f(x, y)\{(1 + \gamma_0)\gamma_5 C\}_{\alpha\beta}u_{\lambda,\gamma} \\
\Gamma_{\alpha\beta\gamma}^{\frac{3}{2}}(x, y)_\lambda &= f(x, y)\{(1 + \gamma_0)\gamma_k C\}_{\alpha\beta}\psi_{k,\gamma}^\lambda.
\end{aligned} \tag{36}$$

The terms $C_{\alpha\beta}\{\gamma_5 u(p)_\lambda\}_\gamma$ and $\frac{1}{m}(\gamma_0\gamma_\mu\gamma_5 C)_{\alpha\beta}\{\gamma_5\psi_\mu^\lambda(p)\}_\gamma$ of Eq. (34) disappear.

These wave functions (36) can be constructed by the two spinors of quarks, $u_{\frac{1}{2}}, u_{-\frac{1}{2}}$ (30) only and there are no contribution from the spinors of antiquarks $v_{\frac{1}{2}}, v_{-\frac{1}{2}}$. Therefore, the effects of antiquark spinors make $f_1 \neq f_2$. In order to explore the cause of the difference between f_1 and f_2 the spectral representation of the wave function of baryon is used

$$\begin{aligned}
B_{\alpha\beta\gamma,ijk}^{i'j'k'}(x, y)_{\lambda U} &= 6Y_a\theta(x_0)\theta(-\frac{x_0}{2}, -y_0)\frac{1}{(2\pi)^6}\int d^4p_n d^4p_l dM_n^2 dM_l^2 \\
&\delta(p_n^2 + m_n^2)\delta(p_l^2 + M_l^2)\theta(p_{n0})\theta(p_{l0})exp[i(p_n - \frac{1}{2}p_l)x - i(p_l - \frac{1}{3}p)y] \\
&f_{\alpha\beta\gamma,ijk}^{i'j'k'}(p_n, p_l, p, M_n^2, M_l^2)_{\lambda U},
\end{aligned} \tag{37}$$

where

$$f_{\alpha\beta\gamma,ijk}^{i'j'k'}(p_n, p_l, p, M_n^2, M_l^2)_{\lambda U} = \sum_{nl}' \langle 0|\psi_{\alpha i}^{i'}(0)|n\rangle \langle n|\psi_{\beta j}^{j'}(0)|l\rangle \langle l|\psi_{\gamma k}^{k'}(0)|B_{\lambda U}(p)\rangle, \tag{38}$$

where \sum'_{nl} is the \sum_{nl} after the factors $\frac{1}{(2\pi)^6} \frac{d^3 p_n}{2E_n} \frac{d^3 p_l}{2E_l} dM_n^2 dM_l^2$ being taken away, Y_a is the antisymmetric operator (see Appendix) to antisymmetrizing $(x_1 \alpha i i'), (x_2 \beta j j'), (x_3 \gamma k k')$.

Using the wave function (37), the expression of f_1 is obtained as

$$\begin{aligned}
\frac{1}{\sqrt{2}} f_1(x, y) \epsilon_{i'j'k'} \epsilon_{ijm} \delta_{kl'} u_{\lambda, \gamma} &= \frac{1}{(2\pi)^6} \int d^4 p_n d^4 p_l dM_n^2 dM_l^2 \delta(p_n^2 + M_n^2) \delta(p_l^2 + M_l^2) \theta(p_{n0}) \theta(p_{l0}) \\
&\sum'_{n,l} \left\{ \theta(x_0) \theta\left(-\frac{x_0}{2} + y_0\right) e^{i(p_n - \frac{1}{2}p_l)x + i(p_l - \frac{2}{3}p)y} < 0 | (\gamma_5 C \psi_{i'}^{i'})_{\beta} | n > < n | \psi_{\beta, j}^{j'} | l > < l | \psi_{\gamma, k}^{k'} | B_{\lambda, l'}^{m'} > \right. \\
&- \theta\left(\frac{x_0}{2} + y_0\right) \theta\left(\frac{x_0}{2} - y_0\right) e^{\frac{i}{2}(p_n + p_l - p)x + i(p_n - p_l - \frac{1}{3}p)y} < 0 | (\gamma_5 C \psi_{i'}^{i'})_{\beta} | n > < n | \psi_{\gamma, k}^{k'} | l > < l | \psi_{\beta, j}^{j'} | B_{\lambda, l'}^{m'} > \\
&- \theta\left(-\frac{x_0}{2} + y_0\right) \theta\left(-\frac{x_0}{2} - y_0\right) e^{-\frac{i}{2}(p_n + p_l - p)x + i(p_n - p_l - \frac{1}{3}p)y} < 0 | (\gamma_5 C \psi_j^{j'})_{\beta} | n > < n | \psi_{\gamma, k}^{k'} | l > < l | \psi_{\beta, i}^{i'} | B_{\lambda, l'}^{m'} > \\
&\left. + \theta(-x_0) \theta\left(\frac{x_0}{2} + y_0\right) e^{-i(p_n - \frac{1}{2}p)x + i(p_l - \frac{2}{3}p)y} < 0 | (\gamma_5 C \psi_j^{j'})_{\beta} | n > < n | \psi_{\beta, i}^{i'} | l > < l | \psi_{\gamma, k}^{k'} | B_{\lambda, l'}^{m'} > \right. \\
&+ \theta\left(-\frac{x_0}{2} - y_0\right) \theta(x_0) e^{i\left[\frac{i}{2}(p_n + p - 2p_l)x - i(p_n - \frac{1}{3}p)y\right]} < 0 | \psi_{\gamma, k}^{k'} | n > < n | (\gamma_5 C \psi_{i'}^{i'})_{\beta} | l > < l | \psi_{\beta, j}^{j'} | B_{\lambda, l'}^{m'} > \\
&\left. - \theta\left(\frac{x_0}{2} - y_0\right) \theta(-x_0) e^{\frac{i}{2}(p_n + p - 2p_l)x - i(p_n - \frac{1}{3}p)y} < 0 | \psi_{\gamma, k}^{k'} | n > < n | (\gamma_5 C \psi_j^{j'})_{\beta} | l > < l | \psi_{\beta, i}^{i'} | B_{\lambda, l'}^{m'} > \right\}. \quad (39)
\end{aligned}$$

Replacing

$$\gamma_5 C \psi \text{ by } \gamma_5 C \gamma_0 \psi \quad (40)$$

in Eq. (39),

$$\frac{1}{\sqrt{2}} f_2(x, y) \epsilon_{i'j'k'} \epsilon_{ijm'} \delta_{kl'} u_{\lambda, \gamma} \quad (41)$$

is obtained. In general the quark field ψ has four components. If only quark spinors ($u_{\pm \frac{1}{2}}$ (30)) are taken into account then $\gamma_0 \psi = \psi$ and $f_1 = f_2$ as mentioned above. For antiquark spinors ($v_{\pm \frac{1}{2}}$ (30)) $\gamma_0 \psi = -\psi$ and $f_1 \neq f_2$.

Theoretically, the relationship between the antiquark spinors v_{\pm} (30) and possible antiquark density of the nucleon is a dynamical question. The dynamical nature of this question is not explored in this paper. However, some arguments are made. in Ref. [14] antiquark density of a nucleon are defined as

$$\bar{q}_i = \frac{1}{2} \langle p | \bar{\psi}_i \psi_i - \bar{\psi}_i \gamma_0 \psi_i | p \rangle . \quad (42)$$

Using the arguments above, this model predicts that

$$\bar{q}_i \neq 0.$$

Detailed calculation of the quantity \bar{q}_i $i = u, d, s$ will be presented in the section of antiquark components.

In this paper when "the contribution of 0 antiquark components" is mentioned it really means that the contributions of the antiquark spinors v_{\pm} .

The wave function of baryon, $\bar{B}_{\alpha\beta\gamma,ijk}(x_1, x_2, x_3)_{\lambda U}$ is required in the calculation of the matrix elements and is defined as (color indices are dropped)

$$\bar{B}_{\alpha\beta\gamma,ijk}(x_1, x_2, x_3)_{\lambda U} = \langle B_{\lambda U}(p) | T \{ \bar{\psi}_{\alpha,i}(x_1) \bar{\psi}_{\beta,j}(x_2) \bar{\psi}_{\gamma,k}(x_3) \} | 0 \rangle . \quad (43)$$

Using time reversal, it is found

$$\bar{B}_{\alpha\beta\gamma,ijk}^{i'j'k'}(x_1, x_2, x_3)_{\lambda U} = \eta(-1)^{J+1} (\gamma_5 C)_{\alpha\alpha'} (\gamma_5 C)_{\beta\beta'} (\gamma_5 C)_{\gamma\gamma'} B_{\gamma'\beta'\alpha',kji}^{k'j'i'}(-x_3, -x_2, -x_1)_{-\lambda U}, \quad (44)$$

where η is a phase factor and it is determined as

$$\begin{aligned} J = \frac{1}{2}, \quad \eta = -i, \\ J = \frac{3}{2}, \quad \eta = i. \end{aligned} \tag{45}$$

Using Eqs. (44,35,33), another sets of wave functions in the moving frame are obtained

$$\begin{aligned} \bar{B}_{\alpha\beta\gamma,ijk}(x,y)_{l,\lambda}^m &= -\frac{1}{6\sqrt{2}}\epsilon_{i'j'k'}\{(\epsilon_{ijm}\delta_{kl} + \epsilon_{ikm}\delta_{jl})\bar{\Gamma}_{\alpha\beta,\gamma}^{\frac{1}{2}}(x,y)_\lambda \\ &\quad + (\epsilon_{jkm}\delta_{il} + \epsilon_{ikm}\delta_{jl})\bar{\Gamma}_{\beta\gamma,\alpha}^{\frac{1}{2}}(x,y)_\lambda, \\ \bar{B}_{\alpha\beta\gamma,ijk}^{lmn}(x,y)_\lambda &= \frac{1}{2\sqrt{2}}\epsilon_{i'j'k'}d_{ijk}^{lmn}\bar{\Gamma}_{\alpha\beta\gamma}^{\frac{3}{2}}(x,y)_\lambda, \end{aligned} \tag{46}$$

$$\begin{aligned} \bar{\Gamma}_{\alpha\beta,\gamma}^{\frac{1}{2}}(x,y,p)_\lambda &= \{C[f_1(-x,-y) + f_2(-x,-y)\frac{i}{m}\gamma \cdot p]\gamma_5\}_{\alpha\beta}\bar{u}(p)_{\lambda,\gamma} \\ &\quad + [f_1(-x,-y) - f_2(-x,-y)]C_{\alpha\beta}\{\bar{u}(p)_\lambda\gamma_5\}_\gamma, \\ \bar{\Gamma}_{\alpha\beta\gamma}^{\frac{3}{2}}(x,y,p)_\lambda &= \{C[f_2(-x,-y) + f_1(-x,-y)\frac{i}{m}\gamma \cdot p]\gamma_\mu\}_{\alpha\beta}\bar{\psi}_\mu^\lambda(p)_\gamma \\ &\quad + [f_1(-x,-y) - f_2(-x,-y)]\frac{i}{m}(C\gamma_mu\gamma \cdot p\gamma_5)_{\alpha\beta}\{\bar{\psi}_\mu^\lambda(p)\gamma_5\}_\gamma. \end{aligned} \tag{47}$$

In Ref. [4] in the rest frame of baryon the $O(3) \times SU(6)$ symmetry has been applied to construct the wave functions of one p-wave and one s-wave(1s1p); one p - wave and one - p wave (1p1p) and one s-wave and 1 d wave (1s1d). For convenience these wave functions are presented in the Appendix.

4 Transit matrix elements and the effective currents

In the relativistic quark model [11] the effective Lagrangian are used to study the electromagnetic and weak properties of baryon. The electromagnetic (EM) effective Lagrangian of quarks is defined as

$$\mathcal{L} = -ie\bar{\psi}Q\{\hat{A}(x) - \frac{i\kappa}{4m_N}\sigma_{\mu\nu}F^{\mu\nu}\}\psi, \quad (48)$$

where

$$Q = \begin{pmatrix} \frac{2}{3} & 0 & 0 \\ 0 & -\frac{1}{3} & 0 \\ 0 & 0 & -\frac{1}{3} \end{pmatrix},$$

κ is the anomalous magnetic moment of quark and it is a parameter in this model.

The general expression of the transit matrix element between baryons is shown in Eq. (1). The kernel G_μ of Eq. (1) is the effect of strong interactions (nonperturbative QCD). In the quark model [11] the mechanism of single quark transition is claimed. On the other hand, in order to satisfy the requirement of SU(6) symmetry the kinetic terms in the kernel G_μ must be ignored. Under this mechanism the kernel G_μ is reduced to

$$M(x'_1, x'_2, x_1, x_2)J_\mu(0),$$

where $M(x'_1, x'_2, x_1, x_2)$ is a scalar function and the $J_\mu(0)$ is the EM or weak current of quarks.

The EM current is shown in Eq. (48) and the weak current will be shown in section 9. The

transit matrix element (1) is rewritten as

$$\begin{aligned} < B_\lambda(p')_{U'} | J_\mu(0) | B_\lambda(p)_U > = P_{k_1 k'_1} \Gamma_{\mu, \gamma \gamma'} \\ \int dx'_1 dx'_2 dx_1 dx_2 M(x'_1, x'_2, x_1, x_2) \bar{B}_{\alpha \beta \gamma, ij k_1}^{\lambda'}(x'_1, x'_2, 0)_{U'} B_{k'_1 j i, \gamma' \beta \alpha}^\lambda(0, x_2, x_1)_U, \end{aligned} \quad (49)$$

where the function $M(x'_1, x'_2, x_1, x_2)$ is unknown and for EM interactions

$$P = Q, \quad \Gamma_\mu = \gamma_\mu + \frac{\kappa}{2m_N} \sigma_{\mu\nu} q_\nu, \quad (50)$$

where q_μ is the transfer momentum. For weak interactions P and Γ_μ have different expressions (see section 9). In Ref. [11] the $M(x'_1, x'_2, x_1, x_2)$ is taken as a constant.

5 EM form factors of baryons

In Ref. [5] the wave functions (33,46), the matrix element (49), and the effective EM current (50) are applied to study the EM form factors of nucleon. The results are presented in this section.

The EM form factors of a baryon are defined as

$$< B(p')_{\lambda'} | J_\mu(0) | B(p)_\lambda > = \bar{u}(p')_{\lambda'} \{ F_1(q^2) \gamma_\mu + F_2(q^2) \frac{\kappa \sigma_{\mu\nu} q_\nu}{2m_p} \} u(p)_\lambda, \quad (51)$$

$$G_E(q^2) = F_1 - \tau \kappa F_2, \quad G_M(q^2) = F_1 + \kappa F_2, \quad (52)$$

$$\tau = \frac{q^2}{4m_p^2}. \quad (53)$$

The electric charge of proton is one. Therefore, there is normalization condition

$$G_E^p(0) = 1, \quad F_1^p(0) = 1. \quad (54)$$

By using the matrix element (49), the effective EM current (50), and the wave functions of baryons (33,46), these matrix elements are calculated and the EM form factors G_E and G_M of baryons are determined in this model.

The matrix elements of electric currents of $\frac{1}{2}^+$ baryon are obtained

$$\langle B_{\lambda}^{\frac{1}{2}}(p_f)_{l_1}' | J_{\mu}(0) | B_{\lambda}^{\frac{1}{2}}(p_i)_{l_2}' \rangle = -\frac{ie}{24} \{A_1 I_1 - A_2 I_2\}, \quad (55)$$

where m , m' and E , E' are the initial and final mass and energy of the baryon respectively,

$$A_1 = Tr \bar{B} Q B, \quad A_2 = Tr \bar{B} B Q. \quad (56)$$

B , \bar{B} are the SU_3 flavor matrices of the initial and final baryon, which are presented in the Appendix.

$$\begin{aligned} I_1 = & -20 \{ D_2(q^2) (1 - \frac{m_+}{5m}) + D_2'(q^2) (1 - \frac{m_+}{5m'}) \\ & + \frac{1}{2mm'} (m_-^2 + q^2 + \frac{\kappa m_+}{5m_p} q^2) D_3(q^2) \} \bar{u}_{\lambda'}(p_f) \gamma_{\mu} u_{\lambda}(p_i) \\ & -20 \{ 2D_1(q^2) - (1 - \frac{2m_p}{5\kappa m}) D_2(q^2) - (1 - \frac{2m_p}{5\kappa m'}) D_2'(q^2) \\ & + \frac{1}{2mm'} (m_+^2 + \frac{3}{5} q^2) D_3(q^2) \} \frac{\kappa}{2m_p} \bar{u}_{\lambda'}(p_f) q_{\nu} \sigma_{\mu\nu} u_{\lambda}(p_i) \\ & -4i \{ \frac{1}{m} D_2(q^2) - \frac{1}{m'} D_2'(q^2) + \frac{\kappa}{2mm'm_p} (m'^2 - m^2) D_3(q^2) \} \end{aligned}$$

$$\begin{aligned}
& q_\mu \bar{u}_{\lambda'}(p_f) u_\lambda(p_i), \\
I_2 = & 4\left\{(1 - 2\frac{m_+}{m})D_2(q^2) + (1 - 2\frac{m_+}{m'})D'_2(q^2)\right. \\
& + \frac{1}{2mm'}(m_-^2 + q^2 + 2\frac{\kappa m_+}{m_p}q^2)D_3(q^2)\big\}\bar{u}_{\lambda'}(p_f)\gamma_\mu u_\lambda(p_i) \\
& - 4\left\{2D_1(q^2) - (1 - \frac{4m_p}{\kappa m})D_2(q^2) - (1 - \frac{4m_p}{\kappa m'})D'_2(q^2)\right. \\
& + \frac{1}{2mm'}(m_+^2 - 3q^2)D_3(q^2)\big\}\frac{\kappa}{2m_p}\bar{u}_{\lambda'}(p_f)q_\nu\sigma_{\nu\mu}u_\lambda(p_i) \\
& + 8i\left\{\frac{1}{m}D_2(q^2) - \frac{1}{m'}D'_2(q^2) + \frac{\kappa(m'^2 - m^2)}{2mm'm_p}D_3(q^2)\right\} \\
& q_\mu \bar{u}_{\lambda'}(p_f) u_\lambda(p_i), \tag{57}
\end{aligned}$$

where

$$q_\mu = p_\mu - p'_{f\mu}, \quad m_+ = m + m', \quad m_- = m' - m, \tag{58}$$

$$\begin{aligned}
D_1(q^2) &= - \int f'_1(-x'_1, -x'_2, 0)M(x'_1, x'_2, x_1, x_2)f_1(0, x_2, x_1)d^4x'_1d^4x'_2d^4x_1d^4x_2, \\
D_2(q^2) &= - \int f'_1(-x'_1, -x'_2, 0)M(x'_1, x'_2, x_1, x_2)f_2(0, x_2, x_1)dx'_1dx'_2dx_1dx_2, \\
D'_2(q^2) &= - \int f'_2(-x'_1, -x'_2, 0)M(x'_1, x'_2, x_1, x_2)f_1(0, x_2, x_1)d^4x'_1d^4x'_2d^4x_1d^4x_2, \\
D_3(q^2) &= - \int f'_2(-x'_1, -x'_2, 0)M(x'_1, x'_2, x_1, x_2)f_2(0, x_2, x_1)d^4x'_1d^4x'_2d^4x_1d^4x_2. \tag{59}
\end{aligned}$$

m, m' are the mass of the initial and final baryon respectively. Eq.(59) shows that when $p' \longleftrightarrow p$ is taken, we have

$$D_2(q^2) \longleftrightarrow D'_2(q^2), \tag{60}$$

therefore, when $m = m'$

$$D_2(q^2) = D_2'(q^2). \quad (61)$$

In Eq. (57) there are three unknown functions, $D_1(q^2)$, $D_2(q^2)$, $D_3(q^2)$.

In Eq.(57), when $m = m'$ is taken, the terms in I_1 and I_2 , which are proportional to q_μ vanish. Thus, when $m = m'$, the current matrix element of $\frac{1}{2}^+$ baryon automatically satisfies the current conservation. In general cases in order to satisfy the current conservation, the following condition must be satisfied

$$D_2'(q^2) - \frac{m'}{m} D_2(q^2) + \frac{m_-}{m} D_3(q^2) = 0. \quad (62)$$

For $\frac{1}{2}^+$ baryons the only matrix element with $m' \neq m$ is $\Sigma^0 - \rightarrow \Lambda$. For this process, we have

$$A_1 = A_2 = \frac{1}{2\sqrt{3}}. \quad (63)$$

The condition(62) guarantees current conservation for the EM process $\Sigma^0 - \rightarrow \Lambda + \gamma$.

Ward identity in this model

It is well known that current conservation is satisfied in the electromagnetic interactions. Why the condition (62) is required in this model ? This question must be answered. As mentioned that in this study a relativistic quark model is exploited. In this model SU(6) symmetry for the wave functions in the rest frame, effective current, and the kernel of the transit matrix elements are assumed. In order to satisfy the current conservation the Ward identity must be satisfied after these assumptions. The Ward identity is the constraint on

these assumptions. In Ref. [15] the conditions for EM transit matrix elements of baryons to satisfy the Ward identity are revealed. As a matter of factor, Eq. (62) is the condition for satisfying the Ward identity.

The condition (62) not only guarantees the current conservation of $B \rightarrow B'$ it will be shown in this paper that the same condition (62) guarantees the current conservation for $p \rightarrow \Delta$ and the same condition (62) prohibits the appearance of the second class current in weak transition of $B \rightarrow B'$ (see section 9). This condition (62) makes the vector form factors of $\Sigma^+ \rightarrow \Lambda + e^+ + \nu$ and $\Sigma^- \rightarrow \Lambda + e^- + \bar{\nu}$ to be proportional to q^2 (Tab. 3) and they are in agreement with the data (see subsection 9.4).

The electromagnetic form factors of $\frac{1}{2}^+$ baryons are obtained from the current matrix elements (57)

$$\begin{aligned}
G_E(q^2) = & -\frac{2}{3}(A_1 + 2A_2)(1 + \frac{q^2}{4m^2})\{D_2(q^2) - \frac{\kappa q^2}{4mm_p}D_3(q^2)\} \\
& + \frac{1}{3}(A_2 + 5A_1)\{D_2(q^2) + \frac{q^2}{4m^2}[D_3(q^2) + \frac{\kappa m}{m_p}D_2(q^2) \\
& - \frac{\kappa m}{m_p}D_1(q^2) - \kappa \frac{m}{m_p}(1 + \frac{q^2}{4m^2})D_3(q^2)]\}. \tag{64}
\end{aligned}$$

$$\begin{aligned}
G_M(q^2) = & \frac{1}{3}(A_2 + 5A_1)\{\frac{m_p}{m}[D_2(q^2) + \frac{q^2}{4m^2}D_3(q^2)] + \kappa[D_1(q^2) \\
& - D_2(q^2) + (1 + \frac{q^2}{4m^2})D_3(q^2)]\}, \tag{65}
\end{aligned}$$

where m is the mass of the baryon and $\frac{e}{2m_p}$ is the unit of the $G_M(q^2)$. The expression of the

magnetic moment of $\frac{1}{2}^+$ baryon is obtained from Eq.(65)

$$\mu = G_M(0) = \frac{1}{3}(A_2 + 5A_1)\left\{\frac{m_p}{m} + \kappa[D_1(0) + D_3(0) - D_2(0)]\right\}. \quad (66)$$

Eq. (66) shows that there are two parts in the magnetic moment of baryon: the term $\frac{m_p}{m}$ is resulted in the recoil effect of the baryon and the second term is the contribution of the anomalous magnetic moment of quark. Eqs. (64,65) show that the two invariant functions f_1 , f_2 and the function $M(x'_1, x'_2, x_1, x_2)$ all appear in the three unknown functions of $D_{1,2,3}(q^2)$.

6 Relationship Between $f_1(x_1, x_2, x_3)$ and $f_2(x_1, x_2, x_3)$

The SU(6) symmetry in the rest frame leads to that in the wave functions of baryons there are two functions $f_1(x_1, x_2, x_3)$ and $f_2(x_1, x_2, x_3)$ and $f_1(x_1, x_2, x_3) \neq f_2(x_1, x_2, x_3)$ is resulted in the effects of antiquarks. In order to explore the effects of antiquarks in the form factors of baryons the possible relationship between the two invariant functions $f_1(x_1, x_2, x_3)$ and $f_2(x_1, x_2, x_3)$ in the frame of center-of-mass is studied [5].

In the rest frame the $\Gamma_{\alpha\beta,\gamma}^{\frac{1}{2}}(p)_\lambda$ (34) can be rewritten as

$$\begin{aligned} \Gamma_{\alpha\beta,\gamma}(x_1, x_2, x_3)_\lambda &= g_1(x_1, x_2, x_3)\{(1 + \gamma_0)\gamma_5 C\}_{\alpha\beta}u_{\lambda,\gamma} \\ &\quad + g_2(x_1, x_2, x_3)\{[(1 - \gamma_0)\gamma_5 C]_{\alpha\beta}u_{\lambda,\gamma} + 2C_{\alpha\beta}(\gamma_5 u_\lambda)_\gamma\}, \\ g_1(x_1, x_2, x_3) &= \frac{1}{2}\{f_1(x_1, x_2, x_3) + f_2(x_1, x_2, x_3)\}, \end{aligned}$$

$$g_2(x_1, x_2, x_3) = \frac{1}{2}\{f_1(x_1, x_2, x_3) - f_2(x_1, x_2, x_3)\}, \quad (67)$$

The wave functions of baryons (2) are the Bethe - Salpeter (BS) amplitudes and they satisfy corresponding BS equations. In order to make the wave functions to satisfy the SU(6) symmetry in the rest frame the BS equation must satisfy the SU(6) symmetry in the rest frame too.

The BS equation of a $\frac{1}{2}^+$ baryon is written as

$$\begin{aligned} & (i\hat{p}_1 + M)_{\alpha\alpha'}(i\hat{p}_2 + M)_{\beta\beta'}(i\hat{p}_3 + M)_{\gamma\gamma'} B_{\alpha'\beta'\gamma',ijk}^{\frac{1}{2}\lambda}(p_1, p_2, p_3)_l^m \\ = & -i(i\hat{p}_3 + M)_{\gamma\gamma'} \int U(q) B_{\alpha\beta\gamma',ijk}^{\frac{1}{2}\lambda}(p_1 - q, p_2 + q, p_3)_l^m d^4q \\ & -i(i\hat{p}_1 + M)_{\alpha\alpha'} \int U(q) B_{\alpha'\beta\gamma,ijk}^{\frac{1}{2}\lambda}(p_1, p_2 - q, p_3 + q)_l^m d^4q \\ & -i(i\hat{p}_2 + M)_{\beta\beta'} \int U(q) B_{\alpha\beta'\gamma,ijk}^{\frac{1}{2}\lambda}(p_1 + q, p_2, p_3 - q)_l^m d^4q \\ & - \int V(q_1, q_2, q_3) \delta^4(q_1 + q_2 + q_3) B_{\alpha\beta\gamma,ijk}^{\frac{1}{2}\lambda}(p_1 + q_1, p_2 + q_2, p_3 + q_3) \\ & \times d^4q_1 d^4q_2 d^4q_3. \end{aligned} \quad (68)$$

It is assumed that $U(q)$ of two bodies interactions and $V(q_1, q_2, q_3)$ of three bodies interactions are independent of the momentum of the baryon and they are scalars to keep possible SU(6) symmetry. The p_1, p_2, p_3 of Eq. (68) satisfy

$$p_1 + p_2 + p_3 = p, \quad (69)$$

where p is the momentum of $\frac{1}{2}^+$ baryon.

It is not the intention to solve this equation and the Eq. (68) is used to study the relationship between $f_{1,2}$ functions. For this purpose in order to keep SU(6) symmetry the spatial part of the matrix \hat{p}_i of Eq. (68) must be ignored. Substituting the wave function of $\frac{1}{2}^+$ (33,34) into Eq.(68), we obtain

$$\begin{aligned}
& (M - \gamma_0 p_{10})_{\alpha\alpha'} (M - \gamma_0 p_{20})_{\beta\beta'} (M - \gamma_0 p_{30})_{\gamma\gamma'} \Gamma_{\alpha'\beta'\gamma'}^{\frac{1}{2}}(p_1, p_2, p_3)_\lambda \\
= & -i(M - \gamma_0 p_{30})_{\gamma\gamma'} \int U(q) \Gamma_{\alpha\beta,\gamma'}^{\frac{1}{2}}(p_1 - q, p_2 + q, p_3)_\lambda d^4 q \\
& -i(M - \gamma_0 p_{10})_{\alpha\alpha'} \int U(q) \Gamma_{\alpha'\beta,\gamma}^{\frac{1}{2}}(p_1, p_2 - q, p_3 + q)_\lambda d^4 q \\
& -i(M - \gamma_0 p_{20})_{\beta\beta'} \int U(q) \Gamma_{\alpha\beta',\gamma}^{\frac{1}{2}}(p_1 + q, p_2, p_3 - q)_\lambda d^4 q \\
& - \int V(q_1, q_2, q_3) \delta^4(q_1 + q_2 + q_3) \Gamma_{\alpha\beta,\gamma}^{\frac{1}{2}}(p_1 + q_1, p_2 + q_2, p_3 + q_3) \\
& \times d^4 q_1 d^4 q_2 d^4 q_3.
\end{aligned} \tag{70}$$

where $\Gamma_{\alpha\beta,\gamma}^{\frac{1}{2}}(p_1, p_2, p_3)_\lambda$ is the expression of $\Gamma_{\alpha\beta\gamma}^{\frac{1}{2}}(x_1, x_2, x_3)_\lambda$ (34) in the momentum representation. Calculations lead to

$$\begin{aligned}
& (M - p_{10})(M - p_{20})(M - p_{30})g_1(p_1, p_2, p_3) \\
= & -i \int U(q) \{ (M - p_{30})g_1(p_1 - q, p_2 + q, p_3) \\
& + (M - p_{10})g_1(p_1, p_2 - q, p_3 + q) \\
& + (M - p_{20})g_1(p_1 + q, p_2, p_3 - q) \} d^4 q \\
& - \int V(q_1, q_2, q_3) \delta^4(q_1 + q_2 + q_3)
\end{aligned}$$

$$\times g_1(p_1 + q_1, p_2 + q_2, p_3 + q_3) d^4 q_1 d^4 q_2 d^4 q_3, \quad (71)$$

$$\begin{aligned} & (M + p_{10})(M + p_{20})(M - p_{30})g_2(p_1, p_2, p_3) \\ = & -i \int U(q) \{ (M - p_{30})g_2(p_1 - q, p_2 + q, p_3) \\ & + (M + p_{10})g_2(p_1, p_2 - q, p_3 + q) \\ & + (M + p_{20})g_2(p_1 + q, p_2, p_3 - q) \} d^4 q \\ & - \int V(q_1, q_2, q_3) \delta^4(q_1 + q_2 + q_3) \\ & \times g_2(p_1 + q_1, p_2 + q_2, p_3 + q_3) d^4 q_1 d^4 q_2 d^4 q_3, \end{aligned} \quad (72)$$

$$\begin{aligned} & (M + p_{10})(M - p_{20})(M + p_{30})g_2(p_1, p_2, p_3) \\ = & -i \int U(q) \{ (M + p_{30})g_2(p_1 - q, p_2 + q, p_3) \\ & + (M + p_{10})g_2(p_1, p_2 - q, p_3 + q) \\ & + (M - p_{20})g_2(p_1 + q, p_2, p_3 - q) \} d^4 q \\ & - \int V(q_1, q_2, q_3) \delta^4(q_1 + q_2 + q_3) \\ & \times g_2(p_1 + q_1, p_2 + q_2, p_3 + q_3) d^4 q_1 d^4 q_2 d^4 q_3, \end{aligned} \quad (73)$$

$$\begin{aligned} & (M - p_{10})(M + p_{20})(M + p_{30})g_2(p_1, p_2, p_3) \\ = & -i \int U(q) \{ (M + p_{30})g_2(p_1 - q, p_2 + q, p_3) \\ & + (M - p_{10})g_2(p_1, p_2 - q, p_3 + q) \} \end{aligned}$$

$$\begin{aligned}
& +(M + p_{20})g_2(p_1 + q, p_2, p_3 - q)\}d^4q \\
& - \int V(q_1, q_2, q_3)\delta^4(q_1 + q_2 + q_3) \\
& \times g_2(p_1 + q_1, p_2 + q_2, p_3 + q_3)d^4q_1d^4q_2d^4q_3.
\end{aligned} \tag{74}$$

Since $V(q_1, q_2, q_3)$ are totally symmetric functions of q_1, q_2, q_3 and $g_1(p_1, p_2, p_3)$ are totally symmetric functions of p_1, p_2, p_3 too. From Eqs.(73,74), we see that $g_2(p_1, p_2, p_3)$ have following symmetries: (1) totally symmetric in p_1, p_2, p_3 . (2) since $U(q)$ and $V(q_1, q_2, q_3)$ are independent of the momentum p , the equation is invariant under the transformations $p_{20} \rightarrow -p_{20}$, $p_{30} \rightarrow -p_{30}$; $p_{10} \rightarrow -p_{10}$, $p_{30} \rightarrow -p_{30}$; $p_{10} \rightarrow -p_{10}$, $p_{20} \rightarrow -p_{20}$. By using the second symmetry of $g_2(p_1, p_2, p_3)$, Eq.(74) becomes Eq.(73) under the transformation $p_{10} \rightarrow -p_{10}$, $p_{20} \rightarrow -p_{20}$, thus $g_1(p_1, p_2, p_3)$ and $g_2(p_1, p_2, p_3)$ satisfy the same equation. $g_1(p_1, p_2, p_3)$ is related to $g_2(p_1, p_2, p_3)$ by

$$g_1(p_1, p_2, p_3) = cg_2(p_1, p_2, p_3), \tag{75}$$

where c is a constant. Eq. (75) leads to

$$f_2(x_1, x_2, x_3) = af_1(x_1, x_2, x_3), \tag{76}$$

where a is another constant. Using Eq. (76), the three functions $D_{1,2,3}(q^2)$ of Eqs. (64,65) are reduced to one unknown function and a parameter a

$$D_1(q^2) = \frac{1}{a}D_2(q^2), \quad D_3(q^2) = aD_2(q^2). \tag{77}$$

Obviously, the discussion above is not a proof of Eq. (76) and it is an argument that the relationship (76) is possible.

Substituting Eq. (76) into the condition of current conservation (62), two solutions are obtained

$$a = 1 \tag{78}$$

or

$$a = \frac{1}{1 - \frac{m_0}{m}} \tag{79}$$

m_0 is a parameter, m is the physical mass of the baryon. As mentioned above $a = 1$ means $f_1 = f_2$ and there is no antiquark effects. In Refs. [5,6,7] the effects of antiquarks are investigated. Therefore, $a \neq 1$ (79) is taken in the studies [5,6,7]. It will be shown that the physical results of this model favor the solution (79) or favor the existence of antiquark components in baryon.

7 EM form factors of proton and neutron

The EM form factors of proton and neutron are derived from Eqs.(64,65) [5]

$$G_E^p(q^2) = D_2(q^2) + \frac{q^2}{4m_N^2} \{D_3(q^2) + \kappa[D_2(q^2) - D_1(q^2) - (1 + \frac{q^2}{4m_N^2})D_3(q^2)]\}, \tag{80}$$

$$G_M^p(q^2) = D_2(q^2) + \kappa[D_1(q^2) + D_3(q^2) - D_2(q^2)] + (1 + \kappa)\frac{q^2}{4m_N^2}D_3(q^2), \tag{81}$$

$$G_E^n(q^2) = -\frac{2}{3}\frac{q^2}{4m_N^2} \{D_3(q^2) - D_2(q^2) + \kappa[D_2(q^2) - D_1(q^2)]\}, \tag{82}$$

$$G_M^n(q^2) = -\frac{2}{3}G_M^p(q^2). \quad (83)$$

The charge normalization of the proton

$$G_E^p(0) = 1 \quad (84)$$

determines

$$D_2(0) = 1. \quad (85)$$

In Eqs. (80-83) the mass difference between proton and neutron is ignored. The isospin symmetry is reserved.

The relationship between the magnetic moments of the proton and neutron

$$\mu_p = G_M^p(0) = 1 + \kappa\{D_1(0) + D_3(0) - 1\}, \quad (86)$$

$$\mu_n = G_M^n(0) = -\frac{2}{3}\mu_p \quad (87)$$

is revealed from Eqs. (81,83). Eq. (87) is the prediction of the SU(6) symmetry and it agrees with the data well. This result shows that the wave function (33,34) has, indeed, SU(6) symmetry. Beside Eq. (87) this model predicts the relation between the two magnetic form factors of proton and neutron (83). Proton and neutron are doublet of isospin. The deviation of Eq. (87) from experimental value is originated in the isospin symmetry breaking which is small.

Eq. (82) shows $G_E^n(0) = 0$ and the charge condition for neutral neutron is automatically satisfied. Nonzero charge form factor of neutron (82) is predicted by this model.

7.1 Magnetic form factors of nucleon

The radius of the magnetic form factors of proton and neutron can be defined

$$\begin{aligned} G_M^p(q^2) &= \mu_p \left\{ 1 - \frac{1}{6} (r^2)_M^p q^2 \right\}, \\ G_M^n(q^2) &= \mu_n \left\{ 1 - \frac{1}{6} (r^2)_M^n q^2 \right\}. \end{aligned} \quad (88)$$

Eq. (88) predicts that

$$r_p^M = r_n^M. \quad (89)$$

There are three reports of the value of the r_p^M : $0.777 \pm 0.013 \pm 0.010 fm$ [16], $0.876 \pm 0.010 \pm 0.016 fm$ [17], $0.854 \pm 0.005 fm$ [18], $0.867 \pm 0.009_{exp} \pm 0.018_{fit} fm$ [18]. One measurement of the r_n^M has been reported as $0.80 \pm 0.10 fm$ [18]. The prediction (89) agrees with the data within the experimental errors.

From Eqs. (83,87)

$$\frac{G_M^p}{\mu_p} = \frac{G_M^n}{\mu_n} \quad (90)$$

is obtained. The measurements of $\frac{1}{\mu_p} G_M^p / G_D$ and $\frac{1}{\mu_n} G_M^n / G_D$ can be found in a review articles [19], where

$$G_D = \frac{1}{(1 + \frac{q^2}{0.71 \text{ GeV}^2})^2}. \quad (91)$$

The prediction (90) is not in contradiction with data within about few percent in the region of $q^2 < 10 \text{ GeV}^2$.

7.2 Charge form factor of neutron and the ratio of the EM form factors of proton

The electric form factor G_E^n is not zero (82). If $f_1 = f_2$ is taken, the Eqs. (59) become

$$D_1(q^2) = D_3(q^2) = D_2(q^2). \quad (92)$$

Substitute Eq. (92) into Eq. (82)

$$G_E^n = 0 \quad (93)$$

is obtained. Therefore, in this model non-zero G_E^n is resulted in the effects of the antiquark components in the wave function of the neutron.

On the other hand, if $f_1 = f_2$ is taken and using Eq. (92), the EM form factors of proton (80,81) become

$$G_E^p(q^2) = D_2(q^2)(1 + \tau)(1 - \kappa q^2), \quad (94)$$

$$G_M^p(q^2) = D_2(q^2)(1 + \kappa)(1 + \tau), \quad (95)$$

and

$$\mu_p = 1 + \kappa, \quad (96)$$

$$R = \frac{\mu_p G_E^p(q^2)}{G_M^p(q^2)} = 1 - \kappa q^2 = 1 - (\mu_p - 1)q^2. \quad (97)$$

are obtained. The ratio R (97) decreases very fast and

$$R \leq 0, \text{ when } q^2 \geq \frac{4m_p^2}{\mu_p - 1} = 1.96 \text{ GeV}^2. \quad (98)$$

This ratio (97) is in strong disagreement with current data [1,2,3].

Therefore, $f_1 = f_2$ is rejected by the ratio of the EM form factors of proton and the charge form factor of neutron.

Now we need to study the case of $f_1 \neq f_2$. Using Eqs.(77,85), it is found

$$\mu_p = 1 + \kappa \left\{ 1 + a - \frac{1}{a} \right\}, \quad (99)$$

$$\mu_n = -\frac{2}{3}\mu_p, \quad (100)$$

$$G_E^p(q^2) = D_2(q^2) \{ 1 + \tau(a + 1 - \mu_p) - a\kappa\tau^2 \}, \quad (101)$$

$$G_M^p(q^2) = \mu_p D_2(q^2) \left\{ 1 + \frac{a}{\mu_p} (1 + \kappa) \tau \right\}, \quad (102)$$

$$G_E^n(q^2) = \mu_n \tau D_2(q^2) \frac{1}{\mu_p} \left(a - 1 \right) \left(1 + \frac{\kappa}{a} \right) \}. \quad (103)$$

The magnetic form factor of the neutron is expressed as Eq. (83). The geometric picture of the form factors of nucleon in this model can be constructed as following. According to the SU(6) symmetry the hadrons of $\underline{56}$ -plet are in s-wave in the rest frame. In the rest frame the $\frac{1}{2}^+$ and $\frac{3}{2}^+$ hadrons have spherical shapes. The wave function of a moving baryon is obtained by boosting the wave function from the rest frame to moving frame by Lorentz transformation. Because of Lorentz contraction the shapes of these baryons are changed to the shape of a football from a sphere. When the transfer momentum q^2 increases the length

of the ball along the direction of motion is shorten and the overlap of the two balls, one is at rest and the second is in motion, is decreasing. This effect makes the overlap function, the form factor, decreases with q^2 .

The $D_2(q^2)$, the κ , and the parameter a or m_0 are unknown and they are taken as three inputs in this model. Inputting the $G_M^p(q^2)$, the $D_2(q^2)$ can be determined

$$D_2(q^2) = \frac{1}{\mu_p} G_M^p(q^2) \left\{ 1 + \frac{a}{\mu_p} (1 + \kappa) \tau \right\}^{-1}. \quad (104)$$

Inputting Eq. (104) into the charge form factor of the neutron, the $G_E^n(q^2)$ (103) has triple poles. Because of the factor $\frac{q^2}{4m^2}$ the $G_E^n(q^2)$ increases with q^2 in small region of q^2 and because of the triple poles of the $D_2(q^2)$ it decreases with q^2 in the range of larger q^2 .

The ration of $R = \frac{\mu_p G_E^p(q^2)}{G_M^p(q^2)}$ is obtained

$$R = \frac{1 + \tau(a + 1 - \mu_p) - a\kappa\tau^2}{1 + \frac{a}{\mu_p}(1 + \kappa)\tau}. \quad (105)$$

If taking $a = 1$ in Eq. (105), the ratio R will go back to Eq. (97). It is interesting to notice that besides the two factors in Eq. (105) which decreases with q^2 if $(a + 1 - \mu_p) > 0$ the factor $(a + 1 - \mu_p)\tau$ increases with q^2 . In this article two versions of comparison with data are presented:

- 1) the original comparison presented in Ref. [5];
- 2) comparison with new data.

Previous comparison with data [5]

In Ref. [5] μ_p (99) and μ_Λ

$$\mu_\Lambda = -\frac{1}{3}\left\{\frac{m_p}{m_\Lambda} + \kappa(a_\Lambda + \frac{1}{a_\Lambda} - 1)\right\} = -0.64. \quad (106)$$

are taken as two inputs and the two parameters κ and m_0 (79) are determined to be

$$\kappa = 0.481, \quad m_0 = 0.778 m_p, \quad a = 4.51. \quad (107)$$

By using Eq. (107),

$$G_E^p(q^2) = D_2(q^2)\{1 + \tau(2.71 - 2.17\tau)\}, \quad (108)$$

$$G_M^p(q^2) = \mu_p D_2(q^2)\{1 + 2.39\tau\}, \quad (109)$$

$$G_E^n(q^2) = 1.39\mu_n\tau D_2(q^2), \quad (110)$$

$$D_2(q^2) = \frac{1}{\mu_p} G_M^p(q^2)(1 + 2.39\tau)^{-1}, \quad (111)$$

$$D_2(q^2) = \frac{1}{(1 + \frac{q^2}{0.71})^2(1 + 2.39\tau)} \quad (112)$$

are obtained, where $\frac{1}{\mu_p} G_M^p(q^2) = 1/(1 + \frac{q^2}{0.71})^2$ is taken. The ratio of the electric and magnetic form factor of proton is obtained

$$R = \frac{\mu_p G_E^p(q^2)}{G_M^p(q^2)} = \frac{1 + \tau(2.71 - 2.17\tau)}{1 + 2.39\tau}. \quad (113)$$

In the range of small q^2 $R = 1 + 0.091q^2$ is revealed. Therefore, the ratio (113) shows that in the range of small q^2 the ratio increases with q^2 slowly, then decreases with q^2 . This behavior is the prediction of this model. Comparisons with data are shown in Fig.1 and 2.

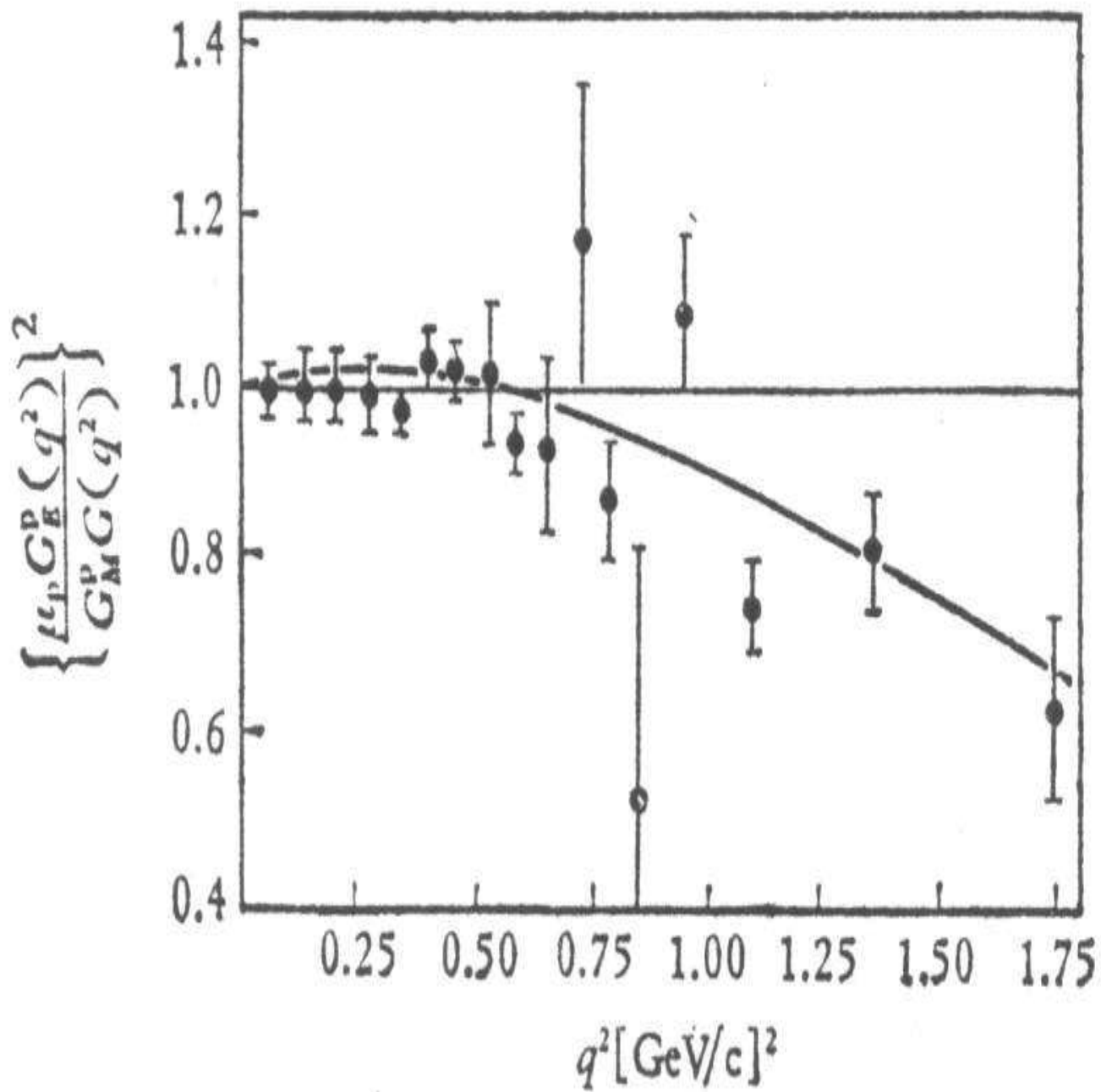


FIG. 1

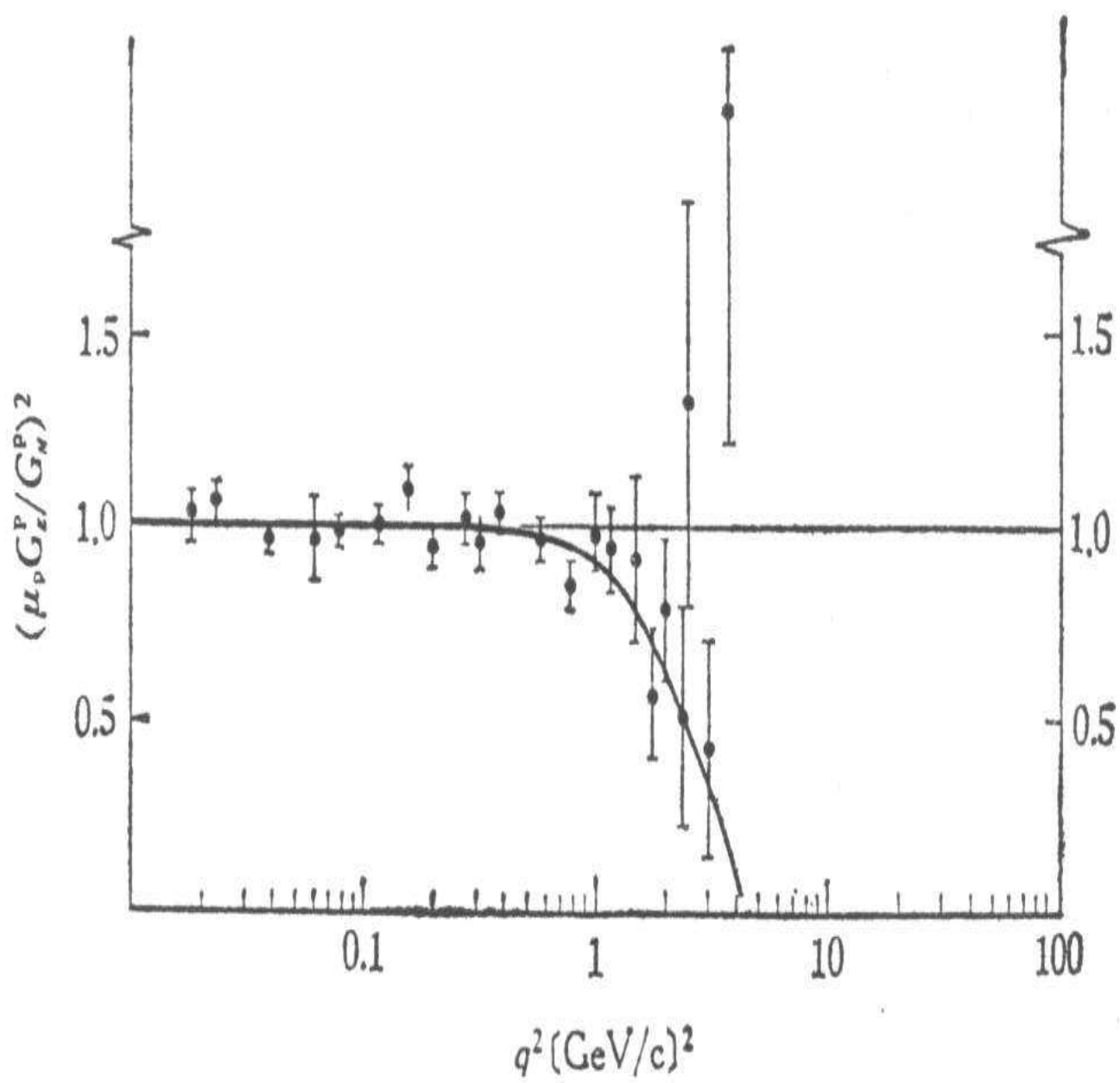


FIG. 2

The experimental data of Fig. 1 is from Ref.[20], and that for Fig. 2 is from Ref.[21]. Fig. 1 and Fig.2 show that in the range of $0 < q^2 < 0.55 \text{ GeV}^2$ the ratio R is about one (a little bit greater than one). After $q^2 = 0.55 \text{ GeV}^2$ the ratio is decreasing with q^2 . At $q^2 = 5.45 \text{ GeV}^2$ the ratio reaches zero and after this value of q^2 the ratio is negative.

The expression of the electric form factor of neutron is obtained

$$G_E^n(q^2) = 1.39\mu_n\tau(1 + 2.39\tau)^{-1}(1 + \frac{q^2}{0.71})^{-2}. \quad (114)$$

The expression of the $G_n^E(q^2)$ obtained in this model is just the Galster type [22]

$$G_E^n(q^2) = A\mu_n\tau G_D(q^2)(1 + B\tau)^{-1}, \quad (115)$$

where $G_D(q^2)$ is the expression of Eq. (91), the two parameters A and B are determined to be

$$A = (a - 1)(1 + \frac{\kappa}{a})\frac{1}{\mu_p}, \quad (116)$$

$$B = 1 + (1 + \kappa)\frac{a}{\mu_p}. \quad (117)$$

Using $a = 4.51$ (107),

$$A = 1.39, \quad B = 2.39 \quad (118)$$

are determined. Therefore, this model predicts a smaller negative charge form factor of neutron. The slope of $G_E^n(q^2)$ at $q^2 = 0$ is

$$\frac{dG_E^n(q^2)}{dq^2} \Big|_{q^2=0} = 1.39\frac{\mu_n}{4m_N^2} = -0.73 \text{ GeV}^{-2}. \quad (119)$$

The experimental data are

$$-0.579 \pm 0.018^{[23]}, -0.512 \pm 0.049^{[24]}, -0.495 \pm 0.010^{[25]}. \quad (120)$$

The data (120) are in the unit of GeV^{-2} . Comparisons of the $G_E^n(q^2)$ (114) with the experimental data are shown in Fig. 3 and Fig. 4.

The experimental data of Fig. 3 comes from Ref. [26] and that for Fig. 4 comes from Ref. [21]. Comparing with the $G_E^p(q^2)$, this model [4,5] predicts a smaller charge form factor of neutron and $|G_E^n(q^2)| < 0.1$. In the range of $q^2 < 0.443 \text{ GeV}^2$ $G_E^n(q^2)$ increases with q^2 and after it decreases. However, the $G_E^n(q^2)$ predicted is greater than the experimental data.

New fit with recent data

There are new data for $\frac{\mu_p G_E^p(q^2)}{G_M^p(q^2)}$ and $G_E^n(q^2)$. The comparison of the $\frac{\mu_p G_E^p(q^2)}{G_M^p(q^2)}$ (105) with new data is shown in Fig. 5

The data of Fig. 5 are taken from Refs. [1,2,3, 27, 28, 29, 30]. The Fig. 5 shows that theoretical prediction agrees with new data as $q^2 < 5 \text{ GeV}^2$ and after this value of q^2 the prediction decreases faster than the data. The value of the parameter a can be increased to fit the data with larger q^2 better. However, the larger a doesn't fit the data of the ratio in the range of smaller q^2 . This is the limitation of this model. This model doesn't work well in the region of larger q^2 . For larger q^2 many new effects, like internal motion of quarks and perturbative gluons, could play roles in these physical quantities. On the other hand, the

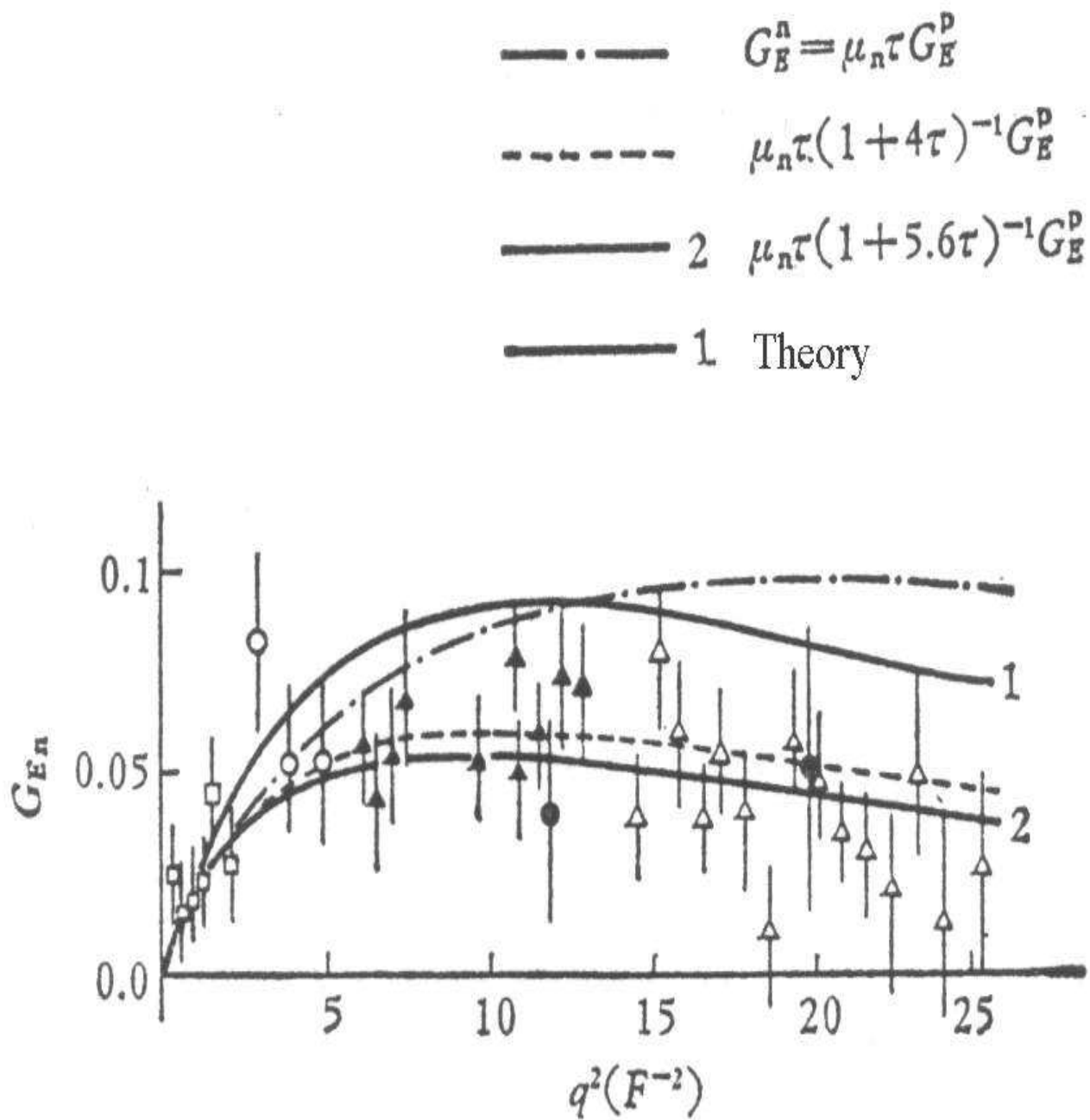


FIG. 3

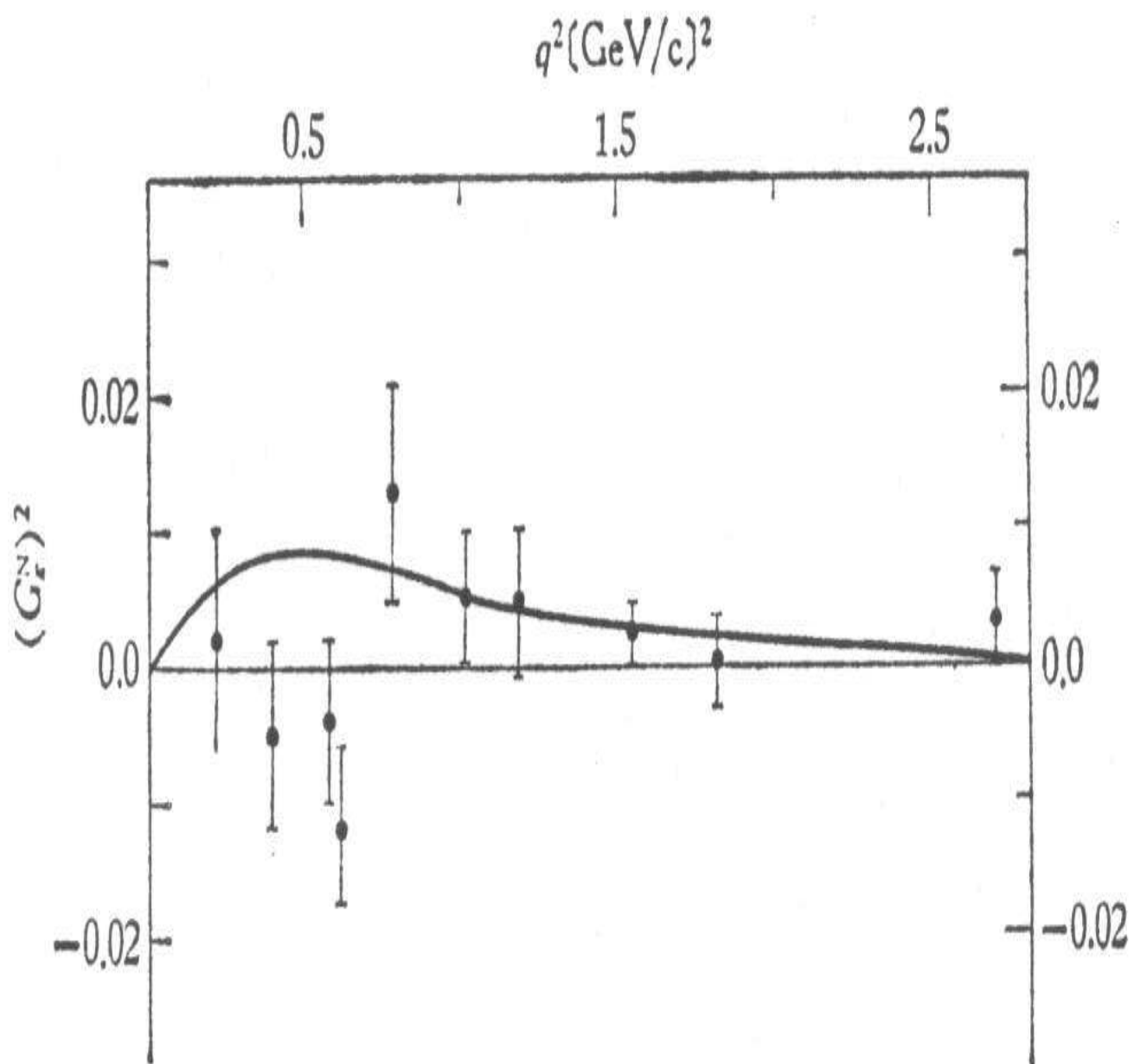
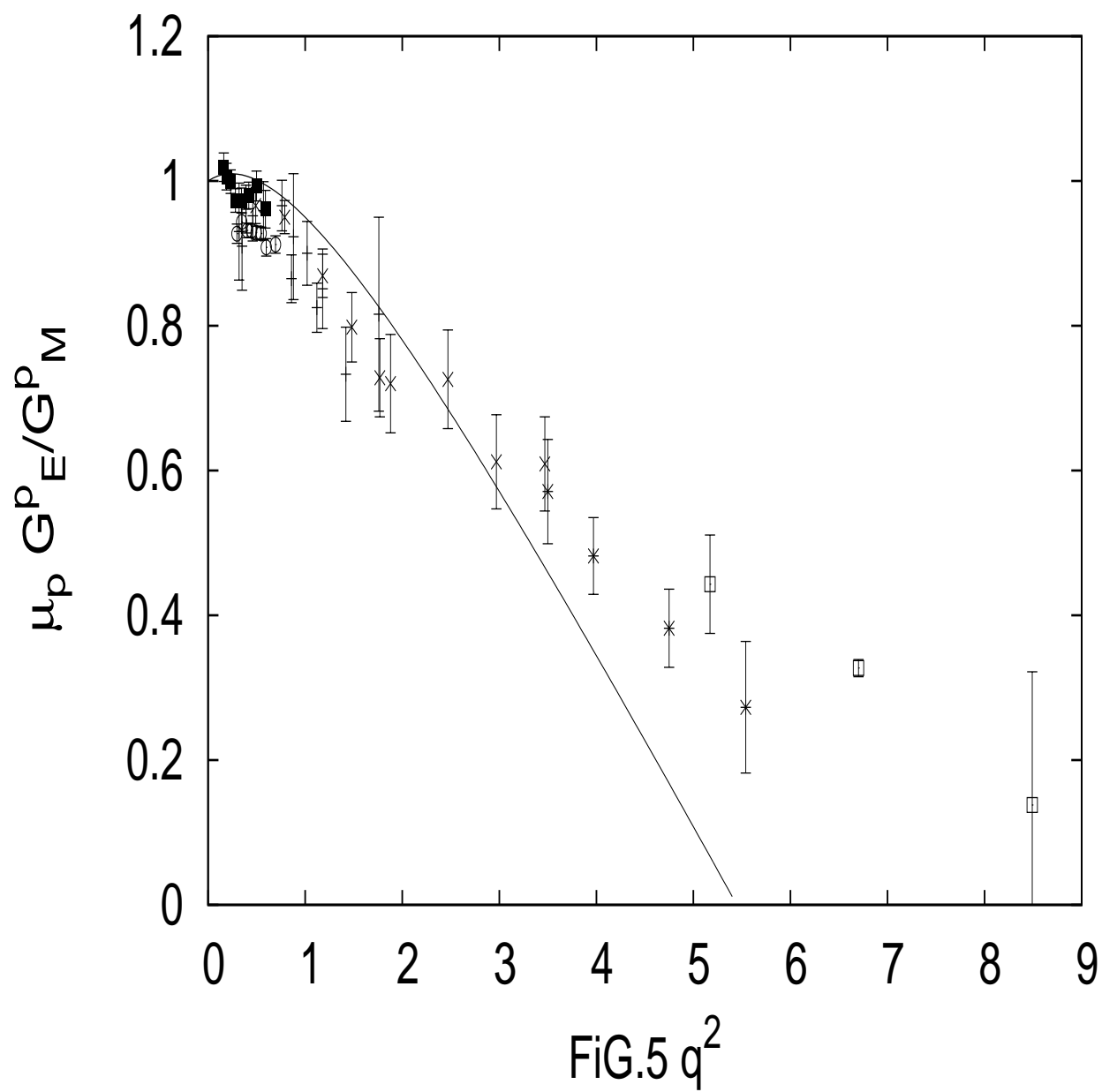


FIG. 4



study shows that the assumption (76) works in the middle range of q^2 and it may not work for larger q^2 .

Fig. 6 shows the comparison of theoretical $G_E^n(q^2)$ with new data. The data of Fig. 6 are from Refs. [32,33,34,35,36,37,38,39,40,41,42,43,44,45]. This model predicts a nonzero and small $G_E^n(q^2)$, $|G_E^n(q^2)| < 0.1$. Fig. 6 shows when $q^2 < 0.3 \text{ GeV}^2$ theory agrees with data. However, when $q^2 > 0.3 \text{ GeV}^2$ theoretical prediction is greater than data by 20% to 30%. Refs. [19,31] are review articles in which reviews of experiments and theoretical models can be found.

7.3 Magnetic moments of $\frac{1}{2}^+$ baryons

In this model the magnetic moments of the $\frac{1}{2}^+$ baryons are obtained from Eqs. (66,77,85) as

$$\mu = \frac{1}{3}(A_2 + 5A_1)\left\{\frac{m_p}{m} + \kappa\left(a + \frac{1}{a} - 1\right)\right\}. \quad (121)$$

The first term of Eq. (121) is from the recoil of the whole baryon and the second term is from the anomalous magnetic moment of quarks. Using the parameters (107), the magnetic moments of other six baryons are determined (Table I) [5]. In this table the experimental data of Ref. [46] are used. The magnetic moments of hyperons have right signs. However, μ_{Σ^+} and μ_{Σ^-} are less than data by about 40% to 50% and μ_{Ξ^0} and μ_{Ξ^-} are less than data by about 28% respectively.

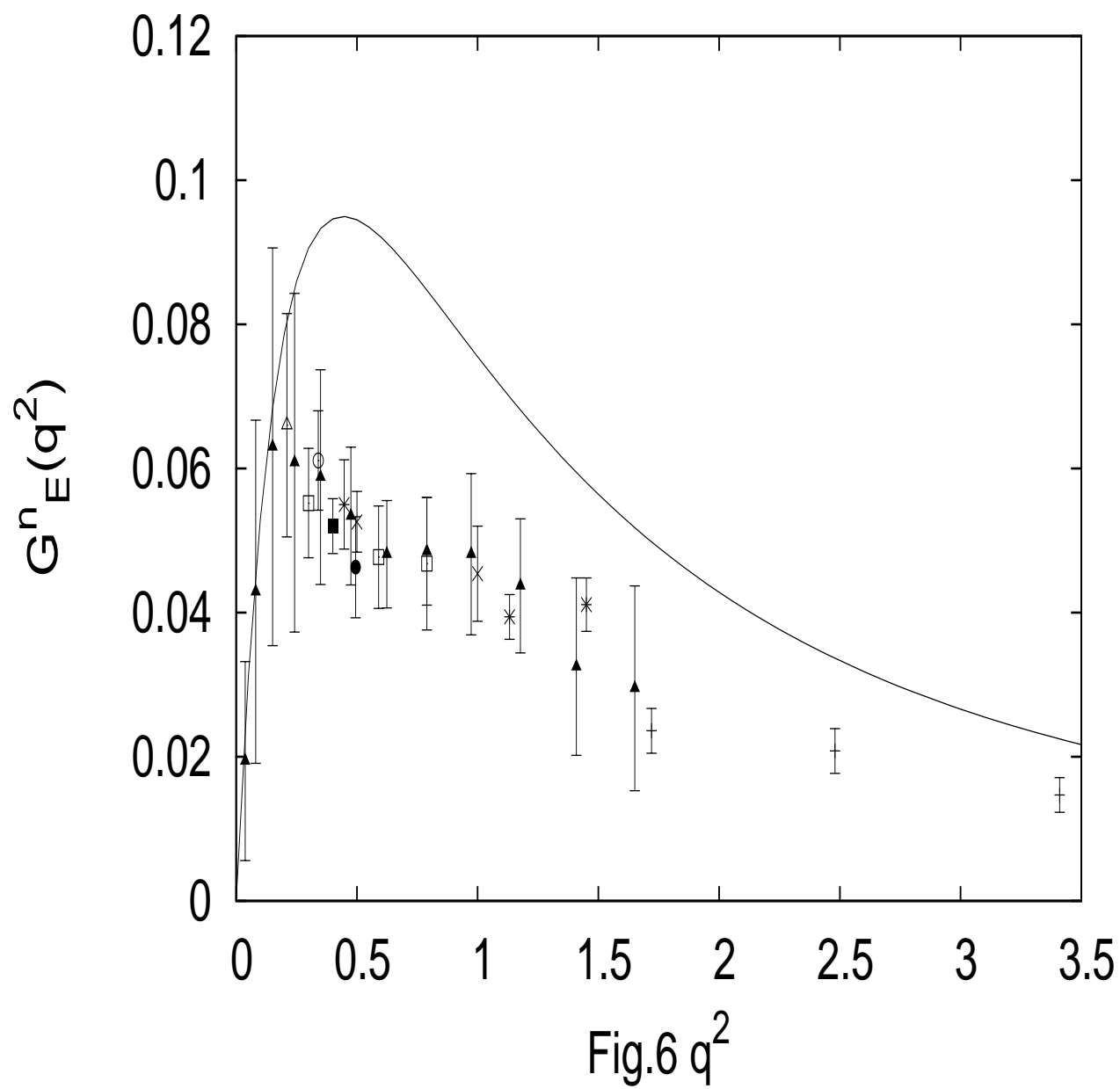


Table 1: Magnetic moments

	μ_p	μ_n	μ_Λ	μ_{Σ^+}	μ_{Σ^0}	μ_{Σ^-}	μ_{Ξ^0}	μ_{Ξ^-}
theory	2.793	-1.862	-0.64	1.74	0.58	-0.57	-0.97	-0.51
	(input)		(input)					
exp	2.793	-1.913	-0.613	2.458		-1.16	-1.250	-0.6507
		± 0.004		± 0.010		± 0.025	± 0.014	± 0.0025

The S-matrix element of $\Sigma^0 \rightarrow \Lambda + \gamma$ is studied

$$\begin{aligned}
 \langle \gamma \Lambda | S | \Sigma^0 \rangle &= -ie(2\pi)^4 \delta(p_i - p_f - q) \frac{e_\mu^\lambda}{\sqrt{2\omega}} \left(\frac{m_\Lambda}{E_\Lambda} \right)^{\frac{1}{2}} \mu_{\Sigma^0 \Lambda} \\
 &\quad \times \frac{\kappa}{2m_p} \bar{u}_{\lambda'}(p_f) q_\nu \sigma_{\nu\mu} u_\lambda(p_i),
 \end{aligned} \tag{122}$$

$$\mu_{\Sigma^0 \Lambda} = \frac{1}{2\sqrt{3}} D_3(0) \left\{ \frac{2}{a_\Lambda a_{\Sigma^0}} - \frac{1}{a_\Lambda} \left(1 - \frac{m_p}{\kappa m_\Sigma} \right) - \frac{1}{a_{\Sigma^0}} \left(1 - \frac{m_p}{\kappa m_\Lambda} \right) + \frac{m_+^2}{2m_\Lambda m_\Sigma} \right\}. \tag{123}$$

The dependencies of $D_1(0)$, $D_2(0)$, $D_1'(0)$ and $D_1'(0)$ on the mass of initial and final baryon need to be found. From Eq. (59,76)

$$\frac{D_2(0)}{D_2'(0)} = \frac{a}{a'}, \tag{124}$$

is obtained, where

$$a = \frac{1}{1 - \frac{m_0}{m_{\Sigma^0}}}, \quad a' = \frac{1}{1 - \frac{m_0}{m_\Lambda}}. \tag{125}$$

On the other hand, Eq.(59) shows if $m \longleftrightarrow m'$ is taken, we have

$$D_2(0) \longleftrightarrow D_2'(0) \quad (126)$$

and

$$D_2(0) = D_2'(0) = 1 \quad (127)$$

when $m = m'$. The general expressions of $D_2(0)$, $D_2'(0)$ which satisfy Eqs.(124,126) can be written as

$$\begin{aligned} D_2(0) &= \left(\frac{a}{a'}\right)^{\frac{1}{2}} f(m, m'), \\ D_2'(0) &= \left(\frac{a'}{a}\right)^{\frac{1}{2}} f(m, m') \end{aligned} \quad (128)$$

where $f(m, m')$ is a symmetric function of m, m' and

$$f(m, m) = 1. \quad (129)$$

When $m \neq m'$, the deviation of $f(m, m')$ from 1 is proportional to $(m - m')^2$. According to Ref. [4], $f(m, m')$ is related to the effect of Lorentz contraction. Possible expression is

$$f(m, m') = \frac{4mm'}{(m + m')^2}. \quad (130)$$

For $\Sigma^0 \rightarrow \Lambda + \gamma$, the deviation of $f(m, m')$ from 1 is only 0.1%. Therefore, for this decay the effect of $f(m, m') = 1$ is taken.

$$\begin{aligned}
D_3(0) &= \sqrt{aa'}, \\
D_1(0) &= \frac{1}{\sqrt{aa'}}.
\end{aligned} \tag{131}$$

are determined too. The magnetic moment of $\Sigma \rightarrow \Lambda$ and the decay rate are computed to be

$$\mu_{\Sigma^0\Lambda} = 1.053 \tag{132}$$

$$\begin{aligned}
\Gamma &= \frac{\alpha}{8} \mu_{\Sigma^0\Lambda}^2 \frac{m_\Sigma^3}{m_p^2} \left(1 - \frac{m_\Lambda^2}{m_\Sigma^2}\right)^3 = 3.79 \times 10^{-3} MeV, \\
\tau &= \frac{1}{\Gamma} = 1.74 \times 10^{-19} sec.
\end{aligned} \tag{133}$$

The current experimental transit magnetic moment of $\Sigma^0 \rightarrow \Lambda + \gamma$ is [46] is

$$|\mu_{\Sigma\Lambda}| = 1.61 \pm 0.08.$$

Theoretical value of this transit magnetic moment is less than data by about 50%.

The SU(6) prediction of the ratio of the magnetic moments of proton and neutron is reproduced in this model and it agrees with data well. Inputting the μ_p and μ_Λ the magnetic moments of Σ 's, Ξ 's, and $\Sigma^0 \rightarrow \Lambda$ are predicted. They have right signs, but they are smaller than data. This problem is resulted in the treatment of the flavor SU(3) symmetry breaking in this model. In the effective EM current (48) the parameter κ is taken to be same for u-, d-, and s-quark. It is possible κ_s is different from $\kappa_{u,d}$. In Eq. (49) the scalar function

$M(x'_1, x'_2, x_1, x_2)$ is assumed to be the same for all three quarks. How to treat the flavor SU(3) symmetry breaking is the key for the improvement of the magnetic moments of hyperons. The study is beyond the scope of this paper.

More discussion about the magnetic moments of baryons

It is known that the effect of isospin symmetry breaking is small. The agreement between Eq. (87) and data is a good example. We can check more relationships between the magnetic moments within the same isospin multiple.

This model predicts that both the magnetic moments of Ξ^- and Ξ^0 (121) are negative and

$$\mu_{\Xi^0} = 2\mu_{\Xi^-} \quad (134)$$

which agrees with data well. It predicts that μ_{Σ^+} is positive and μ_{Σ^-} is negative. These predictions agree with data. However, under isospin symmetry

$$\mu_{\Sigma^-} = -\frac{1}{3}\mu_{\Sigma^+} \quad (135)$$

is predicted. However, this prediction (135) is different from data by about 30% which is much larger than the effect of isospin breaking. In the limit of SU(3) symmetry this model predicts (121)

$$\mu_{\Sigma^+} = \mu_p. \quad (136)$$

The difference between the prediction (136) and the data [46] by an reasonable 12%. The

key point is how to understand the large μ_{Σ^-} . On the other hand, in the limit of isospin symmetry this model predicts

$$\mu_{\Sigma^0} = \frac{1}{3}\mu_{\Sigma^+}. \quad (137)$$

So far, there is no data to test Eq. (137). Finally, it is interesting to point out that the effect of the recoil of the whole baryon plays an important rule in the magnetic moments of baryons. As shown above, this model works well on EM form factors of nucleon (two flavors). However, when s-quark is involved theoretical results of the magnetic moments of hyperons have more than 30% deviation from the data. How to improve the involvement of the effects of SU(3) symmetry breaking is an important task for this model.

7.4 Electric and magnetic radii of nucleon

From Eqs. (101,102) the difference of the charge and the magnetic radii of the proton is predicted as

$$(r_M^p)^2 - (r_E^p)^2 = \frac{3}{2m_p^2} \left\{ a + 1 - \mu_p - \frac{a}{\mu_p}(1 + \kappa) \right\}. \quad (138)$$

Using the values of the parameter a and κ (107),

$$(r_M^p)^2 - (r_E^p)^2 = 0.0215 fm^2 \quad (139)$$

is obtained. This value is very sensitive to the value of the parameter a . This model predicts that both radii are pretty close to each other. Eq. (139) shows that this model predicts that

the r_M^p is little bit greater than the r_E^p . The experimental data of the r_M^p can be found in Refs. [16,17,18]. In review article [47] $r_E^p = 0.8775 \pm 0.0051$ fm is listed. Many more data on r_M^p can be found in Ref. [46].

7.5 Electromagnetic form factors of hyperons

It is useful to list the EM form factors of hyperons. Both the charge and magnetic form factors of the Σ^+ are obtained from Eqs. (64,65) respectively

$$G_E^{\Sigma^+}(q^2) = D_2(q^2) + \tau\{D_3(q^2) + \kappa\frac{m_{\Sigma^+}}{m_p}[D_2(q^2) - D_1(q^2) - (1 + \tau)D_3(q^2)]\}, \quad (140)$$

$$G_M^{\Sigma^+}(q^2) = \frac{m_p}{m_{\Sigma^+}}\{D_2(q^2) + \tau D_3(q^2)\} + \kappa\{D_1(q^2) - D_2(q^2) + (1 + \tau)D_3(q^2)\}. \quad (141)$$

The functions $D_{1,2,3}$ depend on the mass of the Σ^+ . $D_2(0) = 1$ leads to $G_E^{\Sigma^+}(0) = 1$.

The charge and the magnetic forms of the Σ^- are derived from Eqs. (64,65) as

$$G_E^{\Sigma^-}(q^2) = -D_2(q^2) - \frac{1}{3}\tau\{2D_2(q^2) + D_3(q^2) + \kappa\frac{m_{\Sigma^-}}{m_p}[D_2(q^2) - D_1(q^2) - 3(1 + \tau)D_3(q^2)]\} \quad (142)$$

$$G_M^{\Sigma^-}(q^2) = -\frac{1}{3}\{\frac{m_p}{m_{\Sigma^-}}D_2(q^2) + \tau D_3(q^2) + \kappa[D_1(q^2) - D_2(q^2) + (1 + \tau)D_3(q^2)]\} \quad (143)$$

Eq. (142) shows that the charge of the Σ^- is -1.

From Eqs. (64,65) the EM form factors of Σ^0 and Λ are found

$$G_E^{\Sigma^0}(q^2) = \frac{1}{3}\tau\{D_3(q^2) - D_2(q^2) + \kappa\frac{m_{\Sigma^0}}{m_p}[D_2(q^2) - D_1(q^2)]\}, \quad (144)$$

$$G_M^{\Sigma^0}(q^2) = \frac{1}{3}\{\frac{m_p}{m_{\Sigma^0}}(D_2(q^2) + \tau D_3(q^2)) + \kappa[D_1(q^2) - D_2(q^2) + (1 + \tau)D_3(q^2)]\}, \quad (145)$$

$$G_E^\Lambda(q^2) = \frac{1}{3}\tau\{D_2(q^2) - D_3(q^2) + \kappa\frac{m_{\Sigma^0}}{m_p}[D_2(q^2) - D_1(q^2)]\}, \quad (146)$$

$$G_M^\Lambda(q^2) = -\frac{1}{3}\{\frac{m_p}{m_\Lambda}(D_2(q^2) + \tau D_3(q^2)) + \kappa[D_1(q^2) - D_2(q^2) + (1 + \tau)D_3(q^2)]\}. \quad (147)$$

Eqs. (144,146) show that $G_E^{\Sigma^0}(0) = 0$, $G_E^\Lambda(0) = 0$. If ignoring the mass difference between the Σ^0 and the Λ , this model presents

$$G_M^{\Sigma^0}(q^2) = -G_M^\Lambda(q^2),$$

$$\mu_{\Sigma^0} = -\mu_\Lambda. \quad (148)$$

The EM form factors of the Ξ^0 and the Ξ^- are obtained

$$G_E^{\Xi^0}(q^2) = \frac{2}{3}\tau\{D_2(q^2) - D_3(q^2) + \kappa\frac{m_{\Xi^0}}{m_p}[D_1(q^2) - D_2(q^2)]\}, \quad (149)$$

$$G_M^{\Xi^0}(q^2) = -\frac{2}{3}\{\frac{m_p}{m_{\Xi^0}}(D_2(q^2) + \tau D_3(q^2)) + \kappa[D_1(q^2) - D_2(q^2) + (1 + \tau)D_3(q^2)]\}, \quad (150)$$

$$G_E^{\Xi^-}(q^2) = -D_2(q^2) - \frac{1}{3}\tau\{2D_2(q^2)D_3(q^2) + \kappa\frac{m_{\Xi^-}}{m_p}[D_1(q^2) - D_2(q^2) - (1 + \tau)D_3(q^2)]\}, \quad (151)$$

$$G_M^{\Xi^-}(q^2) = -\frac{1}{3}\{\frac{m_p}{m_{\Xi^0}}(D_2(q^2) + \tau D_3(q^2)) + \kappa[D_1(q^2) - D_2(q^2) + (1 + \tau)D_3(q^2)]\}. \quad (152)$$

Eqs. (149, 151) show that $G_E^{\Xi^0}(0) = 0$ and $G_E^{\Xi^-}(0) = -1$. Ignoring the mass difference between Ξ^0 and Ξ^- , this model predicts

$$G_M^{\Xi^-}(q^2) = \frac{1}{2}G_M^{\Xi^0}(q^2). \quad (153)$$

8 EM transition of $p \rightarrow \Delta(1236)$

The electromagnetic transition of $p \rightarrow \Delta(1236)$ has been studied by this model [5] and there is no any new parameter. Using the wave functions of proton and Δ (33,34) and the effective current (48), the matrix elements of EM currents of $p \rightarrow \Delta(1236)$ are obtained

$$\begin{aligned}
\langle B_{\lambda'}^{\frac{3}{2}}(p_f)^{lmn} | J_{\mu}(0) | B_{\lambda}^{\frac{1}{2}}(p_i)_{l'_1}^{l'_1} \rangle = & ied_{l_1jk}^{lmn} \varepsilon_{jk'l'_1} Q_{kk'} \{ 2D_2(q^2) + \kappa [\frac{m_+}{m_p} D_3(q^2) + 2\frac{m}{m_p} D_1(q^2) \\
& - \frac{m}{m_p} D_2(q^2) - \frac{m}{m_p} D'_2(q^2)] \} \frac{1}{mm'} p_{\rho} q_{\sigma} \varepsilon_{\rho\sigma\nu\mu} \bar{\psi}_{\nu}^{\lambda'}(p') u_{\lambda}(p) \\
& + ied_{l_1jk}^{lmn} \varepsilon_{jk'l'_1} Q_{kk'} \{ D_3(q^2) - D_2(q^2) + \frac{\kappa m}{2m_p} [D_2(q^2) + D'_2(q^2) - 2D_1(q^2)] \} \\
& \frac{1}{mm'} (p'_{\mu} q_{\nu} - p' \cdot q \delta_{\mu\nu}) \bar{\psi}_{\nu}^{\lambda'}(p') \gamma_5 u_{\lambda}(p) \\
& + ied_{l_1jk}^{lmn} \varepsilon_{jk'l'_1} Q_{kk'} \{ D'_2(q^2) - \frac{m'}{m} D_2(q^2) + \frac{m_-}{m} D_3(q^2) \} \bar{\psi}_{\mu}^{\lambda'}(p') \gamma_5 u_{\lambda}(p) \quad (154)
\end{aligned}$$

m, m' are the mass of $\frac{1}{2}^+$ baryon and $\frac{3}{2}^+$ baryon respectively and $m_- = m' - m$,

$$P_{\mu} = p_{\mu} + p'_{\mu}.$$

It is interesting to notice that the last term of Eq. (154) violates the current conservation.

However, this term is proportional to

$$D'_2(q^2) - \frac{m'}{m} D_2(q^2) + \frac{m_-}{m} D_3(q^2).$$

According to Eq. (62) it is equal to zero, the current conservation of $p \rightarrow \Delta(1236)$ (154)

is guaranteed by the same condition (62) which guarantees the current conservation for the EM transition matrix elements of $B \rightarrow B$.

8.1 Photoproduction of Δ resonance

The Photoproduction of Δ resonance is related to the transit matrix element (154)

$$\begin{aligned}
& \langle \Delta_{\lambda'}^+(p_f) | J_\mu(0) | p_\lambda(p_i) \rangle = -\frac{ie}{4\sqrt{3}} A \frac{1}{mm'} D_3(q^2) p_{i\rho} q_\sigma \\
& \times \varepsilon_{\rho\sigma\nu\mu} \bar{\psi}_\nu^{\lambda'}(p_f) u_\lambda(p_i) - \frac{ie}{\sqrt{3}} \frac{B}{mm'} D_3(q^2) \\
& \times (p_{f\mu} q_\nu - p_f \cdot q \delta_{\mu\nu}) \bar{\psi}_\nu^{\lambda'}(p_f) \gamma_5 u_\lambda(p_i),
\end{aligned} \tag{155}$$

where

$$\begin{aligned}
A &= \frac{2}{a'} + \kappa \left\{ 1 + \frac{m'}{m_p} + \frac{2}{aa'} - \frac{1}{a} - \frac{1}{a'} \right\}, \\
B &= 1 - \frac{1}{a'} + \frac{\kappa}{2} \left\{ \frac{1}{a} + \frac{1}{a'} - \frac{2}{aa'} \right\},
\end{aligned} \tag{156}$$

m' is the mass of the Δ , and

$$a = \frac{1}{1 - \frac{m_0}{m_p}}, \quad a' = \frac{1}{1 - \frac{m_0}{m_\Delta}} \tag{157}$$

$$A = 1.717, \quad B = 0.699. \tag{158}$$

It is interesting to notice that the condition (62) has been taken into account in Eq. (155)

and the current conservation is satisfied. Eq. (156) shows that $B = 0$ is obtained when

taking $a = a' = 1$. Therefore, the term B in Eq. (155) is directly related to the contribution

of antiquark components. For the $\Delta^+ \rightarrow p + \gamma$ there are both $M1_+$ and $E1_+$ amplitudes.

The S matrix element of $\gamma p \rightarrow \Delta^+ \rightarrow \pi N$ is written as

$$\langle \pi N | S | \gamma p \rangle = -i(2\pi)^4 \delta(p_\gamma + p_i - p_\pi - p_N) \sum_{\lambda'} \langle \pi N | T | \Delta_{\lambda'}^+(p_f) \rangle$$

$$\times < \Delta_{\lambda'}^+(p_f) | T | \gamma p > \frac{E_\Delta}{m_\Delta} \frac{1}{W - m_\Delta + \frac{i}{2}\Gamma(W)}, \quad (159)$$

where W is the mass of the final state, $\Gamma(W)$ is the total width of the strong decay of $\Delta(1236)$. The calculation is done in the rest frame of $\Delta(1236)$. $< \pi N | T | \Delta_{\lambda'}^+(p_f) >$ is the amplitude of the strong decay of $\Delta(1236)$

$$< \pi N | T | \Delta_{\lambda'}^+(p_f) > = g(W) \frac{p_{\pi\mu}}{m_N} \bar{u}(p_N) \psi_\mu^{\lambda'}. \quad (160)$$

The electric transition amplitude in Eq.(159) is expressed as

$$< \Delta_{\lambda'} | T | \gamma p > = -e_\mu < \Delta_{\lambda'} | J_\mu(0) | p >. \quad (161)$$

By using following equation

$$\sum_{\lambda'} \psi_\mu^{\lambda'} \bar{\psi}_{\mu'}^{\lambda'} = \frac{1}{3} (1 + \gamma_0) \{ \delta_{\mu\mu'} + \frac{1}{2} \gamma_5 \gamma_j \varepsilon_{j\mu\mu'} \} \quad (162)$$

where $j, \mu, \mu' = 1, 2, 3$. Using Eq.(155), it is obtained

$$\begin{aligned} \sum_{\lambda'} \bar{u}_\gamma(p_N) \psi_\mu^{\lambda'} &< \Delta_{\lambda'} | J_\nu(0) | p_\lambda > p_{\pi\mu} e_\nu \\ &= \frac{e D_3(0)}{24 \sqrt{3} m_N^2 m_\Delta} \left\{ \frac{m_N(m_N + E_N)}{E_i(m_N + E_i)} \right\}^{\frac{1}{2}} \bar{u}_\gamma \{ [A(m_N + m_\Delta)^2 + B(m_\Delta^2 - m_N^2)] \\ &\quad \times [2\mathbf{k} \cdot (\mathbf{e} \cdot \mathbf{p}_\pi) + i\sigma \cdot \mathbf{e} \mathbf{p}_\pi \cdot \mathbf{k} - i\sigma \cdot \mathbf{k} \mathbf{p}_\pi \cdot \mathbf{e}] \\ &\quad - 3iB(m_\Delta^2 - m_N^2)(\sigma \cdot \mathbf{e} \mathbf{p}_\pi \cdot \mathbf{k} + \sigma \cdot \mathbf{k} \mathbf{p}_\pi \cdot \mathbf{e}) \} u_\lambda, \end{aligned} \quad (163)$$

where E_i is the energy of the initial proton, k is the energy of the photon, and $D_3(0)$ is given by Eq. (131). The amplitudes of the magnetic and electric transitions are obtained by

comparing with the photo production amplitudes in Ref. [48]

$$\begin{aligned}
M1+ &= \frac{eD_3(0)}{96\sqrt{3}\pi m_N^2 m_\Delta} \left\{ \frac{m_N + E_N}{m_\Delta E_i(m + E_i)} \right\}^{\frac{1}{2}} \frac{g(W)p_\pi k}{W - m_\Delta + \frac{i}{2}\Gamma(W)} \\
&\times \{A(m_N + m_\Delta)^2 + B(m_\Delta^2 - m_N^2)\}, \tag{164}
\end{aligned}$$

$$\begin{aligned}
E1+ &= -\frac{eD_3(0)}{96\sqrt{3}\pi m_N^2 m_\Delta} \left\{ \frac{m_N + E_N}{m_\Delta E_i(m + E_i)} \right\}^{\frac{1}{2}} \frac{g(W)p_\pi k}{W - m_\Delta + \frac{i}{2}\Gamma(W)} \\
&\times B(m_\Delta^2 - m_N^2), \tag{165}
\end{aligned}$$

where W is the total energy of the photon and the proton in the frame of center of mass and $g(W)$ is the amplitude of $\Delta \rightarrow \pi + N$, p_π and k are the momenta of the pion and the photon respectively. This model predicts a nonzero amplitude of electric quadrupole $E1+$. Inputting $\Gamma = 0.12\text{GeV}$ at $W = m_\Delta$, $g = 1.66$ is determined. The $M1+$ amplitude at $W = m_\Delta$ is calculated to be

$$M1+ = 47.3 \times 10^{-3}/m_{\pi+}.$$

In Ref. [49] the $\gamma^*p \rightarrow \Delta$ reaction at low q^2 is measured. At $q^2 = 0.06 \text{ GeV}^2$ the average value of the $M1+$ amplitude

$$M1+ = 40.33 \pm 0.27 \pm 0.57 \pm 0.61 \cdot 10^{-3}/m_{\pi+}$$

is presented. Many effective theories [50] are used to fit the data. The theoretical result presented above [5] is at $q^2 = 0 \text{ GeV}^2$. In order to compare with the data at $q^2 = 0.06 \text{ GeV}^2$ [49] the correction by the form factor $D_3(q^2) = \sqrt{aa'}D_2(q^2)$ (112) has to be taken into

account. The correction is 0.82. Therefore, this model [5] predicts

$$M1+ = 38.810^{-3}/m_{\pi^+}$$

at the $q^2 = 0.06 \text{ GeV}^2$. This value is in agreement with the average value of Ref. [49] within the errors. No new parameter is taken in this prediction.

As mentioned above in the rest frame the wave functions of nucleon and Δ resonance are in s-wave only. Eq. (165) shows that

$$E1+ \propto B, \text{ and } E1+ \propto m_{\Delta}^2 - m_N^2.$$

Nonzero B comes from the effects of antiquarks and $m_{\Delta}^2 - m_N^2$ is resulted in the effect of recoil or the effect of Lorentz contraction in the moving frame. The Lorentz contraction makes that the nucleon or Δ in moving frame contain components of many partial waves. Nonzero $E1+$ predicted in this model is resulted in both the antiquark components and the recoil effects. It is interesting to notice that in the rest frame both the proton and the Δ are spherical. This model provides a new mechanism for the $E1+$ amplitude in the process $\Delta \rightarrow p + \gamma$.

At the peak $W = m_{\Delta}$

$$\frac{E1+}{M1+} = \frac{-B(m_{\Delta} - m_N)}{A(m_{\Delta} + m_N) + B(m_{\Delta} - m_N)} = -5.4 \%. \quad (166)$$

In the paper [5] following early data of this ratio are quoted

-0.045 [51], -0.073 [52], -0.024 [53].

In Ref. [46] the newer estimated value of this ratio is presented as

$$-0.025 \pm 0.005$$

for the process $\Delta \rightarrow N + \gamma$. However, the absolute value of the ratio $\frac{E1+}{M1+}$ at the pole is determined as

$$0.065 \pm 0.007 [54], \text{ and } 0.058 [55].$$

This model predicts a negative and small $\frac{E1+}{M1+}$ at the pole by this mechanism.

8.2 $\Delta \rightarrow N + \gamma$ decay

Using Eq. (155), the width of the $\Delta^+(1236) \rightarrow p + \gamma$ is derived

$$\Gamma_\gamma = \frac{k^2 m_N}{2\pi m_\Delta} \{ |A_{\frac{3}{2}}|^2 + |A_{\frac{1}{2}}|^2 \}, \quad (167)$$

$$\begin{aligned} A_{\frac{3}{2}} &= -\frac{eD_3(0)(m_\Delta + m_N)(m_\Delta^2 - m_N^2)}{8\sqrt{6}(m_N m_\Delta)^{3/2}} \left\{ A + 2B \frac{m_\Delta - m_N}{m_\Delta + m_N} \right\} \\ &= -0.21 \text{ GeV}^{-\frac{1}{2}}, \\ A_{\frac{1}{2}} &= -\frac{eD_3(0)(m_\Delta + m_N)(m_\Delta^2 - m_N^2)}{24\sqrt{2}(m_N m_\Delta)^{3/2}} \left\{ A - 2B \frac{m_\Delta - m_N}{m_\Delta + m_N} \right\} \\ &= -0.10 \text{ GeV}^{-\frac{1}{2}}. \end{aligned} \quad (168)$$

The experimental data are [54]

$$A_{\frac{3}{2}} = -0.24 \text{ GeV}^{-\frac{1}{2}}, \quad A_{\frac{1}{2}} = -0.14 \text{ GeV}^{-\frac{1}{2}}. \quad (169)$$

The new data are [46]

$$A_{\frac{3}{2}} = -0.250 \pm 0.008 \text{ GeV}^{-\frac{1}{2}}, \quad A_{\frac{1}{2}} = -0.135 \pm 0.006 \text{ GeV}^{-\frac{1}{2}}. \quad (170)$$

The decay width is computed to be

$$\Gamma_{\Delta \rightarrow N\gamma} = 0.64 \text{ MeV}, \quad (171)$$

The experimental data [56] is 0.65 MeV. The new data [46] is (0.63 - 0.78) MeV. Theoretical results agree with data pretty well.

8.3 The electromagnetic form factors of $p \rightarrow \Delta^+(1236)$

The differential cross section of the

$$e + p \rightarrow e + \Delta^+(1236)$$

$$\hookrightarrow N + \pi$$

is expressed as

$$\frac{1}{\Gamma_t} \frac{d^2\sigma}{d\Omega dE'} = \sigma_T + \varepsilon\sigma_S. \quad (172)$$

where E' is the energy of the outgoing electron, σ_T and σ_S are the cross sections of the transverse and longitudinal photons respectively, and ε is the polarization parameter. Using of the Eq. (155) and the equation

$$\sum_{\lambda} \psi_{\mu}^{\lambda}(p) \bar{\psi}_{\mu'}^{\lambda}(p) = \frac{1}{2} \left(1 - \frac{i}{m'} \hat{p}\right) \{ \delta_{\mu\mu'} + \frac{2}{3} \frac{p_{\mu} p_{\mu'}}{m'^2} - \frac{1}{3} \gamma_{\mu} \gamma_{\mu'} \}$$

$$-\frac{i}{3m'}(p_\mu\gamma_{\mu'} - p_{\mu'}\gamma_\mu)\}, \quad (173)$$

it is obtained

$$\begin{aligned} \sigma_T = & \frac{m\alpha q^{*2}}{m_\Delta(W^2 - m^2)} \frac{\Gamma(W)}{(W - m_\Delta)^2 + \frac{1}{4}\Gamma^2(W)} \frac{D_3^2(q^2)}{18m^2} \{A^2(q^2 + m_+^2) \\ & + 2AB(m_\Delta^2 - m^2 - q^2) + 4B^2(q^2 + m_-^2)(1 - \frac{q^2}{q^{*2}})\}, \end{aligned} \quad (174)$$

$$\sigma_S = \frac{m\alpha q^{*2}}{m_\Delta(W^2 - m^2)} \frac{\Gamma(W)}{(W - m_\Delta)^2 + \frac{1}{4}\Gamma^2(W)} \frac{2D_3^2(q^2)}{9m^2} B^2(q^2 + m_+^2) \frac{q^2}{q^{*2}}, \quad (175)$$

where

$$W^2 = -(p_i + p_e - p_{e'})^2, \quad q^{*2} = q^2 + \frac{1}{4m_\Delta^2}(m_\Delta^2 - m^2 - q^2)^2, \quad (176)$$

p_i is the momentum of the proton, m is the mass of nucleon, and $m_+ = m_\Delta + m$, and $m_- = m_\Delta - m$. a Eq. (175) shows that the cross section of the longitudinal photon $\sigma_S \propto B^2$ and B is originated in the effect of antiquark components of the proton and the Δ . Therefore, the cross section σ_S is the consequence of the antiquark components in this model. The ratio of σ_S and σ_T is obtained

$$\begin{aligned} R = \frac{\sigma_S}{\sigma_T} = & 4B^2(q^2 + m_-^2) \frac{q^2}{q^{*2}} / \{(Am_+ + Bm_-)^2 \\ & + (A - B)^2 q^2 + 3B^2(q^2 + m^2) - 4B^2(q^2 + m_-^2) \frac{q^2}{q^{*2}}\}. \end{aligned} \quad (177)$$

The behavior of R is expressed as

$$\begin{aligned} q^2 &= 0, \quad R = 0; \\ q^2 &\rightarrow \infty, \quad R \sim \frac{1}{q^2} \rightarrow 0. \end{aligned} \quad (178)$$

In the range of $q^2 > 3 \text{ GeV}^2$, $R \sim 0.27$.

According to the definition of multiples [57], the magnetic transition form factor $G_{M1+}^2(q^2)$, the electric quadrupole transition form factor $G_{E1+}^2(q^2)$ and the Coulomb transition form factor $G_{S1+}^2(q^2)$ are found

$$G_{M1+}^2(q^2) = \frac{D_3^2(q^2)}{18m^2} \{ (Am_+ + Bm_-)^2 + (A - B)^2 q^2 - B^2(q^2 + m_-^2) \frac{q^2}{q^{*2}} \}, \quad (179)$$

$$G_{E1+}^2(q^2) = \frac{D_3^2(q^2)}{18m^2} B^2(q^2 + m_-^2) \left(1 - \frac{q^2}{q^{*2}}\right), \quad (180)$$

$$G_{S1+}^2(q^2) = \frac{D_3^2(q^2)}{18m^2} B^2(q^2 + m_-^2). \quad (181)$$

Eqs. (179-181) show that besides the magnetic form factor $G_{M1+}(q^2)$ this model predicts nonzero $E1+$, $S1+$ form factors $G_{E1+}(q^2)$ and $G_{S1+}(q^2)$. There is a relationship between $G_{E1+}(q^2)$ and $G_{S1+}(q^2)$

$$G_{E1+}^2(q^2) = \left(1 - \frac{q^2}{q^{*2}}\right) G_{S1+}^2(q^2).$$

Both the $G_{E1+}(q^2)$ and the $G_{S1+}(q^2)$ are proportional to B . Therefore, these two form factors are from the contributions of the antiquark components of the nucleon.

The differential cross section (172) is expressed as

$$\begin{aligned} \frac{1}{\Gamma_t} \frac{d^2\sigma}{dE' d\Omega} &= \frac{m\alpha q^{*2}}{m'(W^2 - m^2)} \{ G_{M1+}^2(q^2) + 3G_{E1+}^2(q^2) \\ &\quad + 4\epsilon G_{S1+}^2(q^2) \frac{q^2}{q^{*2}} \} \frac{\Gamma(W)}{(W - m')^2 + \frac{1}{4}\Gamma^2(W)}. \end{aligned} \quad (182)$$

From Eq.(179), the transit magnetic moment of $p \rightarrow \Delta^+(1236)$ is derived

$$\mu_{p \rightarrow \Delta} = G_{M1+}(0) = \frac{D_3(0)}{3\sqrt{2}m} (Am_+ + Bm_-) = 1.23 \frac{2\sqrt{2}}{3} \mu_p. \quad (183)$$

The data are

$$1.22\frac{2\sqrt{2}}{3}\mu_p^{[53]}, \quad 1.28\frac{2\sqrt{2}}{3}\mu_p^{[56]}. \quad (184)$$

Taking $a = a' = 1$ and $m = m'$ in Eq. (183), the prediction of SU(6), $\mu_{p \rightarrow \Delta} = \frac{2\sqrt{2}}{3}\mu_p$, is revealed. The correction factor 1.23 in Eq. (183) is from the effects of recoil and antiquarks in this model. Theory agrees with the data.

The expression

$$\sigma_T^R = \frac{m\alpha q^{*2}}{m'(W^2 - m^2)} \frac{\Gamma(W)}{(W - m')^2 + \frac{1}{4}\Gamma^2(W)} G_M^{*2}(q^2) \quad (185)$$

has been used to determine $G_M^{*2}(q^2)$. G_M^* is obtained from Eq.(174) that

$$\begin{aligned} G_M^{*2}(q^2) &= G_{M1+}^2(q^2) + 3G_{E1+}^2(q^2) \\ &= \frac{D_3^2(q^2)}{18m^2} \{ (Am_+ + Bm_-)^2 + (A - B)^2 q^2 + B^2(q^2 + m_-^2)(3 - 4\frac{q^2}{q^{*2}}) \}. \end{aligned} \quad (186)$$

The $D_3(q^2)$ for $p \rightarrow \Delta^+(1236)$ is expressed as

$$D_3(q^2) = \frac{4mm'\sqrt{aa'}}{(m + m')^2} (1 + 2.39\frac{q^2}{4m^2})^{-1} (1 + \frac{q^2}{0.71})^{-2}. \quad (187)$$

The $G_{M1+}^2(q^2)$ form factor dominates the $G_M^{*2}(q^2)$. Eq. (186) shows that

$$G_M^*(q^2) \propto D_3(q^2)$$

and $D_3(q^2)$ has triple poles. Therefore, this model predicts the form factor $G_M^*(q^2)$ decreases with q^2 faster than the $G_M^p(q^2)$ which is in form of dipole. Comparisons with experimental data are shown in Fig.7 and Fig.8 (a).

The data for Fig.7 comes from Ref.[26] and that for Fig.8 are from Ref.[61].

These two figures show that:

- 1) this model predicts that $G_M^*(q^2)$ decreases faster than $G_D(q^2)$ or $G_M^p(q^2)$;
- 2) theoretical prediction of $G_M^*(q^2)$ agrees with data in the region of low q^2 ;
- 3) in the larger region theoretical $G_M^*(q^2)$ decreases faster than data.

There are new measurements of the form factor $G_M^*(q^2)$ [63,64,65] in the region of larger q^2 . These new data show that the $G_M^*(q^2)$ indeed decreases faster than $G_M^p(q^2)$ ($\sim \mu_p G_D(q^2)$). However, theoretical prediction of $G_M^*(q^2)$ decreases faster than these new data too. SU(6) symmetry breaking is the possible reason. As shown in the transit magnetic moment (183) the effect of SU(6) symmetry breaking by the mass difference of nucleon and Δ is about 23%. Therefore, in order to improve the behavior of the $G_M^*(q^2)$ in the region of larger q^2 the effects of SU(6) symmetry breaking must be taken into account. In the expression of the $D_3(q^2)$ (187) the factor

$$1/(1 + 2.39q^2/(4m_p^2))/(1 + q^2/0.71)^2$$

is determined from the magnetic form factor of the proton. The $G_M^p(q^2)$ the quantity with dimension of *mass* is proportional to m_p . Based on SU(6) symmetry Eq. (187) has been applied to the magnetic form factor $G_{M1+}(q^2)$. In order to include the effect of the SU(6) symmetry breaking it is natural to include m_Δ in this factor of Eq. (187). In this paper

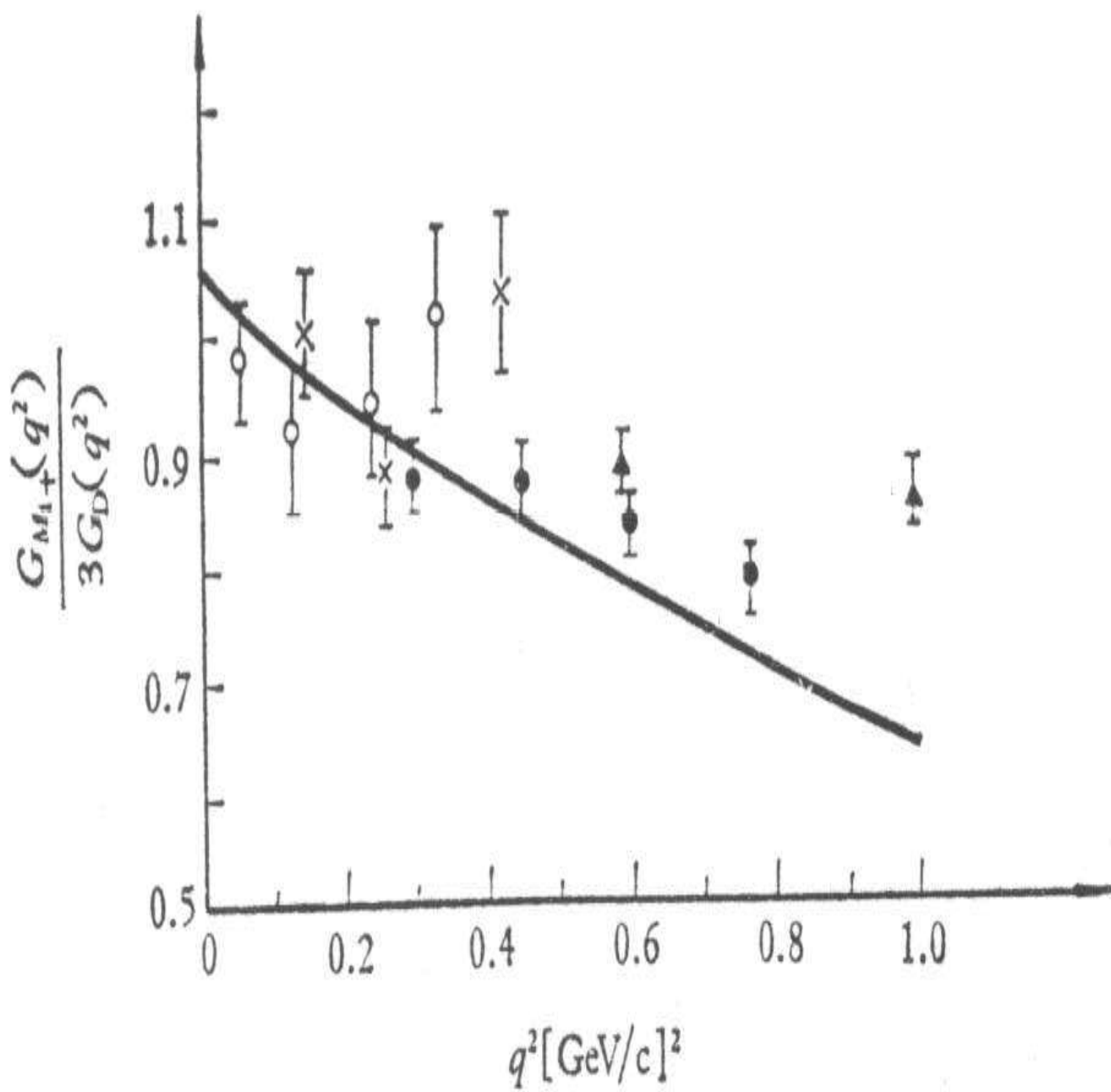


Fig. 7

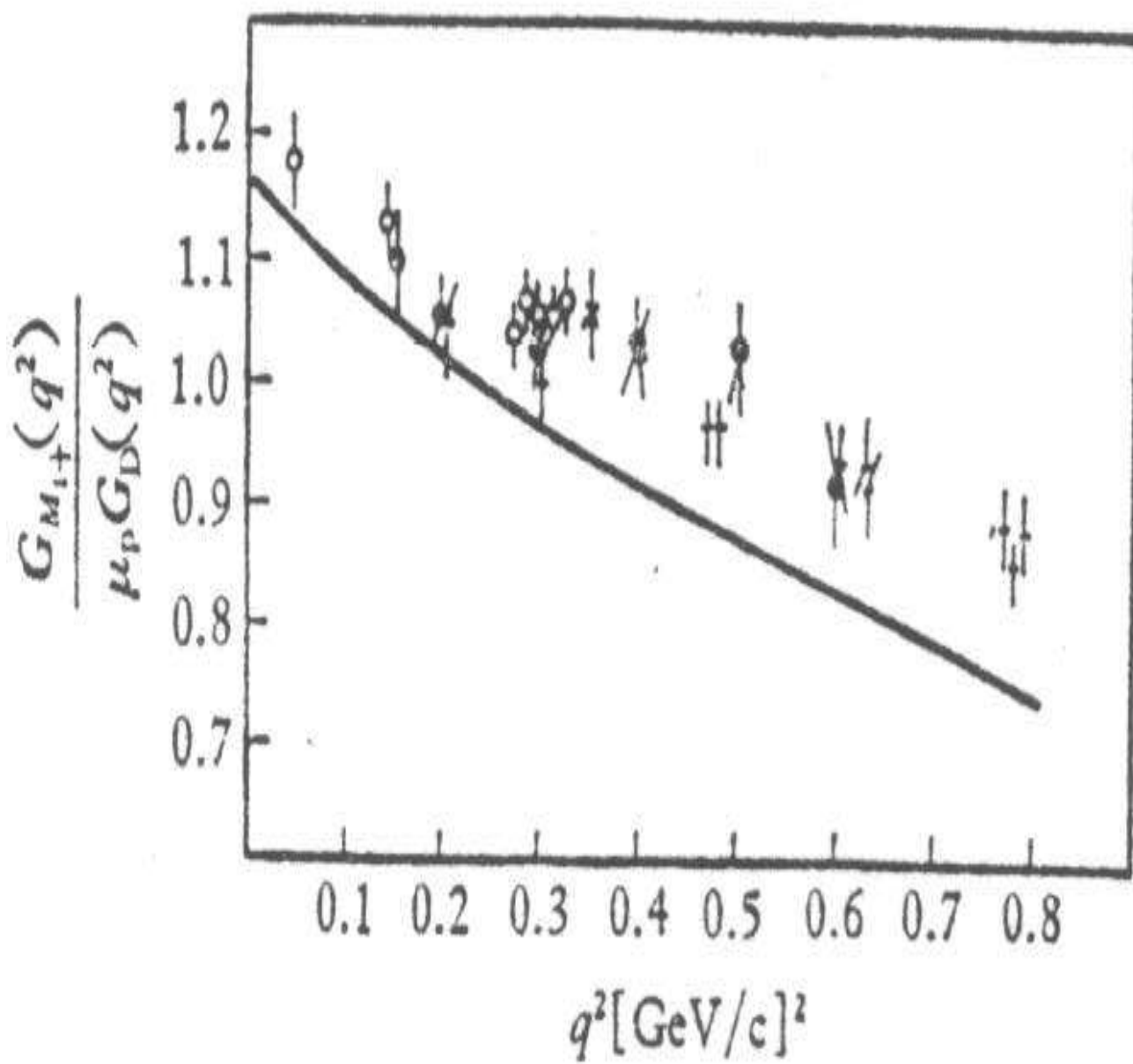


Fig. 8 (a)

following possibility

$$m_p \rightarrow \frac{1}{2}(m_p + m_\Delta)$$

is tried. The quantity 0.71GeV^2 can be rewritten as

$$0.71 \rightarrow 0.71(m_p + m_\Delta)^2/(4m_p^2)$$

and the $2.39/(4m_p^2)$ in Eq. (187) can be replaced as

$$2.39/(m_p + m_\Delta)^2.$$

The comparison between this scheme and the data [63,64,65] is presented in Fig. 8(b).

Fig. 8(b) shows that the theoretical results of the $G_{M1+}(q^2)$ are indeed improved. However, when $q^2 > 6 \text{ GeV}^2$ theoretical $G_{M1+}(q^2)/(3G_D(q^2))$ decreases still faster than current data. As mentioned above that this model may not be working well for large q^2 .

At the peak of the Δ resonance the electric multiple moments are obtained from Eq.(180,181)

$$E1+ = G_{E1+}(0) = -\frac{D_3(0)}{3\sqrt{2}m}Bm_- = -0.17, \quad (188)$$

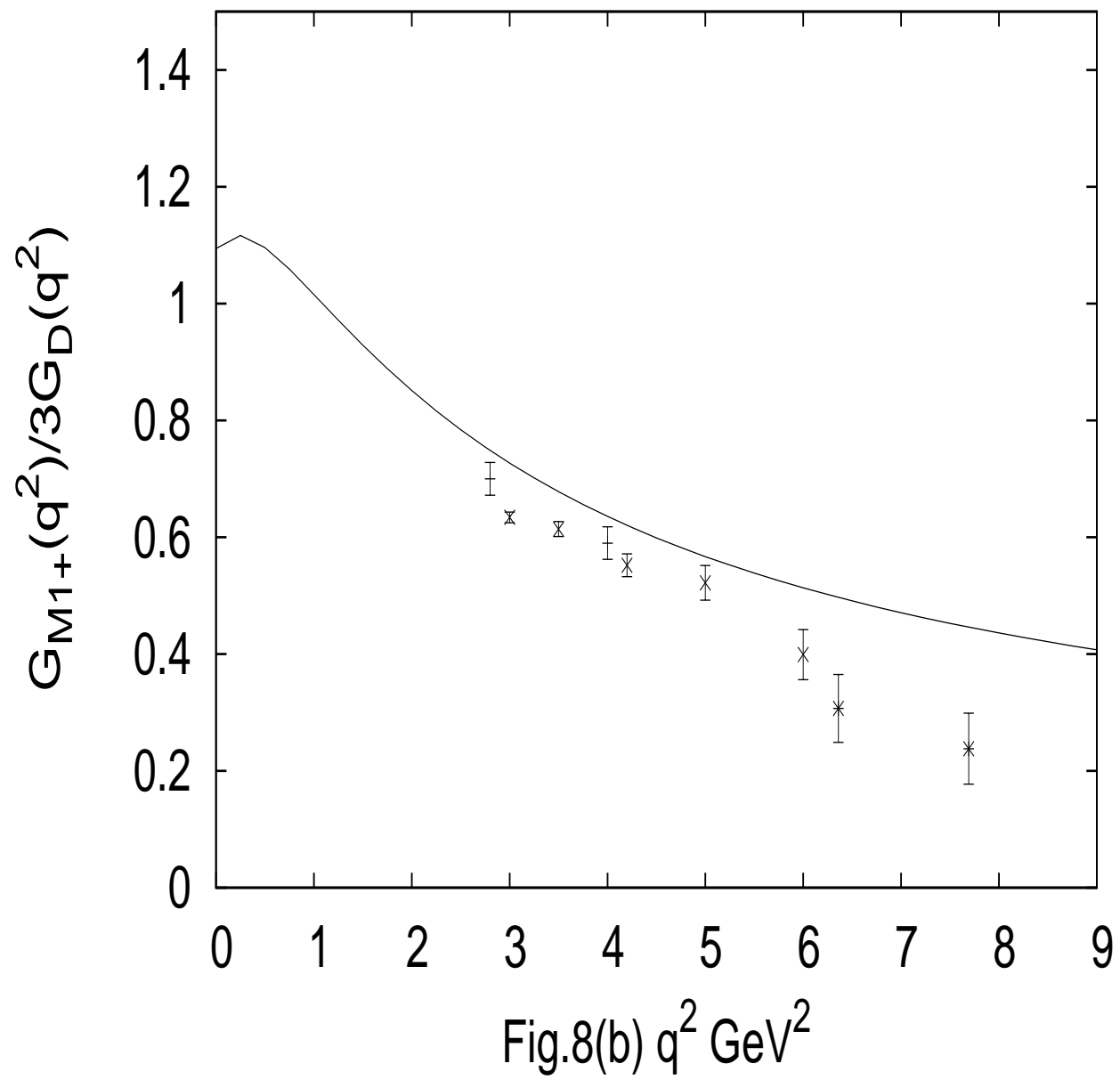
$$S1+ = G_{S1+}(0) = -\frac{D_3(0)}{3\sqrt{2}m}Bm_- = -0.17. \quad (189)$$

This model predicts small and negative $E1+$, $S1+$, and

$$S1+ = E1+,$$

$$R_{SM} = \frac{S1+}{\mu_{p \rightarrow \Delta}} = -5.4\%, \quad (190)$$

$$R_{EM} = \frac{E1+}{\mu_{p \rightarrow \Delta}} = -5.4\%. \quad (191)$$



The data [26] is

$$\frac{S1+}{\mu_{p \rightarrow \Delta}} = (-5 \pm 3)\%. \quad (192)$$

Theoretical result agree with this experimental data. There are many new measurements on the ratios of $\frac{E1+}{\mu_{p \rightarrow \Delta}}$ and $\frac{S1+}{\mu_{p \rightarrow \Delta}}$ in different regions of q^2 [66-74]. All the new data show both the R_{EM} and R_{SM} are negative and small, which are the predictions of this model. The value of the R_{SM} predicted by this model is compatible with these new data. However, the value of the R_{EM} predicted by this model is about half the value measured.

The cross section σ_S (175) is calculated in Ref. [5]. Taking

$$W = m' = 1.236 \text{ GeV}, \quad \Gamma(m') = 0.12 \text{ GeV}, \quad (193)$$

we obtain

$$\sigma_S = 48.4 q^2 (q^2 + 0.0888) (1 + 0.679 q^2)^{-2} \left(1 + \frac{q^2}{0.71}\right)^{-4} \times 10^{-28} \text{ cm}^2. \quad (194)$$

Comparison with the data [62] is shown in Fig.9.

9 The axial-vector and pseudoscalar form factors of baryons

This model has been applied to study the weak semileptonic decays of baryons and the charged quasielastic neutrino reactions of baryons in Ref. [6] and the review of this study is

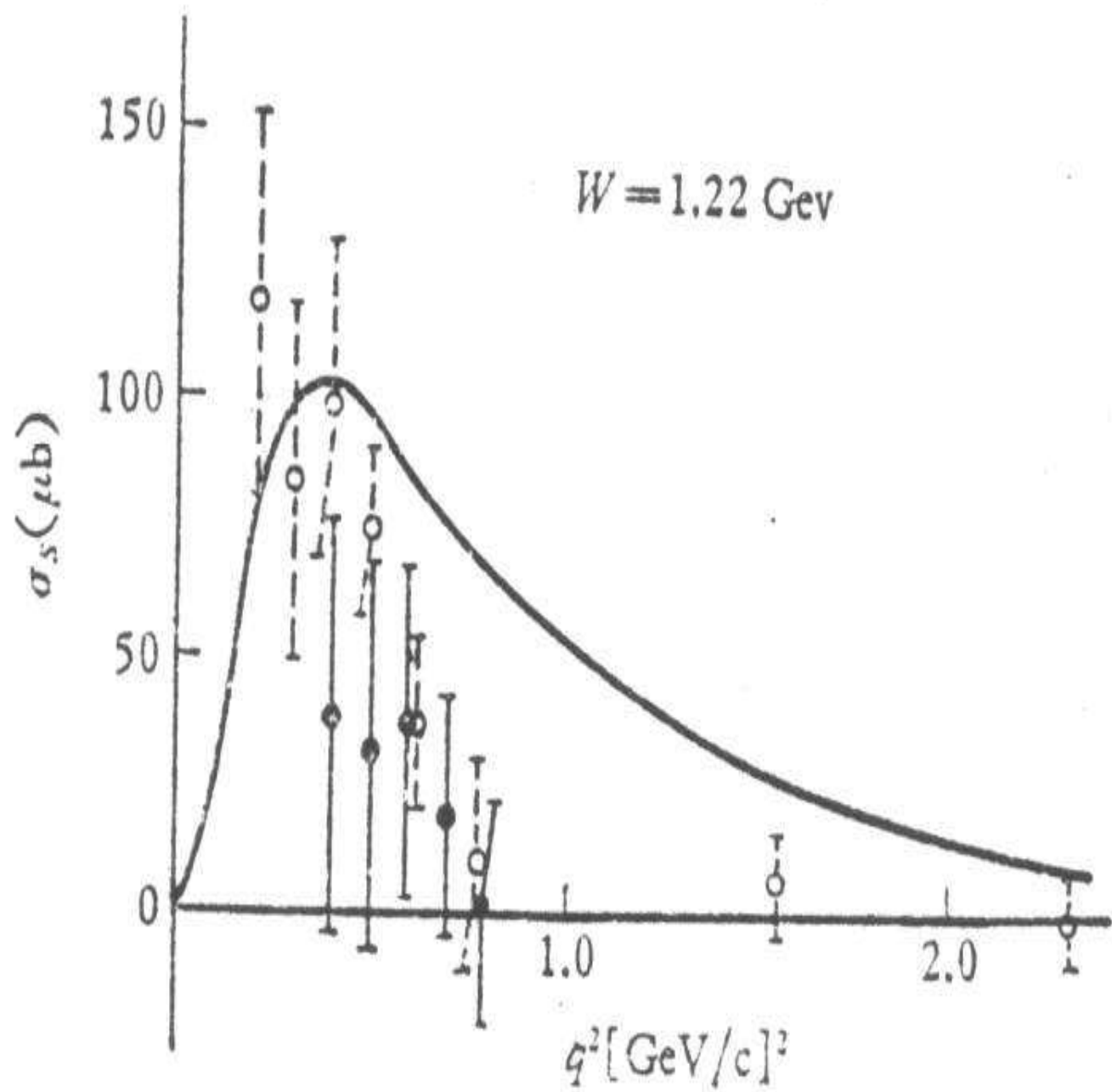


Fig. 9.

presented in this section.

The effective Lagrangian of weak interactions of charged currents between quark and lepton is

$$\mathcal{L}_w = \frac{G}{\sqrt{2}} \bar{l}(x)(1 + \gamma_5)\gamma_\mu \nu J_\mu^W + h.c.. \quad (195)$$

where J_μ^W is the charged weak currents of quarks. The effects of strong interactions must be taken into account. In J_μ^W there are both vector and axial-vector parts. Because of CVC the vector part is well determined from Eq. (48). It is known that the G_A of the β decay of the neutron cannot be determined by SU(6) symmetry, therefore, a new parameter λ has to be introduced. The effective charged current of quarks are expressed as [6]

$$J_\mu^W = \bar{\psi}(x)Q_W\{\gamma_\mu + \lambda\gamma_\mu\gamma_5 + \frac{\kappa}{2m_N}\sigma_{\mu\nu}q_\nu\}\psi(x), \quad (196)$$

where $Q_w = \cos\theta\lambda_{12} + \sin\theta\lambda_{13}$, θ is Cabbibo angle, λ is a new parameter, and the parameter κ has been determined already (107).

9.1 Weak matrix elements of $\frac{1}{2}^+$ baryons

Using the baryon wave functions (33,35,46,47), the effective Lagrangian of weak interaction (196), and the expression of the matrix elements similar to (49), the transition matrix elements of charged weak currents are calculated

$$< B^{\frac{1}{2}c'}(p_f) | J_\mu^W(0) | B^{\frac{1}{2}c}(p_i) > = -\frac{1}{2} \int d^4x_1 d^4x_2 M(x_1, x_2, x'_2, x_1) \bar{B}_{\alpha\beta\gamma,ijk}^{\frac{1}{2}c',i'j'k'_1}(x_1, x_2, 0)_{l'_1}^{l'_1} Q_{Wk_1k_2}^{k'_1k'_2}$$

$$\{\gamma_\mu + \frac{\kappa}{2m_p}\sigma_{\mu\nu}q_\mu + \lambda\gamma_5\gamma_\mu\}_{\gamma\gamma'} B_{\gamma'\beta\alpha,k_1ji}^{\frac{1}{2}c,k_2j'i'}(0, x_2, x_1)_{l_2}' = \bar{u}_{c'}(p_f)\{A_1 I_1 + A_2 I_2\}u_c(p_i) \quad (197)$$

where

$$A_1 = Tr \bar{B} Q_w B, \quad A_2 = Tr \bar{B} B Q_w, \quad (198)$$

and

$$\begin{aligned} I_1 = & \frac{1}{6} \{ [(4 - \frac{m'}{m})D_2(q^2) + (4 - \frac{m}{m'})D_2'(q^2) + 5(\frac{q^2 + m_-^2}{2mm'} + \frac{\kappa m_+ q^2}{10mm'm_p})D_3(q^2)]\gamma_\mu \\ & + [10D_1(q^2) - (5 - \frac{2m_p}{\kappa m})D_2(q^2) - (5 - \frac{2m_p}{\kappa m'})D_2'(q^2) \\ & + \frac{3q^2 + 5m_+^2}{2mm'}D_3(q^2)]\frac{\kappa}{2m_p}\sigma_{\mu\nu}q_\nu + 5\lambda[D_2(q^2) + D_2'(q^2) + \frac{q^2 + m_-^2}{2mm'}D_3(q^2)]\gamma_\mu\gamma_5 \\ & + i(1 + \frac{\kappa m_+}{2m_p})\frac{m_-}{mm'}D_3(q^2)q_\mu - i\lambda[\frac{1}{m}D_2(q^2) + \frac{1}{m'}D_2'(q^2) - \frac{m_+}{mm'}D_3(q^2)]q_\mu\gamma_5\}, \quad (199) \end{aligned}$$

$$\begin{aligned} I_2 = & \frac{1}{6} \{ [-(1 + 2\frac{m'}{m})D_2(q^2) - (1 + 2\frac{m}{m'})D_2'(q^2) + (\frac{q^2 + m_-^2}{2mm'} + \frac{\kappa m_+ q^2}{mm'm_p})D_3(q^2)]\gamma_\mu \\ & + [2D_1(q^2) - (1 - \frac{4m_p}{\kappa m})D_2(q^2) - (1 - \frac{4m_p}{\kappa m'})D_2'(q^2) \\ & + \frac{m_+^2 - 3q^2}{2mm'}D_3(q^2)]\frac{\kappa}{2m_p}\sigma_{\mu\nu}q_\nu + \lambda[D_2(q^2) + D_2'(q^2) + \frac{q^2 + m_-^2}{2mm'}D_3(q^2)]\gamma_\mu\gamma_5 \\ & + 2i(1 + \frac{\kappa m_+}{2m_p})\frac{m_-}{mm'}D_3(q^2)q_\mu - 2i\lambda[\frac{1}{m}D_2(q^2) + \frac{1}{m'}D_2'(q^2) - \frac{m_+}{mm'}D_3(q^2)]q_\mu\gamma_5\}, \quad (200) \end{aligned}$$

where $m_\pm = m' \pm m$, m and m' are the masses of the initial and final baryons respectively.

The functions $D_1(q^2)$, $D_2(q^2)$, $D_2'(q^2)$, $D_3(q^2)$ are defined by Eq. (59).

It is necessary to point out that the condition of the current conservation (62) prohibits the appearance of the second class current,

$$\bar{u}\gamma_5 q_\nu \sigma_{\mu\nu} u,$$

in Eq. (199,200).

The amplitude (197) can be expressed as

$$\begin{aligned}
\langle B^{\frac{1}{2}c'}(p_f) | J_\mu^W(0) | B^{\frac{1}{2}c}(p_i) \rangle = & b D_1(q^2) \bar{u}(p_f)_{c'} \\
& \{ f_V(q^2) \gamma_\mu + f_T(q^2) \sigma_{\mu\nu} q_\nu + i f_S(q^2) q_\mu \\
& + g_A(q^2) \gamma_\mu \gamma_5 + i g_P(q^2) q_\mu \gamma_5 \} u(p_i)_c,
\end{aligned} \tag{201}$$

where b is a coefficients and

$$D_1(q^2) = \frac{1}{\sqrt{aa'}(1 + 2.39\tau)(1 + \frac{q^2}{0.71})^2}. \tag{202}$$

All these form factors of the weak matrix elements (201) are predicted by this model and b ,

f_V, f_T, f_S, g_A, g_P are listed in Table 2.

9.2 Axial-vector form factor of nucleon

Using the Table 2, the axial-vector form factor of $n \rightarrow p$ is obtained

$$G_A(q^2) = \frac{5}{6} \lambda D_1(q^2) \{a + a' + \zeta_- aa'\}, \tag{203}$$

where the definition of the ζ_- can be found in Tab. 2. Ignoring the mass difference of proton and neutron and using the definitions of $D_{2,3}(q^2)$, Eq. (203) is expressed as

$$G_A(q^2) = G_A(0) \{D_2(q^2) + \tau D_3(q^2)\}, \tag{204}$$

where

$$G_A(0) = \frac{5}{3}\lambda. \quad (205)$$

Eq.(205) is the result of SU(6).

After ignoring the mass difference of proton and neutron, the vector form factor of $n \rightarrow p$ is found from Tab. 2

$$f_V = \frac{1}{6}\{6a + \tau(10 + 4\kappa)a^2\}D_1(q^2), \quad (206)$$

$$f_V = D_2(q^2) + \frac{1}{3}\tau(5 + 2\kappa)D_3(q^2). \quad (207)$$

Therefore,

$$f_V(0) = 1. \quad (208)$$

In Ref. [6] inputting $\frac{G_A}{G_V} = 1.242$ (where $G_V = f_V$) the parameter λ is found to be

$$\lambda = 0.745. \quad (209)$$

The new data is $\frac{G_A}{G_V} = 1.2701 \pm 0.0025$ [46] and $\lambda = 0.762$ is determined. The difference is about 2%.

From Eqs.(52,80,81), the Dirac form factor $F_1(q^2)$ of proton is found to be

$$F_1(q^2) = D_2(q^2) + \tau D_3(q^2). \quad (210)$$

Therefore, this model predicts

$$G_A(q^2) = \frac{5}{3}\lambda F_1(q^2), \quad (211)$$

$$F_1^p(q^2) = \frac{1}{1+\tau} \{G_E^p(q^2) + \tau G_M^p(q^2)\}. \quad (212)$$

Following the notation in literature, the the axial-vector form factor is rewritten as

$$\frac{5}{3} \lambda G_A(q^2). \quad (213)$$

In the study of $\nu + N$ scattering the axial-vector form factor is taken as a form of dipole

$$G_A(q^2) = \frac{1}{(1 + \frac{q^2}{M_A^2})^2}. \quad (214)$$

The relationship between parameter M_A and the charge radius of proton (80) is predicted

$$\frac{1}{M_A^2} = \frac{1}{12} < r_E^2 > - (\mu_p - 1) \frac{1}{8m_p^2}, \quad (215)$$

where $< r_E^2 >$ is the charge radius of proton squared. Using Eq. (139) and inputting $< r_M^2 > = (0.777 \pm 0.013 \pm 0.010)^2 fm^2$, it is predicted

$$M_A = 1.002 \text{ GeV}. \quad (216)$$

On the other hand, if ignoring the contribution of the antiquarks, as mentioned above, $a = 1$ should be taken and

$$G_A(q^2) = (1 + \frac{q^2}{0.71})^{-2} = \frac{1}{\mu_p} G_M^p(q^2). \quad (217)$$

The form factor $G_A(q^2)$, indeed, takes the form of dipole and $M_A = 0.84 \text{ GeV}$. Comparing with the data, this $G_A(q^2)$ decreases too fast. Using the parametrization (77), the axial-vector form factor of nucleon, $G_A(q^2)$, is expressed as

$$G_A(q^2) = \frac{1 + 4.5\tau}{(1 + 2.39\tau)(1 + \frac{q^2}{0.71})^2}. \quad (218)$$

The axial-vector form factor predicted by this model is not in the form of dipole. However, because of the factor

$$\frac{1 + 4.5\tau}{1 + 2.39\tau}$$

the $G_A(q^2)$ (218) decreases with q^2 slower than $(1 + \frac{q^2}{0.71})^{-2}$ and an equivalent M_A is determined (216). The comparison between the expression (218) predicted by this model and the form of dipole (214) with $M_A = 1.002$ GeV is shown in Fig. 10 .

The Fig. 10 shows that in a wide range of q^2 these two expressions of $G_A(q^2)$ are almost identical. There are many measurements of the M_A . In Ref. [18] two groups of the experimental values of the M_A are presented. One group from quasi-elastic neutrino and antineutrino scattering experiments and the resulting world average is

$$M_A = (1.026 \pm 0.021)\text{GeV}. \quad (219)$$

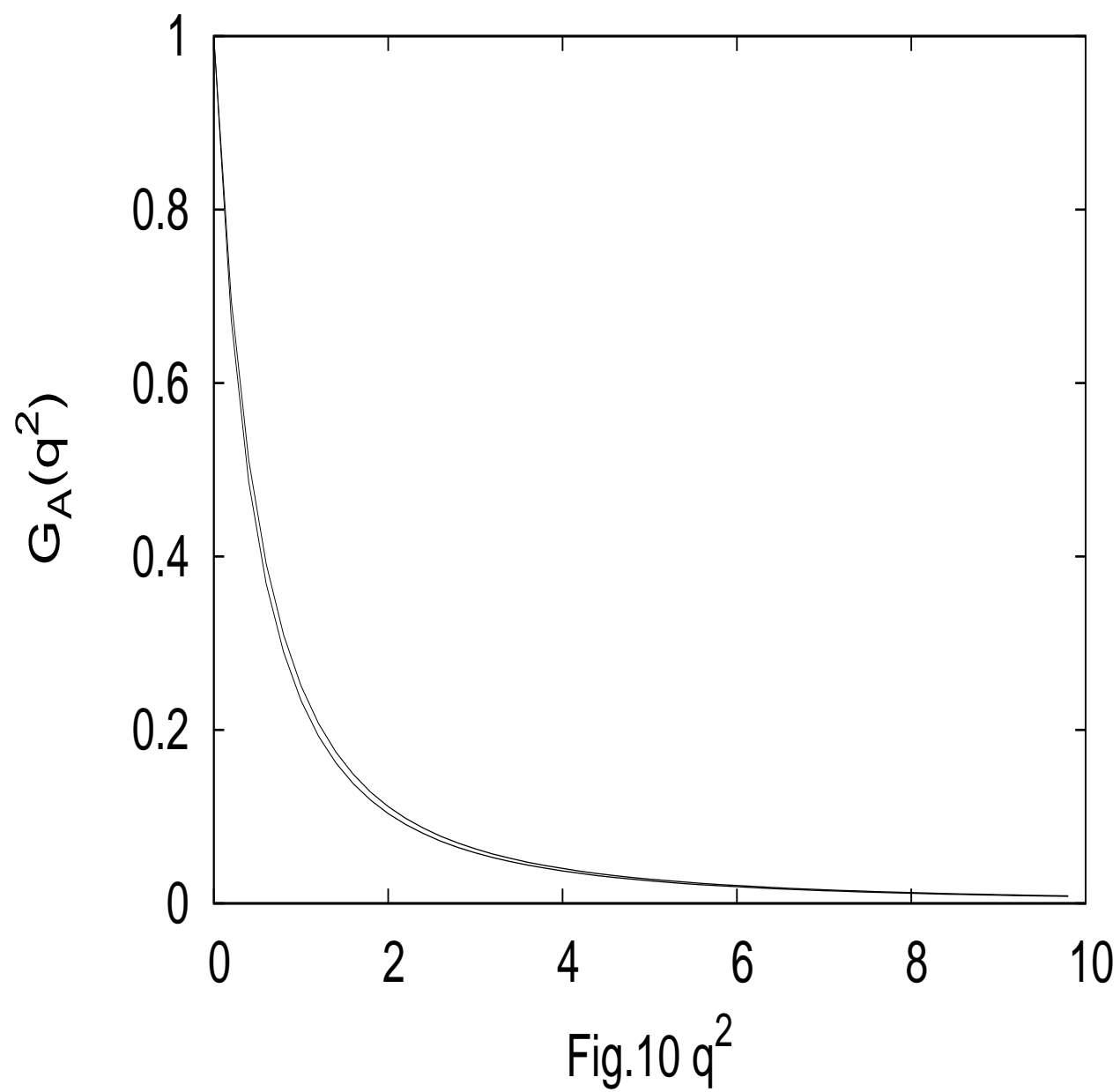
The other determinations of the $G_A(q^2)$ are based on the analysis of charged pion electro-production off proton and the world average is

$$M_A = (1.069 \pm 0.016)\text{GeV}. \quad (220)$$

In Ref. [79]

$$M_A^{\text{world-average}} = 1.014 \pm 0.014\text{GeV} \quad (221)$$

is presented. In Ref. [87] a list of the value of M_A used by many experiments of $\nu_\mu + N$ and



$\bar{\nu}_\mu + N$ is presented. The prediction of the M_A (216) by this model is in good agreement with these values (219,220,221) within the experimental errors.

9.3 Pseudoscalar form factor of $n \rightarrow p$

Ignoring the mass difference between neutron and proton, the pseudoscalar form factor of $n \rightarrow p$ is predicted by this model (Table 2) (after the g_P form factor in Eq. (201) is rewritten as $g_P \frac{q_\mu}{m} \gamma_5$)

$$g_P = \frac{1}{3} \lambda (a - 1) D_2(q^2). \quad (222)$$

If $a = 1$ is taken, $g_P = 0$ is revealed. Therefore, in this model the pseudoscalar form factor of nucleon is resulted in antiquark components of nucleon. For very small q^2

$$g_P(0) = \frac{1}{3} \lambda (a - 1) = 0.872. \quad (223)$$

Based on the work presented in Refs.[81,82] and systematic chiral expansion of low energy QCD Green function the authors of Ref. [78] obtain

$$g_P = 8.26 \pm 0.16. \quad (224)$$

In Ref. [95] a measurement of the g_P from low energy pion electroproduction has been reported as

$$g_P(q^2) = 0.082 \pm 0.018 \, m_N/\text{MeV}, \text{ at } q^2 = 0.012 \, \text{GeV}^2.$$

It is claimed that the measurements are consistent with the pion pole dominance in the region of small q^2

$$g_P(q^2) \sim (1 - q^2/m_\pi^2).$$

Using this form factor, it is obtained

$$g_P(0) = 2.33 \pm 0.51.$$

The value of the g_P (223) obtained in this model is smaller than these two values obtained in Refs. [78, 95]. On the other hand, the $g_P(q^2)$ obtained in this model (222) in the region of small q^2 is expressed as

$$1 - q^2/0.286.$$

The constant 0.286 is more than 10 times of the m_π^2 . Therefore, the pion pole of the $g_P(q^2)$ is not revealed from this model. There is an issue about satisfaction of PCAC in this model. On the other hand, in this model g_P is resulted in antiquark components of nucleon. The antiquark components of nucleon can come from pion clouds. It is interesting to study the relationship between the factor, a - 1 (223) and the pion clouds. This study is beyond the scope of this paper. Phenomenologically, the contributions of the g_P to the semileptonic decays and the cross sections of the quasielastic neutrino scatterings are small.

9.4 Semileptonic decays of baryons

For the semileptonic decays of $\frac{1}{2}^+$ baryons the transfer momenta are very small and only the $g_A(0)$ and the $f_V(0)$ contribute to the decays. After inputting the value of the λ , the $g_A(0)$ is obtained and the $f_V(0)$ is found from Table 2. The Cabbibo angle is chosen to be

$$\theta = 0.22.$$

The branching ratios of these semileptonic decays are predicted. The results and comparisons with data [46] are shown in Table 3.

Table 3 shows that theoretical predictions of the branching ratios and $\frac{G_A}{G_V}$ (or $\frac{G_V}{G_A}$ in some cases) are in good agreement with data.

It is interesting to notice (see Table 2) that the vector form factors of $\Sigma^\pm \rightarrow \Lambda$ are expressed as

$$G_V(q^2) = \frac{q^2}{2\sqrt{6}m_\Lambda m_\Sigma} \left(1 + \kappa \frac{m_\Lambda + m_\Sigma}{2m_p} a_\Lambda a_\Sigma\right) D_1(q^2), \quad (225)$$

where $a_\Lambda = (1 - \frac{m_0}{m_\Lambda})^{-1}$, and $a_\Sigma = (1 - \frac{m_0}{m_\Sigma})^{-1}$. Therefore, at $q^2 = 0$ the vector form factors for both processes are equal to zero

$$\frac{G_V}{G_A} = 0. \quad (226)$$

This prediction originates in the condition of current conservation (62). In 70's the experimental data was -0.37 ± 0.20 . The newer data is 0.01 ± 0.10 [46]. Theory agrees with data very well. As a matter of fact in both $\Sigma^\pm \rightarrow \Lambda + e^+(e^-) + \nu(\bar{\nu})$ decays transfer momenta are very small and the maximum of q^2 are $0.55 \times 10^{-2} \text{ GeV}^2$, $0.67 \times 10^{-2} \text{ GeV}^2$ respectively. For the q_{max}^2

$$G_V(q_{max}^2) = 0.164 \times 10^{-2}, \quad 0.199 \times 10^{-2}$$

respectively for both decays. Therefore, for both decays

$$\frac{G_V}{G_A} \sim 0. \quad (227)$$

These predictions are in good agreements with data.

The coefficient between lepton and neutrino, $\alpha_{e\nu}$, and the asymmetric parameters, α_e , α_ν , α_B , are predicted by this model (see Table 4). In Table 5 the related data [76] of the process $\Lambda \rightarrow pe^-\bar{\nu}$ are listed.

The experimental value of α_e of the $\Sigma^- \rightarrow ne^-\bar{\nu}$

$$\alpha_e = -0.26 \pm 0.37$$

can be found in Ref. [77]. Theoretical results of these coefficients are compatible with the existing data. In Ref. [87] it has been reported

$$\alpha_{e\nu} = -0.27 \pm 0.013, \quad G_A(0)/G_V(0) = 0.731 \pm 0.016$$

for the decay $\Lambda \rightarrow p + e^- + \bar{\nu}$. In Ref. [88] for the decay $\Sigma^- \rightarrow n + e^- + \bar{\nu}$ following quantities have been measured

$$\alpha_e = -0.519 \pm 0.104, \quad \alpha_n = 0.509 \pm 0.102, \quad \alpha_\nu = -0.230 \pm 0.061.$$

Theoretical values of these quantities (see Tab. 4) are compatible with the measured values.

10 Charged quasielastic reactions of neutrino and nucleon

10.1 $\Delta S = 0$ scatterings of neutrino (antineutrino) and nucleon

There are two $\Delta S = 0$ charged quasielastic reactions

$$\nu_\mu + n \rightarrow p + \mu^-, \quad \bar{\nu}_\mu + p \rightarrow n + \mu^+.$$

As shown in Eqs. (218,219) the $G_A(q^2)$ and the M_A are all predicted in this model. The vector form factors of these two processes are determined completely and the cross sections of them can be calculated without any new parameter. Therefore, the cross sections of these scattering processes are the predictions of this model.

$$\nu_\mu + n \rightarrow p + \mu^-$$

Using Eq. (201) and ignoring the mass difference between proton and neutron, the matrix element of the charged weak quark current can be written

$$\langle p(p_f) | j_\mu^W(0) | n(p_i) \rangle = \frac{1}{3} \bar{u}_{c'}(p_f) \{ 5G_M^p(q^2) \gamma_\mu + 5\lambda G_A(q^2) \gamma_\mu \gamma_5 + \frac{i}{m} P_\mu J(q^2) \} u_c(p_i), \quad (228)$$

where $P_\mu = p_{i\mu} + p_{f\mu}$, the form factors $G_M^p(q^2)$ and $G_A(q^2)$ are shown in Eqs. (95,218) respectively,

$$\begin{aligned} J(q^2) &= D_2(q^2) + \frac{5}{2} \kappa \{ D_1(q^2) - D_2(q^2) + (1 + \frac{5}{3} \tau) D_3(q^2) \} \\ &= \{ 1 + \frac{5}{2} (\mu_p - 1) + \frac{3}{2} \kappa a \tau \} D_2(q^2). \end{aligned} \quad (229)$$

$D_2(q^2)$ is shown in Eq. (112).

The cross section of $\nu_\mu + n \rightarrow p + \mu^-$ is derived as

$$\frac{d\sigma}{dq^2} = \frac{G^2}{9\pi x} \cos^2\theta \left\{ \frac{\tau}{x} W_1 + \left[\frac{x}{2} - \tau \left(1 + \frac{1}{2x} \right) \right] W_2 - \frac{\tau}{x} (x - \tau) W_3 \right\}, \quad (230)$$

where $x = \frac{E_\nu}{m}$, E_ν is the energy of neutrino,

$$\begin{aligned} W_1 &= 25 \{ \tau G_M^p(q^2)^2 + (1 + \tau) \lambda^2 G_A^2(q^2) \}, \\ W_2 &= \{ 5 G_M^p(q^2) - 2 J(q^2) \}^2 + 25 \lambda^2 G_A^2(q^2) + 4 \tau J^2(q^2), \\ W_3 &= -50 \lambda G_A(q^2) G_M^p(q^2). \end{aligned} \quad (231)$$

Using

$$q^2 = \frac{4m^2 x^2 \sin^2 \frac{\alpha}{2}}{1 + 2x \sin^2 \frac{\alpha}{2}} \quad (232)$$

(α is the scattering angle of muon), the limits of q^2 are found

$$0 \leq q^2 \leq \frac{4m^2 x^2}{1 + 2x}. \quad (233)$$

Integrating over q^2 , the total cross section as a function of E_ν is obtained. The comparison between theory and experimental data [83] is shown in Fig. 11.

The comparison with newer data is shown in Fig. 12

The experimental data of Fig. 12 are taken from Refs. [84,85,86]. When $E_\nu > 15\text{GeV}$ theoretical $\sigma(\nu_\mu + n \rightarrow p + \mu^-)$ is very flat (see below). In this calculation there is no new adjustable parameter. Theory agrees with data very well.

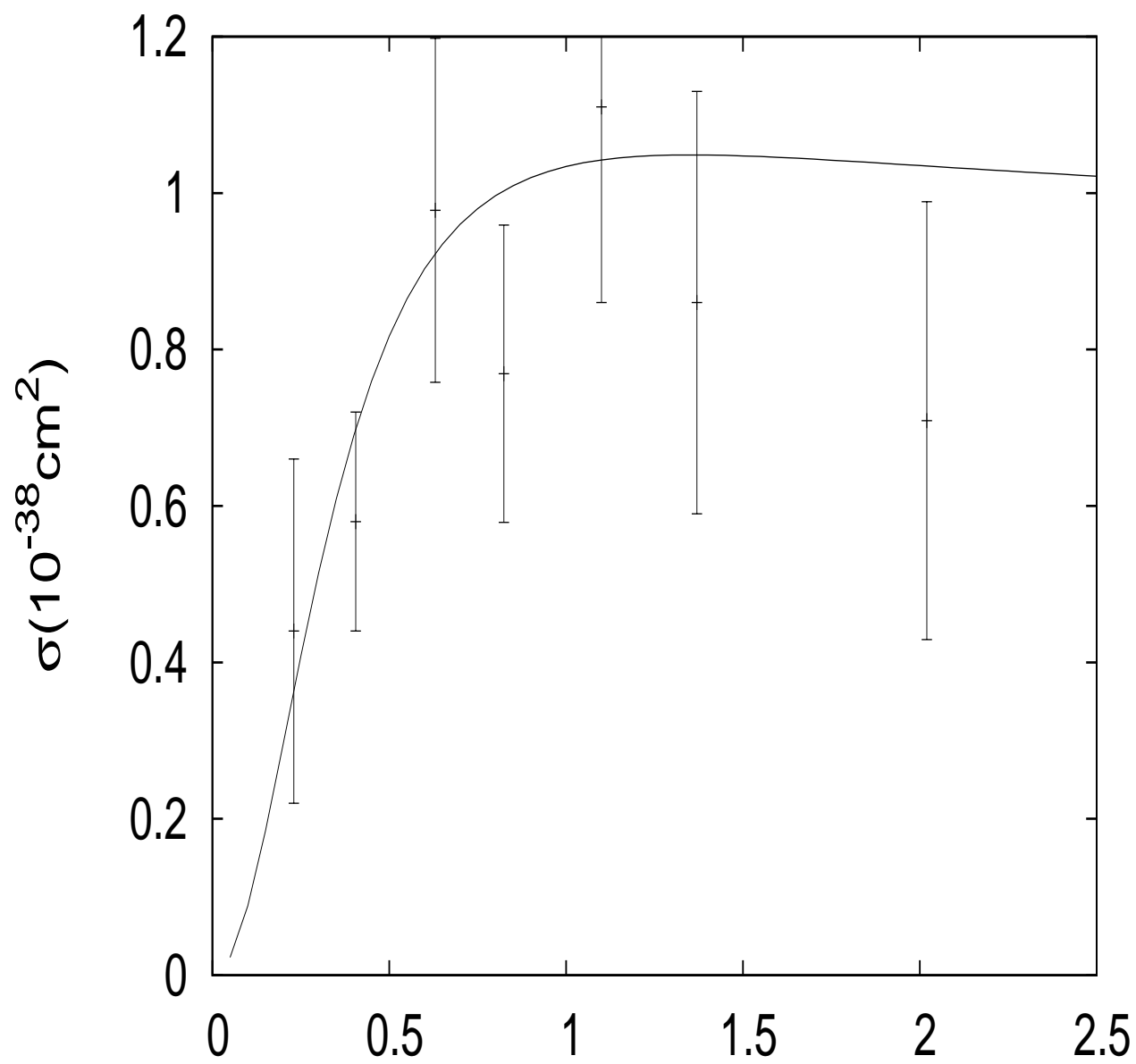
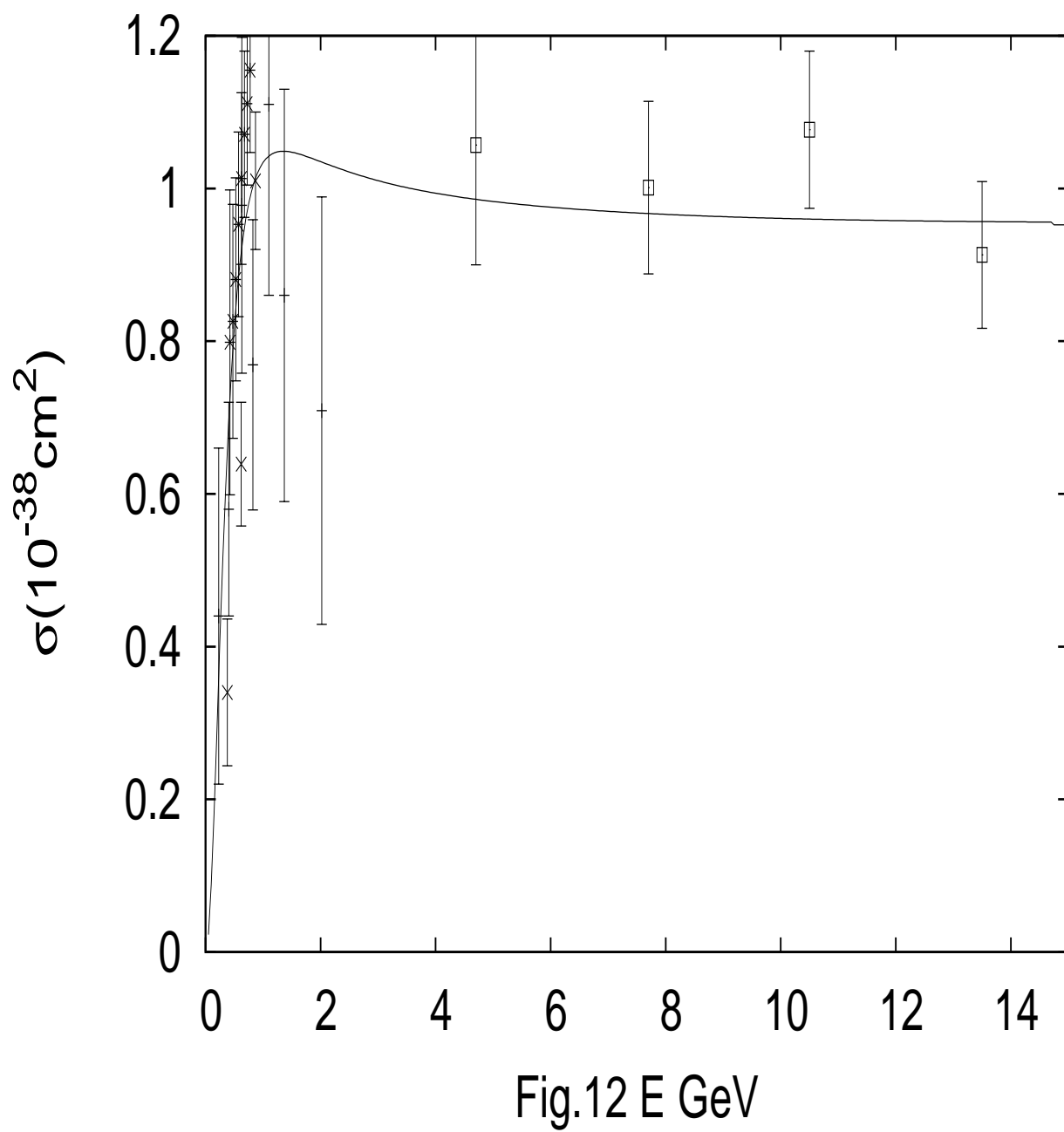


Fig.11 E GeV



$$\bar{\nu}_\mu + p \rightarrow n + \mu^+$$

The cross section of this process is obtained from Eq. (230) by changing the minus sign associated with the W_3 to plus

$$\frac{d\sigma}{dq^2} = \frac{G^2}{9\pi x} \cos^2\theta \left\{ \frac{\tau}{x} W_1 + \left[\frac{x}{2} - \tau \left(1 + \frac{1}{2x} \right) \right] W_2 + \frac{\tau}{x} (x - \tau) W_3 \right\}, \quad (234)$$

where $W_{1,2,3}$ are shown in Eqs. (231). The theoretical values of the cross section is shown in Fig. 13. The data is taken from Ref. [86] Theory agrees with the data well. When $E_\nu \rightarrow \infty$ $W_{1,3}$ make no contributions to the cross section. Therefore,

$$\lim_{E_\nu \rightarrow \infty} \sigma(\bar{\nu}_\mu + p \rightarrow n + \mu^+) = \lim_{E_\nu \rightarrow \infty} \sigma(\nu + n \rightarrow p + \mu) = 0.89 \times 10^{-38} \text{ cm}^2. \quad (235)$$

10.2 $\Delta S = 1$ quasielastic reactions of neutrino and nucleon

$$\bar{\nu}_\mu + p \rightarrow \Lambda + \mu^+$$

The decays $\Lambda \rightarrow p + e^- + \bar{\nu}_e$, $p + \mu^- + \bar{\nu}_\mu$ have been studied and the results are shown in Table 2. Theory agrees with data. The matrix element of the weak current of this process is obtained from Eq. (201) and Table 2

$$\langle \Lambda(p_f) | J_\mu^W(0) | p(p_i) \rangle = \frac{3}{2\sqrt{6}} \bar{u}_{c'}(p_f) \{ G_V^\Lambda(q^2) \gamma_\mu + \lambda G_A^\Lambda(q^2) \gamma_\mu \gamma_5 + \frac{i}{m_+} G(q^2) P_\mu \} u_c(p_i), \quad (236)$$

where $m_+ = m_\Lambda + m_p$,

$$G_A^\Lambda(q^2) = D_2(q^2) + D_2'(q^2) + \frac{q^2 + (m_\Lambda - m_p)^2}{2m_p m_\Lambda} D_3(q^2),$$

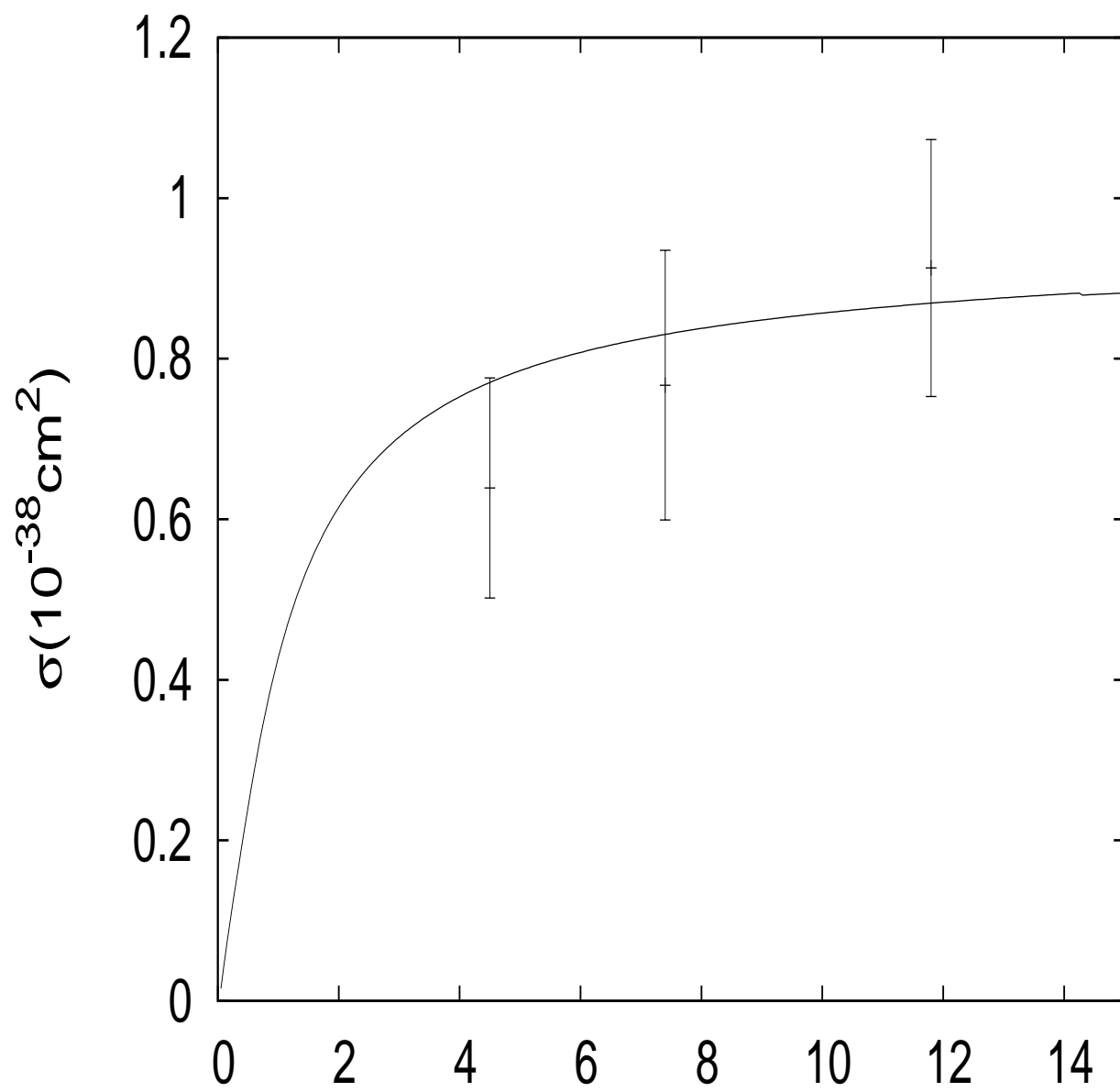


Fig.13 E GeV

$$G(q^2) = \frac{\kappa(m_\Lambda + m_p)}{2m_p} \{2D_1(q^2) - D_2(q^2) - D_2'(q^2) + \frac{q^2 + (m_\Lambda + m_p)^2}{2m_p m_\Lambda} D_3(q^2)\},$$

$$G_V^\Lambda(q^2) = G_A^\Lambda(q^2) + G(q^2). \quad (237)$$

According to Eq.(77), there are

$$D_2(q^2) = a_p D_1(q^2), \quad D_2'(q^2) = a_\Lambda D_1(q^2), \quad D_3(q^2) = a_p a_\Lambda D_1(q^2), \quad (238)$$

where a_p and a_Λ are obtained from Eq.(79). Using Eq. (238), we have

$$G_A^\Lambda(q^2) = D_1(q^2) \{a_p + a_\Lambda + \frac{q^2 + (m_\Lambda - m_p)^2}{2m_p m_\Lambda} a_p a_\Lambda\},$$

$$G(q^2) = \frac{\kappa(m_\Lambda + m_p)}{2m_p} D_1(q^2) \{2 - a_p - a_\Lambda + \frac{q^2 + (m_\Lambda + m_p)^2}{2m_p m_\Lambda} a_p a_\Lambda\}. \quad (239)$$

All the form factors of this process are determined.

The experimental estimation of the parameter M_A of the axial-vector form factor (239) is 0.6 ± 0.2 GeV [83]. Eq.(239) shows that the axial-vector form factor $G_A^\Lambda(q^2)$ decreases faster than the axial-vector form factor (218) of $\nu_\mu + n \rightarrow p + \mu^-$. Comparing with the dipole form factor, for Λ production

$$M_A = 0.865 \text{ GeV}.$$

is determined. It is compatible with the experimental estimation.

The cross section of $\bar{\nu}_\mu + p \rightarrow \Lambda + \mu^+$ is written as

$$\frac{d\sigma}{dq^2} = \frac{3G^2 \sin^2 \theta}{8\pi m_p^2 x^2} \left\{ \tau W_1 + \left[x \left(\frac{x}{2} - \frac{m_\Lambda^2 - m_p^2}{4m_p^2} \right) - \tau \left(\frac{1}{2} + x \right) \right] W_2 - \tau \left(\tau - x + \frac{m_\Lambda^2 - m_p^2}{4m_p^2} \right) W_3 \right\}, \quad (240)$$

where $x = \frac{E_\nu}{m_p}$,

$$\begin{aligned} W_1 &= \frac{1}{4m_p^2} \{ [q^2 + (m_\Lambda - m_p)^2] G_V^\Lambda(q^2)^2 + \lambda^2 [q^2 + (m_\Lambda + m_p)^2] G_A^\Lambda(q^2)^2 \}, \\ W_2 &= (1 + \lambda^2) [G_A^\Lambda(q^2)^2 + \frac{q^2}{(m_\Lambda + m_p)^2} G^2(q^2)], \\ W_3 &= -2\lambda G_A^\Lambda(q^2) G_V^\Lambda(q^2). \end{aligned} \quad (241)$$

q^2 is expressed as

$$q^2 = \frac{2x(2m_p^2x + m_p^2 - m_\Lambda^2) \sin^2 \frac{\alpha}{2}}{1 + 2x \sin^2 \frac{\alpha}{2}}. \quad (242)$$

The limits of q^2 is determined as

$$0 \leq q^2 \leq \frac{4m_p^2x(x - \frac{m_\Lambda^2 - m_p^2}{2m_p^2})}{1 + 2x}. \quad (243)$$

The lower limit of the energy of neutrino is

$$E_\nu > \frac{m_\Lambda^2 - m_p^2}{2m_p}. \quad (244)$$

The total cross section is obtained and shown in Fig.14. In the calculation there is no new adjustable parameter. In the range of neutrino energies from 0.9-3.3 GeV the experimental value of the cross section [83] is

$$\sigma = (1.3_{-0.7}^{+0.9}) \times 10^{-40} \text{ cm}^2/\text{proton}. \quad (245)$$

It is at the order of 10^{-40} cm^2 which is smaller than the cross section of $\nu_\mu + n \rightarrow p + \mu^-$ by two order of magnitude. The reason is that this cross section is $\propto \sin^2 \theta$.

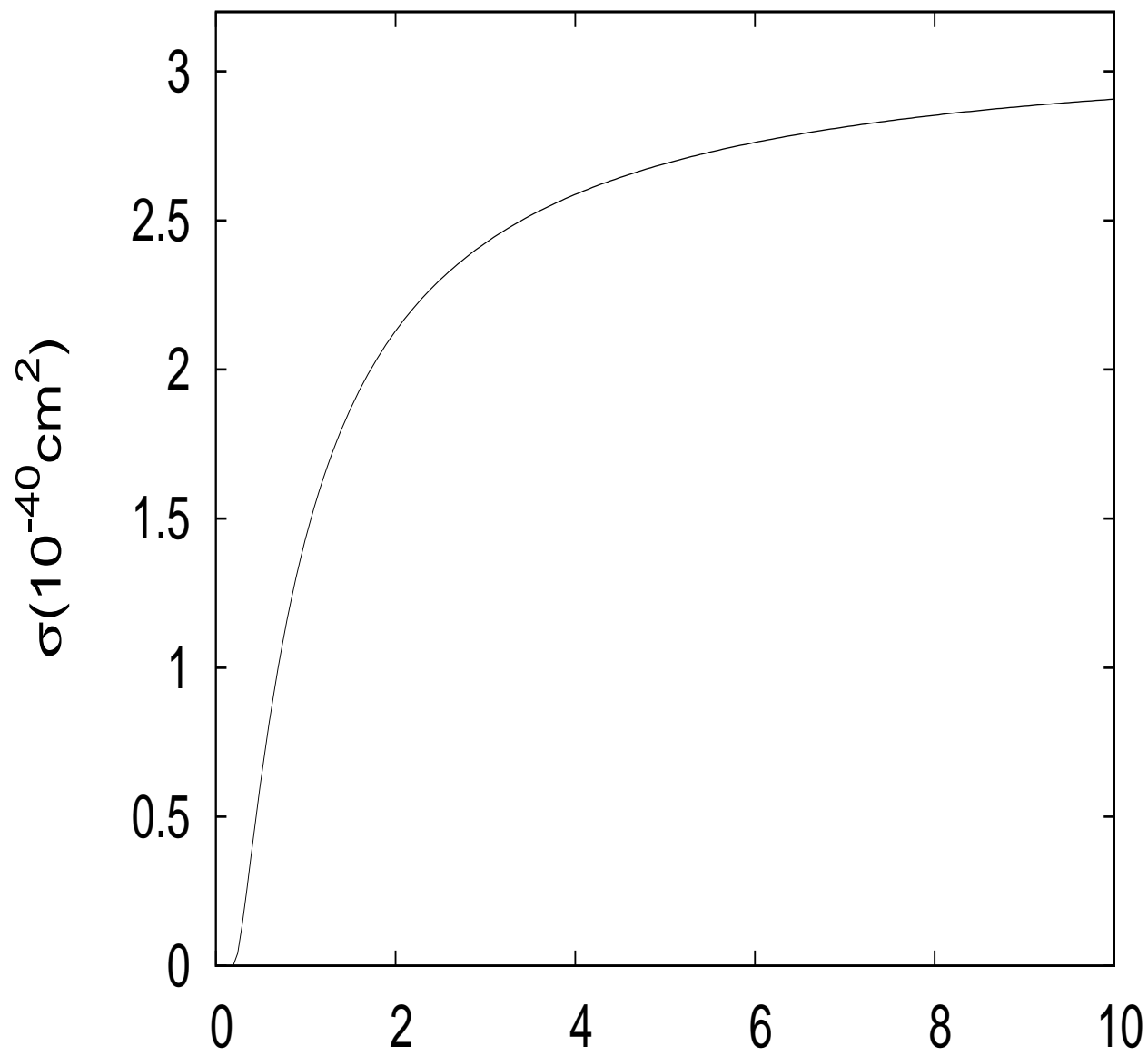


FIG.14 E GeV

When $E_\nu \rightarrow \infty$ the cross section approaches a constant

$$\lim_{E_\nu \rightarrow \infty} \sigma = 2.69 \times 10^{-40} \text{ cm}^2. \quad (246)$$

Theory is compatible with data.

$$\bar{\nu}_\mu + p \rightarrow \Sigma^0 + \mu^+$$

The matrix element of this process is obtained from Eq. (201)

$$\langle \Sigma_c^0(p_f) | J_\mu^W(0) | p_c(p_i) \rangle = \frac{3}{2\sqrt{6}} \bar{u}_c(p_f) \{ G_V^\Sigma(q^2) \gamma_\mu + \lambda G_A^\Sigma(q^2) \gamma_\mu \gamma_5 + \frac{i}{m_\Sigma} G^\Sigma(q^2) P_\mu \} u_c(p_i), \quad (247)$$

where

$$\begin{aligned} G_V^\Sigma(q^2) &= \frac{1}{3\sqrt{3}} \{ D_2(q^2) + D_2'(q^2) + \frac{q^2 + (m_\Sigma - m_p)^2}{2m_p m_\Sigma} D_3(q^2) \\ &+ \frac{\kappa(m_\Sigma + m_p)}{2m_p} [2D_1(q^2) - D_2(q^2) - D_2'(q^2) + \frac{q^2 + (m_\Sigma - m_p)^2}{2m_p m_\Sigma} D_3(q^2)] \}, \\ &= (0.988 + 1.6\tau)/(1 + 2.39\tau)/(1 + 4.96\tau)^2, \end{aligned} \quad (248)$$

$$\begin{aligned} G_A^\Sigma(q^2) &= \frac{1}{3\sqrt{3}} \{ D_2(q^2) + D_2'(q^2) + \frac{q^2 + (m_\Sigma - m_p)^2}{2m_p m_\Sigma} D_3(q^2) \} \\ &= (0.42 + 1.03\tau)/(1 + 2.39\tau)/(1 + 4.96\tau)^2, \end{aligned} \quad (249)$$

$$\begin{aligned} G^\Sigma(q^2) &= \frac{2}{3\sqrt{3}} \{ D_2'(q^2) + \frac{m_\Sigma}{m_p} D_2(q^2) - \frac{\kappa q^2}{2m_p^2} D_3(q^2) + \frac{\kappa m_\Sigma}{4m_p} [2D_1(q^2) - D_2(q^2) - D_2'(q^2) \\ &+ \frac{q^2 + (m_\Sigma - m_p)^2}{2m_p m_\Sigma} D_3(q^2)] \} \\ &= (1.26 - 0.95\tau)/(1 + 2.39\tau)/(1 + 4.96\tau)^2. \end{aligned} \quad (250)$$

Using the substitution $m_\Lambda \rightarrow m_\Sigma$ in Eq. (240), the cross section of $\bar{\nu}_\mu + p \rightarrow \Sigma^0 + \mu^+$ is

obtained and the $W_{1,2,3}$ of this process are defined as

$$\begin{aligned}
W_1 &= \frac{1}{4m_p^2} \{ [q^2 + (m_\Sigma - m_p)^2] G_V^\Sigma(q^2)^2 + \lambda^2 [q^2 + (m_\Sigma + m_p)^2] G_A^\Sigma(q^2)^2 \}, \\
W_2 &= \left[\frac{m_\Sigma + m_p}{m_\Sigma} G^\Sigma(q^2) - G_V^\Sigma(q^2) \right]^2 + \lambda^2 G_A^\Sigma(q^2)^2 + \frac{q^2}{m_\Sigma^2} G^\Sigma(q^2)^2, \\
W_3 &= -2\lambda G_A^\Sigma(q^2) G_V^\Sigma(q^2).
\end{aligned} \tag{251}$$

There is no new adjustable parameter. When $E_\nu \rightarrow \infty$ the cross section approaches a constant

$$\lim_{E_\nu \rightarrow \infty} \sigma = 0.38 \times 10^{-40} \text{ cm}^2. \tag{252}$$

The numerical results are shown in Fig.15. Comparing Fig.15 with Fig.14, it is found

$$\sigma(\bar{\nu}_\mu + p \rightarrow \Sigma^0 + \mu^+) \sim \frac{1}{6} \sigma(\bar{\nu}_\mu + p \rightarrow \Lambda + \mu^+).$$

In the experiment of quasielastic hyperon production by antineutrino [83] 10 Λ and 2 Σ^0 are found. Theory is compatible with data.

11 $\nu_\mu + p \rightarrow \Delta^{++} + \mu^-$ scattering

Using the same approach, the $\nu_\mu + p \rightarrow \Delta^{++} + \mu^-$ scattering process has been studied in Ref. [7]. In this section the review of the study done in Ref. [7] is presented.

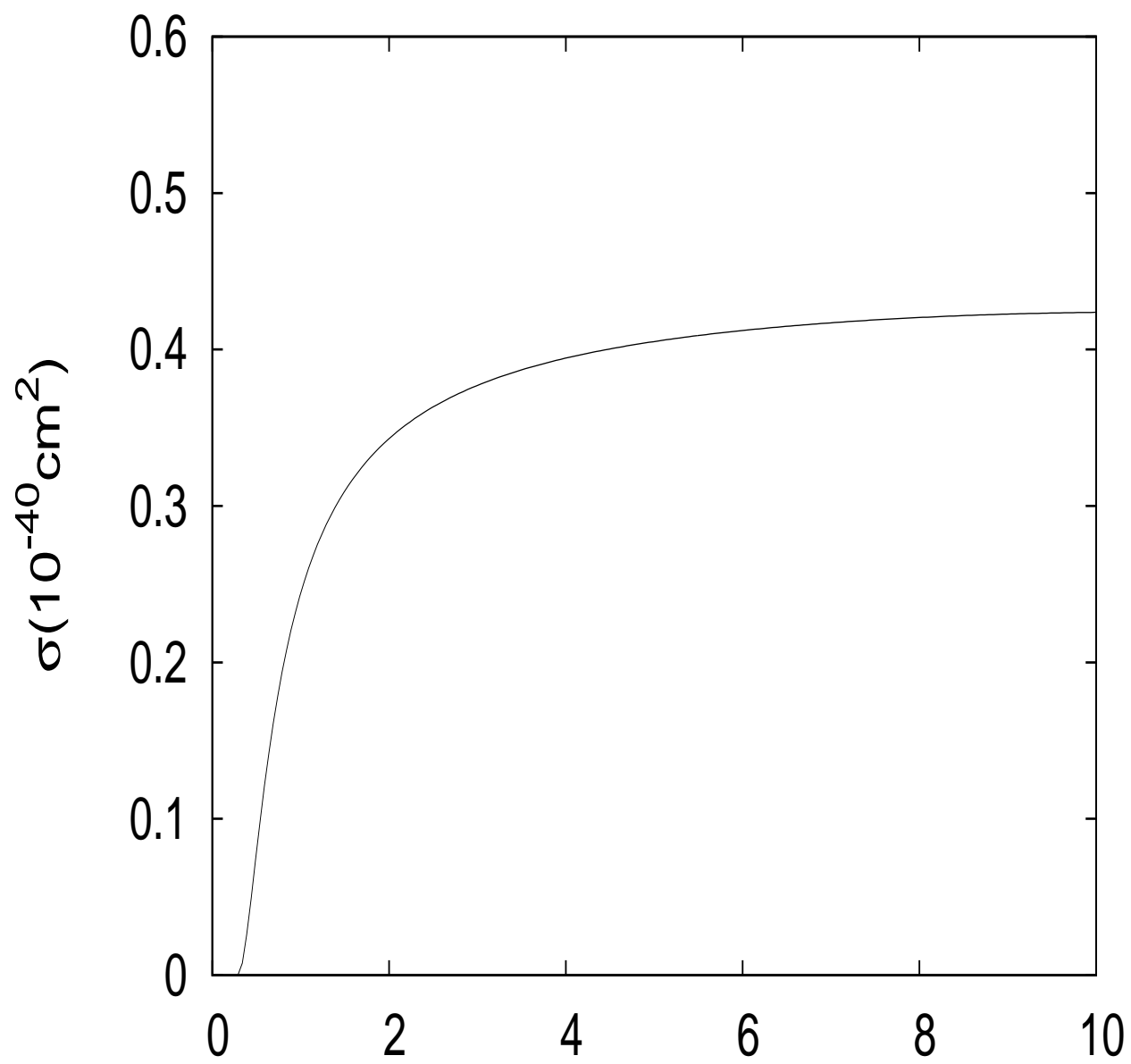


Fig.15 E GeV

11.1 Form factors of $p \rightarrow \Delta^{++}$

The S-matrix element of neutrino production of Δ is written as

$$\langle \mu^- \Delta^{++} | S | \nu_\mu p \rangle = -i(2\pi)^4 \delta^4(p_i + p_\nu - p_f - p_\mu) \frac{G}{\sqrt{2}} \cos\theta \langle \mu^- | j_\mu(0) | \nu_\mu \rangle \langle \Delta^{++} | J_\mu^W(0) | p \rangle. \quad (253)$$

The hadronic matrix element is expressed as

$$\begin{aligned} \langle \Delta^{++} | J_\mu^W(0) | p \rangle &= -\frac{i}{2} \int d^4x' d^4y' d^4x d^4y \bar{B}_{\alpha\beta\gamma}^{\frac{3}{2}\lambda'}(x', y', 0)_{ij1,111}^{i'j'k'} M(y', x', x, y) \\ &\quad \{ \gamma_\mu (1 + \lambda\gamma_5) + \frac{\kappa}{2m_p} \sigma_{\mu\nu} q_\nu \}_{\gamma\gamma'} B_{\gamma'\beta\alpha}^{\frac{1}{2}\lambda}(0, y, x)_{2ji,1}^{k'j'i',3}. \end{aligned} \quad (254)$$

Using the wave functions(33,46,47), the matrix element (254) is expressed as

$$\begin{aligned} \langle \Delta^{++} | J_\mu^W(0) | p \rangle &= \frac{1}{4} D_3(q^2) \bar{\psi}_\sigma^{\lambda'}(p') \{ \frac{A}{mm'} P_\rho q_\nu \epsilon_{\rho\nu\sigma\mu} + \frac{4B}{mm'} (p'_\mu q_\sigma - p' \cdot q \delta_{\mu\sigma}) \gamma_5 \\ &\quad + 4\lambda [C \delta_{\sigma\mu} - \frac{1}{mm'a'} (p' \cdot q \delta_{\sigma\mu} - p'_\mu q_\sigma)] + \frac{2\lambda D}{mm'} p_\rho q_\nu \epsilon_{\rho\nu\sigma\mu} \gamma_5 \} u_\lambda(p), \end{aligned} \quad (255)$$

where m , E , m' , E' are the masses and energies of proton and Δ respectively,

$$\begin{aligned} A &= \frac{2}{a'} + \kappa \{ \frac{2}{aa'} - \frac{1}{a} - \frac{1}{a'} + 1 + \frac{m'}{m} \}, \\ B &= 1 - \frac{1}{a'} + \frac{\kappa}{2} (\frac{1}{a} + \frac{1}{a'} - \frac{2}{aa'}), \\ C &= \frac{1}{a} + \frac{m'}{m} \frac{1}{a'}, \\ D &= 1 - \frac{1}{a'}, \end{aligned} \quad (256)$$

where a and a' are the proportional constants of proton and Δ respectively, $P_\mu = p_\mu + p'_\mu$,

$D_3(q^2)$ is given by Eq. (187), A and B are the same as Eqs. (156). Eq.(256) shows that the

coefficients B and D are resulted in the effects of antiquarks of nucleon. The conservation of the vector current is satisfied.

According to Ref. [7], there are 8 form factors

$$\begin{aligned}
T &\equiv \frac{G}{\sqrt{6}} \langle \Delta^{++} | J_\mu^W(0) | p \rangle \langle \mu^- | j_\mu(0) | \nu_\mu \rangle \\
&= \frac{G}{\sqrt{2}} \cos\theta \bar{\psi}(p')_\alpha \left\{ -\left[\frac{1}{m} G_3^V(q^2) \gamma_\mu + \frac{1}{m^2} G_4^V(q^2) p'_\mu + \frac{1}{m^2} G_5^V(q^2) p_\mu \right] \gamma_5 F^{\mu\nu} \right. \\
&\quad \left. G_6^V(q^2) j^\alpha \gamma_5 - \left[\frac{1}{m} G_3^A(q^2) \gamma_\mu + \frac{1}{m^2} G_4^A(q^2) p'_\mu \right] F^{\mu\nu} + G_5^A(q^2) j^\alpha + \frac{1}{m^2} G_6^A(q^2) q_\alpha q \cdot j \right\} u(p), \quad (257)
\end{aligned}$$

where

$$j_\alpha = \langle \mu^- | j_\alpha(0) | \nu \rangle,$$

$$F^{\mu\nu} = q_\mu j_\nu - q_\nu j_\mu, \quad (258)$$

p and p' are the momenta of the proton and the Δ respectively, $q = p - p'$. Comparing with

Eq. (255), it is obtained

$$G_3^V(q^2) = \frac{A}{2\sqrt{3}} D_3(q^2), \quad (259)$$

$$G_4^V(q^2) = -\frac{1}{2\sqrt{3}} \frac{m}{m'} (A - 2B) D_3(q^2), \quad (260)$$

$$G_5^V(q^2) = G_6^V(q^2) = 0, \quad (261)$$

$$G_3^A(q^2) = \frac{\lambda D}{\sqrt{3}} D_3(q^2), \quad (262)$$

$$G_4^A(q^2) = -\frac{\lambda}{\sqrt{3}} \left(\frac{1}{a'} - D \right) \frac{m}{m'} D_3(q^2), \quad (263)$$

$$G_5^A(q^2) = \frac{1}{\sqrt{3}} \lambda C D_3(q^2), \quad (264)$$

$$G_6^A(q^2) = 0. \quad (265)$$

Three axial-vector form factors are predicted. The $G_5^A(q^2)$ has been mentioned in Refs. [85,86]. $G_5^A(0)$ is computed

$$G_5^A(0) = \frac{1}{\sqrt{3}} \lambda C \sqrt{aa'} = 1.09. \quad (266)$$

In Ref.[85] many values of $G_5^A(0)$ have been listed. Using PCAC,

$$G_5^A(0) = \frac{g_\Delta f_\pi}{2\sqrt{3}M} = 1.2$$

is obtained [85] in the limit $m_\pi \rightarrow 0$ and

$$G_5^A(0) = 0.84, 1.07, 1.9,$$

are presented too from different approaches [85]. From Eq. (264) the $G_5^A(q^2)$ is expressed as

$$G_5^A(q^2) = G_5^A(0)(1 + 2.39\tau)^{-1}(1 + \frac{q^2}{0.71})^{-2}. \quad (267)$$

In Refs. [85,86] a dipole expression

$$G_5^A(q^2) = G_5^A(0)(1 + \frac{q^2}{M_A^2})^{-2} \quad (268)$$

has been applied to fit the data of the cross section of $\nu + p \rightarrow \mu^- + \Delta^{++}$ and the parameter M_A are determined to be

$$M_A = 0.92 \pm 0.14 \text{ GeV}, \quad M_A = 0.84 \pm 0.15 \text{ GeV},$$

and

$$M_A = 0.98 \text{ GeV}, \quad 0.95 \text{ GeV}$$

respectively. Obviously, unlike the form of dipole [85,86] the axial-vector form factor of $p \rightarrow \Delta^{++}$ (267) predicted in this model takes the form of triple pole and it is very different from the one of the dipole (268). However, when q^2 is small the parameter M_A is determined from Eq. (267) to be

$$M_A = 0.76 \text{ GeV}. \quad (269)$$

Besides the $G_5^A(q^2)$ this model predicts other two axial-vector form factors for the transition $p \rightarrow \Delta^{++}$

$$G_3^A(q^2) = -0.8434(1 + 2.39\tau)^{-1}(1 + \frac{q^2}{0.71})^{-2}, \quad (270)$$

$$G_4^A(q^2) = 0.1965(1 + 2.39\tau)^{-1}(1 + \frac{q^2}{0.71})^{-2}. \quad (271)$$

Therefore, in this model the $G_3^A(q^2)$ and the $G_5^A(q^2)$ are the two major axial-vector form factors for the transition $p \rightarrow \Delta^{++}$. The two vector form factors of this process (259,260) are determined to be

$$G_3^V(q^2) = 1.645(1 + 2.39\tau)^{-1}(1 + \frac{q^2}{0.71})^{-2}, \quad (272)$$

$$G_4^V(q^2) = -0.2323(1 + 2.39\tau)^{-1}(1 + \frac{q^2}{0.71})^{-2}, \quad (273)$$

$$G_4^V(q^2) = -0.141G_3^V(q^2). \quad (274)$$

The $G_3^V(q^2)$ is the major vector form factor of this process and it is the magnetic form factor.

This model predicts that two major axial-vector and one vector form factors contribute to the process $\nu + p \rightarrow \mu^- + \Delta^{++}$. These three form factors are in the forms of triple poles.

11.2 Cross section

Using Eq.(255), the differential cross section is written as

$$\frac{d^2\sigma}{d\Omega dE'} = \frac{G^2}{512\pi^3} \cos^2\theta E'^2 \tau_{\mu\nu} W_{\mu\nu} \frac{\Gamma(m')}{(m' - m_\Delta)^2 + \frac{1}{4}\Gamma^2(\Delta)}, \quad (275)$$

where

$$\begin{aligned} \tau_{\mu\nu} W_{\mu\nu} &= \frac{2}{3mm'\epsilon\epsilon'} D_3^2(q^2) \{4m^2 q^2 W_1 + [4m\epsilon(2m\epsilon + m^2 - m'^2) - 2mq^2(m + 2\epsilon)] W_2 \\ &\quad - q^2(q^2 - 4m\epsilon + m'^2 - m^2) W_3\} \\ W_1 &= \frac{1}{m^2} (q^2 + m_+^2) (4\lambda^2 C'^2 + \frac{A^2}{m^2} q^{*2}) + \frac{4}{m^2} (q^2 + m_-^2) [B^2 \frac{p'q}{m^2 m'^2} + \frac{\lambda^2 D^2}{m^2} q^{*2}] \\ &\quad + 4 \frac{q^{*2}}{m^2} (AB \frac{p'q}{m^2} - 2\lambda^2 C' D \frac{m'}{m}), \\ W_2 &= \frac{q^2 + m_+^2}{mm'} \{4\lambda^2 [\frac{m}{m'} C'^2 + \frac{2C'}{a'} \frac{p'q}{m'^2} + \frac{q^{*2}}{mm'a'}] + \frac{A^2}{mm'} q^2\} \\ &\quad + \frac{4q^2}{m^2 m'^2} (q^2 + m_-^2) (B^2 + \lambda^2 D^2) + \frac{4q^2}{mm'} [AB \frac{p'1}{mm'} - 2\lambda^2 C' D], \\ W_3 &= 8\lambda A (\frac{q^2 + M_+^2}{mm'} C' - \frac{q^{*2}}{m^2} D) + 16\lambda B \frac{p'q}{mm'} (C' - D \frac{q^2 + m_-^2}{mm'}), \end{aligned} \quad (276)$$

ϵ is the energy of neutrino, $m'^2 = (p + p_\nu - p_\mu)^2$, $\Gamma(m')$ is the decay width of Δ . Using Eq. (257), the cross sections and the differential cross section of $\nu + p \rightarrow \mu^- + \Delta^{++}$ are calculated.

The comparison between theoretical results and the experimental data are shown in Fig. 16, 17, 18, 19.

The data of Fig. 16 and Fig. 17 are taken from Ref. [85].

Newer experimental data [86] of $\sigma(\nu + p \rightarrow \mu^- + \Delta^{++}(p + \pi^+))$ and $\frac{d\sigma}{dq^2}$ are shown in Fig. 18 and Fig. 19. The data used in Fig. 18 and Fig. 19 [86] are the cross sections of $\nu + p \rightarrow \mu^- p + \pi^+$ when $M_{N\pi} < 1.4$ GeV. The background has not been subtracted. Fig. 16, 17, 18, 19 show that theoretical predictions are compatible with data.

11.3 Density matrix

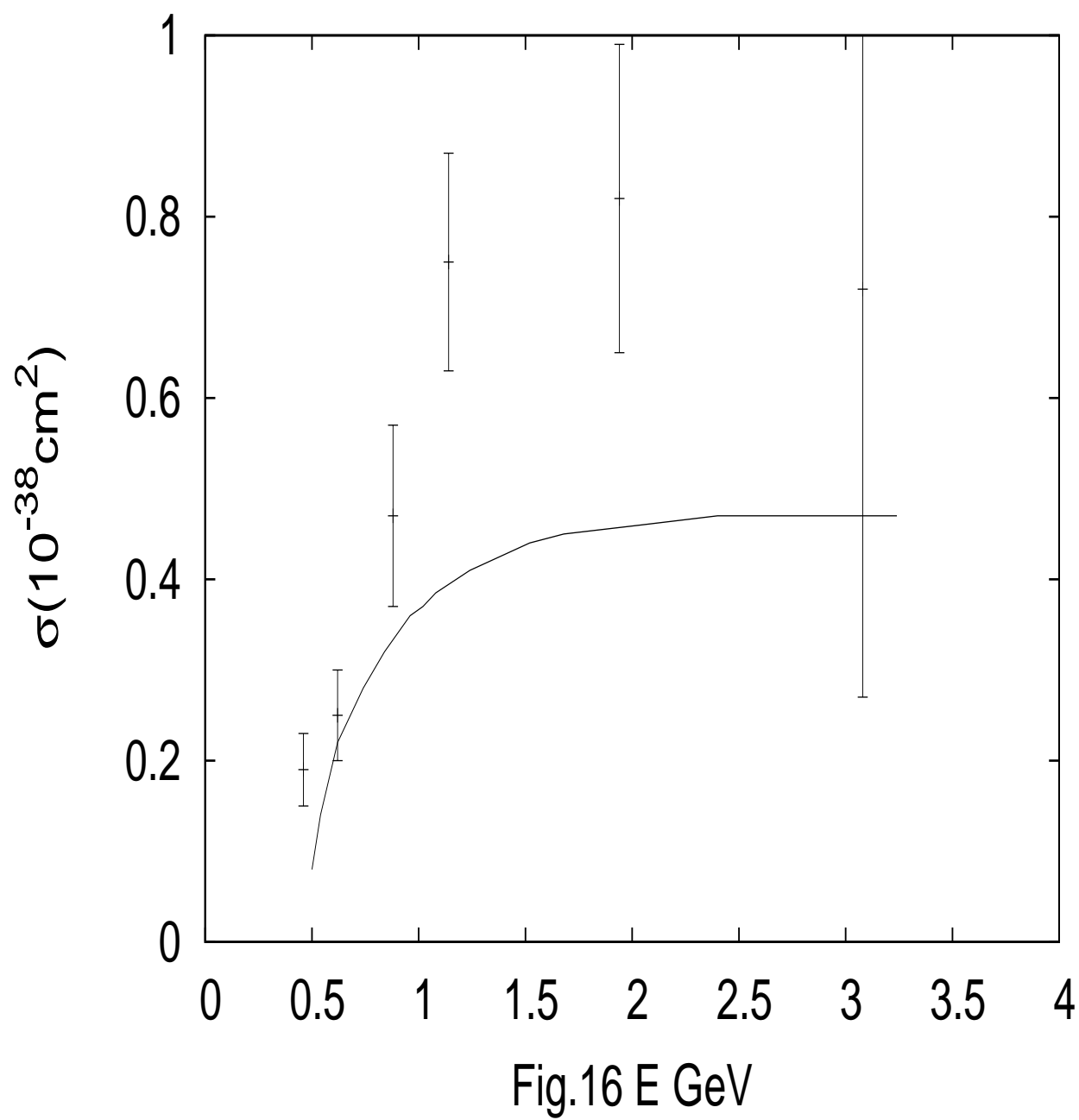
When pions produced from the decay of the Δ are measured the differential cross section is written as

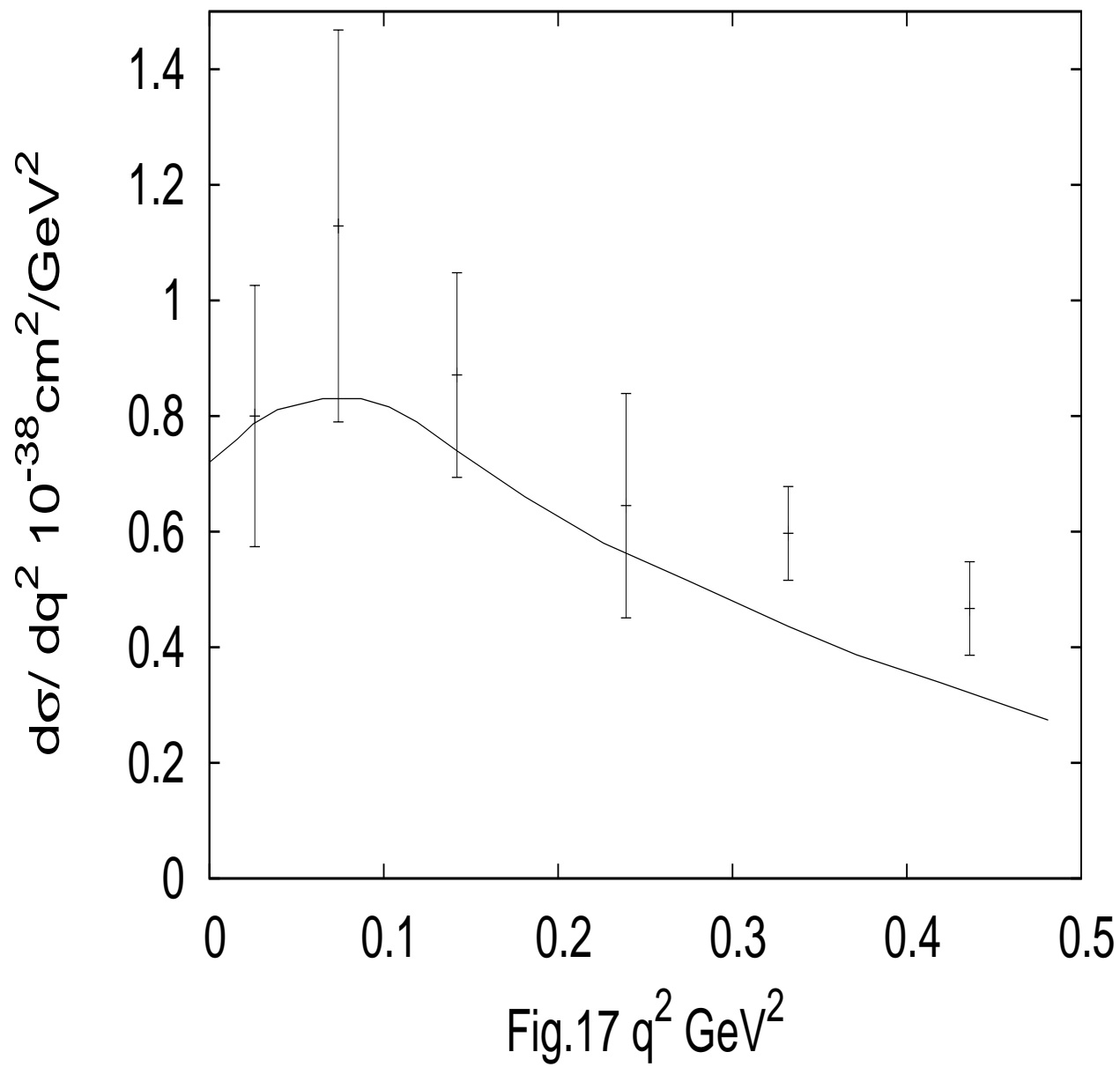
$$\begin{aligned} \frac{d^4\sigma}{dq^2 dm'^2 d\Omega_\pi} = & \frac{1}{4\pi} \frac{d^2\sigma}{dq^2 dm'^2} \left\{ Y_{00} - 2\sqrt{5}(\rho_{33} - \frac{1}{2})Y_{20} \right. \\ & \left. + \frac{4}{\sqrt{10}}\rho_{31}ReY_{21} - 4\sqrt{10}\rho_{3-1}ReY_{22} \right\}, \end{aligned} \quad (278)$$

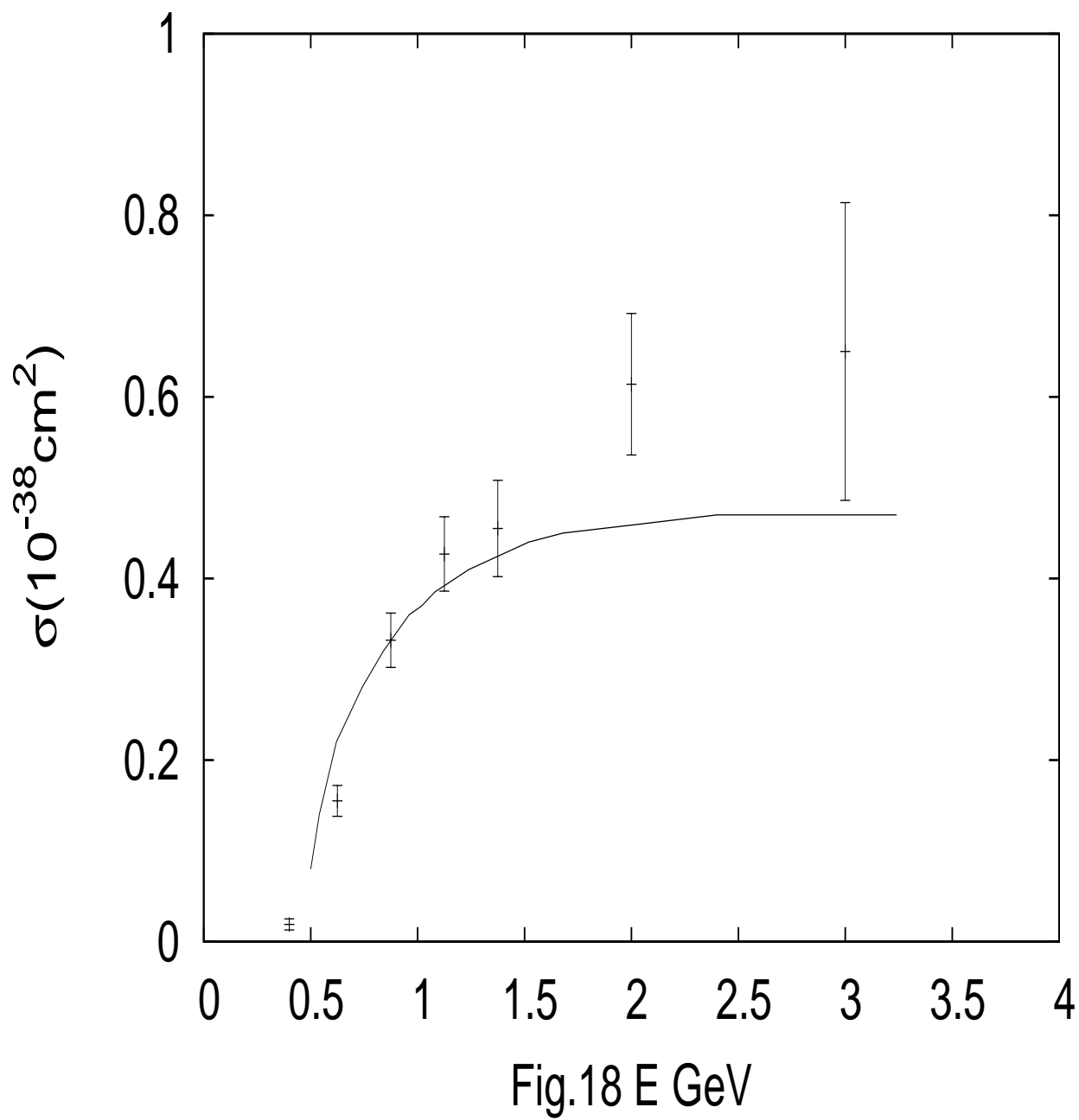
$\frac{d^2\sigma}{dq^2 dm'^2}$ is derived from Eq.(257). The results are shown in Table 6.

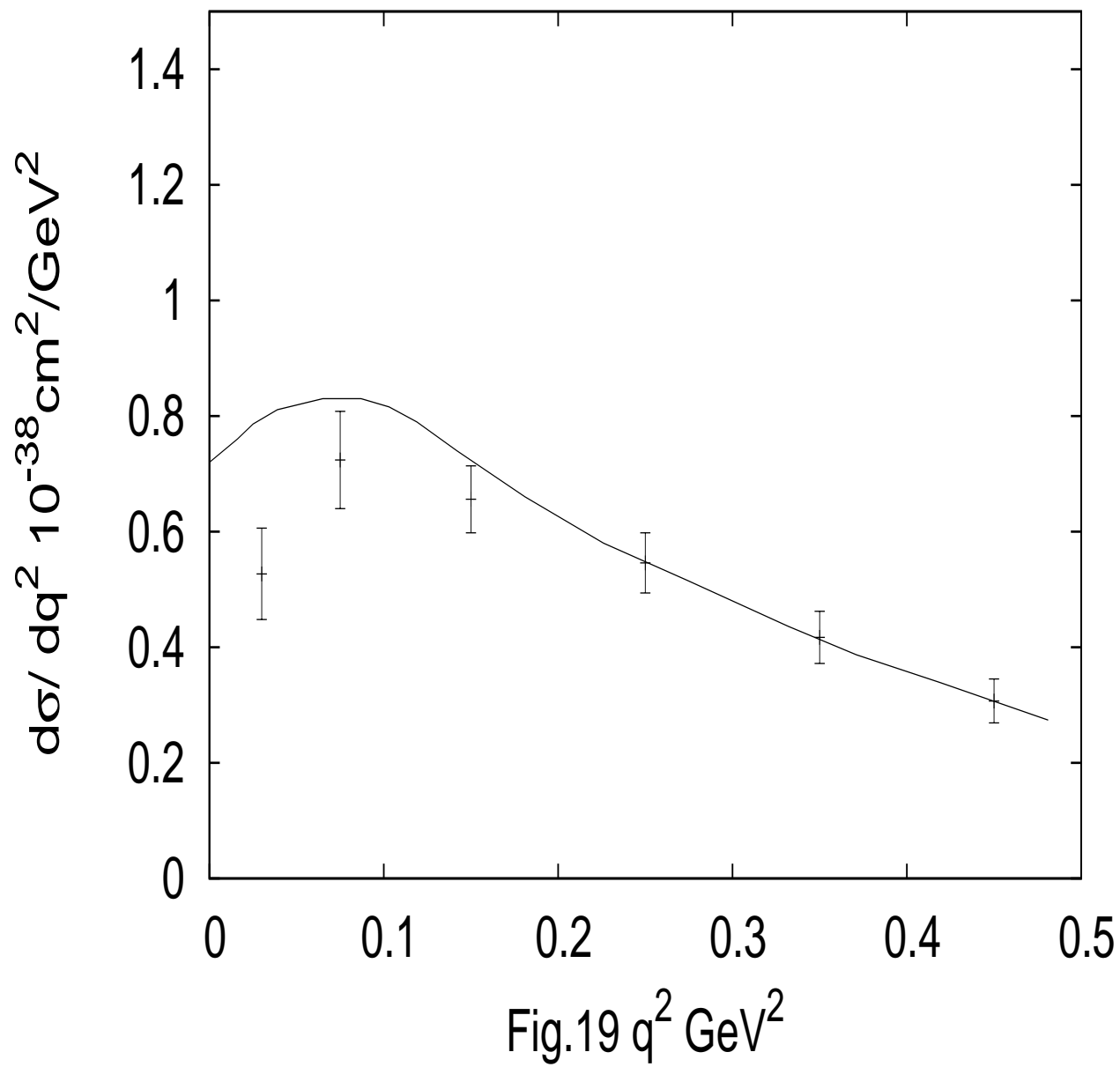
12 σ term of nucleon

In this model there are two Lorentz invariant functions, f_1 and f_2 , in the wave functions. It is shown in section 1 that the difference between f_1 and f_2 represents the antiquark spinors.









If $f_1 = f_2$ the effects of the antiquark spinors disappear and theoretical results disagree with data. As shown in this paper the contribution of the antiquarks plays essential role in the EM and weak form factors of nucleon or the structure of nucleon.

The σ term of nucleon is calculated

$$\sigma = \langle p | m_u \bar{u}u + m_d \bar{d}d | p \rangle = (a + \frac{1}{a} - 1)(2m_u + m_d) = 3.73 (2m_u + m_d). \quad (279)$$

There is a wide range for m_u and m_d [46]: $m_u = 2.3^{+0.7}_{-0.5}$ MeV, $m_d = 4.8^{+0.7}_{-0.3}$ MeV. The σ term of nucleon is determined to be

$$\sigma = 30.2 - 42.9 \text{ MeV}. \quad (280)$$

If $a = 1$ is taken,

$$\sigma = 2m_u + m_d = 8.1 - 11.5 \text{ MeV}$$

is obtained. This value of the σ term is much smaller than the one (280) and much smaller than other results.

In Ref. [88] $\sigma \sim 45$ MeV is determined. In Refs. [92,94] the σ term determined by Lattice calculations are listed

$$15 - 25 \text{ MeV}, 40 - 60 \text{ MeV}, 50 \pm 3 \text{ MeV}, 45 - 55 \text{ MeV}, 18 \pm 5 \text{ MeV}, 49 \pm 3 \text{ MeV}.$$

In Ref. [14] $\sigma = 37 \pm 8 \pm 6$ MeV is reported. $\sigma = 52 \pm 3 \pm 8$ MeV is obtained in Ref. [93].

The value of the σ term obtained in this paper is compatible with these values.

13 Antiquark components of nucleon

As mentioned in this paper that the antiquark spinors v_{\pm} (30) of baryons play very important role in understanding the structure of baryon. Eq. (42) shows that the antiquark spinors contribute to the density of the antiquarks of nucleon.

In Ref. [14] the antiquark content of proton is defined as Eq. (42). This definition (42) has been used to study the quark sea of nucleon and the σ term of nucleon. Eq. (42) can be used to argue the existence of the contents of \bar{u} and \bar{d} in a proton.

From the expressions of the wave functions of nucleon (33,34) if $f_1 = f_2$ is taken only the quark components contribute. The matrix γ_0 doesn't affects the wave function in the rest frame, therefore,

$$\langle p | \bar{\psi}_i \psi_i | p \rangle = \langle p | \bar{\psi}_i \gamma_0 \psi_i | p \rangle$$

the antiquark content of nucleon is zero. However, if $f_1 \neq f_2$ antiquark spinors are part of the wave functions. When γ_0 acts on antiquark spinors a minus sign is generated. Then

$$\langle p | \bar{\psi}_i \psi_i | p \rangle \neq \langle p | \bar{\psi}_i \gamma_0 \psi_i | p \rangle$$

and according to Eq. (42), $\bar{q}_i \neq 0$. Of course, meson clouds contribute to the antiquark contents of nucleon.

Using the wave functions (33,34), the antiquark densities

$$\bar{u} = \frac{1}{2} \langle p | \bar{u} (1 - \gamma_0) u | p \rangle,$$

$$\begin{aligned}
\bar{d} &= \frac{1}{2} \langle p | \bar{d} (1 - \gamma_0) d | p \rangle, \\
\bar{s} &= \frac{1}{2} \langle p | \bar{s} (1 - \gamma_0) s | p \rangle
\end{aligned} \tag{281}$$

are calculated

$$\begin{aligned}
\bar{u} &= \frac{2}{a} (a - 1)^2, \\
\bar{d} &= \frac{1}{a} (a - 1)^2, \\
\bar{s} &= 0.
\end{aligned} \tag{282}$$

In this model there is no strange quark component. Therefore, $\bar{s} = 0$ is natural. The antiquark density, \bar{u} and \bar{d} , vanish when $a = 1$ as expected. Obviously, there are other contributors for the density of the antiquarks of nucleon. Eq. (281) shows the contribution of the antiquark spinors of nucleon to the density of antiquark of proton only. It is very interesting to explore the dynamics of nonzero antiquark density. This investigation is beyond the scope of this paper.

14 Summary

A review of an approach of the study of EM and weak structure of nucleon done in Refs. [4,5,6,7] in 70's is presented. In these study a nucleon in the rest frame is spherical. The wave functions of $\frac{1}{2}^+$ and $\frac{3}{2}^+$ in the frame of center of mass are SU(6) symmetric and are boosted

to moving frame by Lorentz transformation. Antiquark components (spinors of antiquarks) are naturally cooperated in these wave functions. These wave functions, effective Lagrangian of electromagnetic and weak interactions [1] have been applied to study the electromagnetic and weak form factors of nucleons and $p \rightarrow \Delta$. There are three inputs: $G_M^p(q^2)$, μ_p , and μ_Λ . A new expression of $R = \frac{\mu_p G_E^p(q^2)}{G_M^p(q^2)}$ is obtained. In small region of q^2 the ratio is flat and $R \sim 1$ and it agrees with data. As q^2 increases the ratio decreases and is consistent with data when $q^2 < 5 \text{ GeV}^2$. The ratio predicted by this model decreases faster than the data when $q^2 > 5 \text{ GeV}^2$. Nonzero small electric form factor $G_E^n(q^2)$ is predicted and agrees with data when $q^2 < 0.3 \text{ GeV}^2$. When $q^2 > 0.3 \text{ GeV}^2$ $G_E^n(q^2)$ is larger than the experimental data. In this model the $G_E^n(q^2)$ is resulted in the contribution of the antiquark components. The magnetic moments of hyperons predicted by this model have the right signs but smaller than data by about 30%. The SU(3) symmetry breaking must be taken into account. The transit magnetic moment $\mu_{p \rightarrow \Delta}$ predicted by this model agrees well with data. Two helicity amplitudes of $\Delta \rightarrow N + \gamma$ are predicted. The the magnetic transition is dominated and $E1+$ moment contributes about 5% of the magnetic amplitude. The magnetic amplitude agrees with data. The helicity amplitudes and the decay rate predicted are in good agreement with data. For the process $e + p \rightarrow \Delta^+ + e$ three form factors, G_{M1+} , G_{E1+} , G_{S1+} , are determined. The G_{M1+} decreases faster with q^2 than $G_M^p(q^2)$ and agrees with data in small q^2 region. In the region of larger q^2 the G_{M1+} predicted decreases faster. In the form factor

G_{M1+} $SU(6)$ symmetry is applied and the $\frac{1}{\mu_p}G_M^p(q^2) = \frac{1}{(1+\frac{q^2}{0.71})^2}$ is inputted to G_{M1+} and the mass difference between proton and Δ is ignored. Phenomenologically, when the effect of the physical mass of the Δ is taken into account the G_{M1+} agrees with data when $q^2 < 5 \text{ GeV}^2$. Therefore, the $SU(6)$ symmetry breaking effect plays an important role in the behavior of the G_{M1+} at larger q^2 . This model presents a new picture for the structure of nucleon. Both the negative and small $E1 + (q^2)$ and the $S1 + (q^2)$ form factors are resulted in both the contribution of antiquark components and Lorentz contraction. In the rest frame both the proton and the Δ are spherical. The $S1 + (q^2)$ form factor is consistent with data and the $E1 + (q^2)$ is small and about twice of the data. This model doesn't work well in the range of large q^2 . In the range of large q^2 many new physical effects like internal motions of quarks and perturbative gluons should play roles. The assumption $f_2 = af_1$ may not work well for large q^2 too. This is the limitation of this model.

The new wave functions of baryons are applied to study the weak interactions of baryons. There is an additional parameter λ for the axial-vector currents of quarks [1], which is determined by inputting $G_A(0)$ of the β decay of nucleon. The axial-vector constants of hyperons, G_A , are predicted. The theoretical predictions of the semi-leptonic decays of neutron and all hyperons are in good agreement with data. The axial-vector form factor $G_A(q^2)$ of nucleon is predicted to be $G_A(q^2) = F_1^p(q^2)$. It is not in the form of dipole exactly. However, numerical calculation shows that the $G_A(q^2)$ predicted is in good agreement with

the form of dipole with $M_A = 1.002\text{GeV}$. It is interesting to notice that the pseudoscalar form factor of nucleon is caused by the antiquark components. The theoretical predictions of the cross sections of $\nu + n \rightarrow p + \mu$, $\bar{\nu} + p \rightarrow n + \mu^+$ agree with data well. The $\Delta S = 1$ quasielastic neutrino scattering $\bar{\nu} + p \rightarrow \Lambda + \mu^+$ and $\bar{\nu} + p \rightarrow \Sigma^0 + \mu^+$ are predicted. This approach has been applied to study $\nu + p \rightarrow \Delta^{++} + \mu^-$ without new parameters. There are three vector form factors and three axial-vector form factors. One vector and two axial-vector form factors play dominant roles. The form factors, especially the axial-vector form factors are not in the form of dipoles, but in the form of tripoles. The cross section, differential cross section, and density matrix elements are predicted. Theory are consistent with data.

The study presented in this review paper shows that antiquark components of nucleon play an essential role in understanding nucleon structure.

Appendix

Appendix I Flavor wave functions of baryons

The flavor wave functions for $\frac{1}{2}^+$ baryons:

$$\begin{aligned}
 p, \quad B &= \begin{pmatrix} 0 & 0 & 1 \\ 0 & 0 & 0 \\ 0 & 0 & 0 \end{pmatrix}, \quad n, \quad B = \begin{pmatrix} 0 & 0 & 0 \\ 0 & 0 & 1 \\ 0 & 0 & 0 \end{pmatrix}, \\
 \Sigma^+, \quad B &= \begin{pmatrix} 0 & 1 & 0 \\ 0 & 0 & 0 \\ 0 & 0 & 0 \end{pmatrix}, \quad \Sigma^-, \quad B = \begin{pmatrix} 0 & 0 & 0 \\ 1 & 0 & 0 \\ 0 & 0 & 0 \end{pmatrix}, \\
 \Sigma^0, \quad B &= \frac{1}{\sqrt{2}} \begin{pmatrix} 1 & 0 & 0 \\ 0 & -1 & 0 \\ 0 & 0 & 0 \end{pmatrix}, \quad \Lambda, \quad B = \frac{1}{\sqrt{6}} \begin{pmatrix} 1 & 0 & 0 \\ 0 & 1 & 0 \\ 0 & 0 & -2 \end{pmatrix}, \\
 \Xi^-, \quad B &= \begin{pmatrix} 0 & 0 & 0 \\ 0 & 0 & 0 \\ 1 & 0 & 0 \end{pmatrix}, \quad \Xi^0, \quad B = \begin{pmatrix} 0 & 0 & 0 \\ 0 & 0 & 0 \\ 0 & 1 & 0 \end{pmatrix},
 \end{aligned}$$

The flavor wave functions of $\frac{3}{2}^+$ baryons are defined as

$$\begin{aligned}
 d_{111}^{111} &= \Delta^{++}, \quad d_{112}^{112} = \frac{1}{\sqrt{3}}\Delta^+, \quad d_{122}^{122} = \frac{1}{\sqrt{3}}\Delta^0, \quad d_{222}^{222} = \Delta^-, \\
 d_{113}^{113} &= \frac{1}{\sqrt{3}}\Sigma^{*+}, \quad d_{123}^{123} = \frac{1}{\sqrt{6}}\Sigma^{*0}, \quad d_{223}^{223} = \frac{1}{\sqrt{3}}\Sigma^{*-},
 \end{aligned}$$

$$d_{133}^{133} = \frac{1}{\sqrt{3}}\Xi^{*0}, \quad d_{233}^{233} = \frac{1}{\sqrt{3}}\Xi^{*-}, \quad d_{333}^{333} = \Omega^-.$$

Appendix II Permutation operators

The four operators of permutation are expressed as

$$O_1 = \frac{1}{6}\{2e + 2(12) - (13) - (32) - (123) - (132)\} \quad (283)$$

$$O_2 = \frac{1}{6}\{2e - 2(12) + (13) + (32) - (123) - (132)\} \quad (284)$$

$$Y_s = \frac{1}{6}\{e + (12) + (13) + (32) + (123) + (132)\} \quad (285)$$

$$Y_a = \frac{1}{6}\{e - (12) - (13) - (32) + (123) + (132)\} \quad (286)$$

The O_1 and O_2 projectors satisfy

$$O_1 \cdot O_1 = O_1$$

$$O_2 \cdot O_2 = O_2$$

$$O_1 \cdot O_2 = 0. \quad (287)$$

Appendix III Wave functions of excited baryons

As mentioned in the paper the electromagnetic and weak interactions of baryons which are in s-wave in the rest frame have been studied by this approach reasonably well. This approach can be extended to study the EM and neutrino(antineutrino) productions of the low-lying excited baryons. The effective electromagnetic currents and the weak currents are the same as Eqs. (48,196). The wave functions of excited baryons can be constructed in the same way.

The wave functions of low lying excited baryons have been constructed in Ref. [4] and are presented in this section of Appendix. In the rest frame of the center of mass the $O(3) \times SU(6)$ symmetry is assumed for these states. In the rest frame $O(3)$ symmetry determines the part of orbital angular momentum of baryon and the $SU(6)$ symmetry determines the parts of the spin and the flavor. The flavor, spin, and the orbital wave functions of the baryon is totally symmetric. Of course the color part is antisymmetric. According to $SU(6)$ symmetry, baryons can be classified as 56, 70, 20 states. These states are decomposed as states of spin ($S = \frac{1}{2}$ or $S = \frac{3}{2}$) and flavor (octet, decuplet, or singlet)

$$\begin{aligned}
\text{56} &= (\frac{3}{2}, 10) + (\frac{1}{2}, 8), \\
\text{70} &= (\frac{3}{2}, 8) + (\frac{1}{2}, 8) + (\frac{1}{2}, 10) + (\frac{1}{2}, 1), \\
\text{20} &= (\frac{1}{2}, 8) + (\frac{3}{2}, 1).
\end{aligned} \tag{288}$$

The wave functions of baryons of the 56 in s-wave have been studied and presented in this paper. The wave functions in p wave and d waves [4] are constructed below. Baryon is a system of three quarks. There are two independent relative coordinates $x = x_1 - x_2$, $y = \frac{1}{2}(x_1 + x_2) - x_3$. Therefore, in the rest frame of the baryon there are two relative orbital angular momentum.

(1s1p) wave functions of baryon

In the rest frame there are two spacial wave functions

$$f_1(x, y)x_j, \quad f_2(x, y)y_j, \quad (289)$$

where $j = 1, 2, 3$, x_j and y_j have O_2 or O_1 symmetry respectively

$$O_2 x_j = x_j, \quad O_1 y_j = y_j, \quad (290)$$

$f_{1,2}(x, y)$ are new Lorentz invariant functions which are total symmetric in x_1, x_2, x_3 . The parity of the baryon of p-wave is negative and they are 20-plet. The spacial, the spin, and the flavor wave function must be total symmetric. The wave functions are constructed

1. $S = \frac{1}{2}$ and Octet

$$\begin{aligned} B_{\alpha\beta\gamma,ijk}^{JM}(x, y)_l^m &= \frac{1}{2}\epsilon_{i'j'k'} \sum_{\lambda,c} C_{1\lambda\frac{1}{2}c}^{JM} x \cdot e^\lambda(p) \{ \Gamma_{\gamma\beta,\alpha}^{\frac{1}{2}}(x, y, p)_c \epsilon_{jkm} \delta_{il} \\ &\quad + \Gamma_{\alpha\gamma,\beta}^{\frac{1}{2}}(x, y, p)_c \epsilon_{ikm} \delta_{jl} \} + \frac{1}{3}\epsilon_{i'j'k'} \sum_{\lambda,c} C_{1\lambda\frac{1}{2}c}^{JM} y \cdot e^\lambda(p) \\ &\quad \{ \Gamma_{\gamma\beta,\alpha}^{\frac{1}{2}}(x, y, p)_c (\epsilon_{jim} \delta_{kl} + \epsilon_{kim} \delta_{jl}) + \Gamma_{\alpha\gamma,\beta}^{\frac{1}{2}}(x, y, p)_c (\epsilon_{jim} \delta_{kl} + \epsilon_{jkm} \delta_{il}) \}. \end{aligned} \quad (291)$$

2. $S = \frac{3}{2}$ and Octet

$$\begin{aligned} B_{\alpha\beta\gamma,ijk}^{JM}(x, y)_l^m &= \epsilon_{i'j'k'} \sum_{\lambda,c} C_{1\lambda\frac{3}{2}c}^{JM} \Gamma_{\alpha\beta\gamma}^{\frac{3}{2}}(x, y, p)_c \{ \frac{1}{2} x \cdot e^\lambda(p) \\ &\quad \epsilon_{ijm} \delta_{kl} + \frac{1}{3} y \cdot e^\lambda(p) (\epsilon_{jim} \delta_{kl} + \epsilon_{jkm} \delta_{il}) \} \end{aligned} \quad (292)$$

3. $S = \frac{1}{2}$ and Decuplet

$$B_{\alpha\beta\gamma,ijk}^{JM,lmn}(x,y) = \frac{1}{2}\epsilon_{i'j'k'}d_{ijk}^{lmn}\sum_{\lambda,c}C_{1\lambda\frac{1}{2}c}^{JM}\{x\cdot e^\lambda(p)\Gamma_{\alpha\beta,\gamma}^{\frac{1}{2}}(x,y,p)_c \\ + \frac{2}{3}y\cdot e^\lambda(p)[\Gamma_{\gamma\alpha,\beta}^{\frac{1}{2}}(x,y,p)_c + \Gamma_{\gamma\beta,\alpha}^{\frac{1}{2}}(x,y,p)_c]\} \quad (293)$$

4. $S = \frac{1}{2}$ and Singlet

$$B_{\alpha\beta\gamma}^{JM}(x,y) = \epsilon_{i'j'k'}\epsilon_{ijk}\sum_{\lambda,c}C_{1\lambda\frac{1}{2}c}^{JM}\{\frac{1}{2}x\cdot e^\lambda(p)[\Gamma_{\beta\gamma,\alpha}^{\frac{1}{2}}(x,y,p)_c \\ + \Gamma_{\alpha\gamma,\beta}^{\frac{1}{2}}(x,y,p)_c] + y\cdot e^\lambda(p)\Gamma_{\alpha\beta,\gamma}^{\frac{1}{2}}(x,y,p)_c\} \quad (294)$$

(1p1p) and (1s1d) wave functions of baryons

The parity of those states are positive. For states of (1p1p) there are three orbital angular momentum

$$L = 2, 1, 0.$$

Their spacial wave functions and property of symmetry of these states are

$$\begin{aligned} L = 2, \quad f(x,y) \sum_{\lambda_1,\lambda_2} C_{1\lambda_1,1\lambda_2}^{(2\lambda)} x\cdot e^{\lambda_1}(p) y\cdot e^{\lambda_2}(p) \quad O_2 \\ L = 1, \quad f(x,y) \sum_{\lambda_1,\lambda_2} C_{1\lambda_1,1\lambda_2}^{(1\lambda)} x\cdot e^{\lambda_1}(p) y\cdot e^{\lambda_2}(p) \quad Y_a \\ L = 0, \quad f(x,y) \{x\cdot y + \frac{1}{m^2}p\cdot xp\cdot y\}, \quad O_2. \end{aligned} \quad (295)$$

The spacial wave functions of the (1s1d) states are $L = 2$ and

$$\begin{aligned} f_1(x, y) C_{1\lambda_1, 1\lambda_2}^{(2\lambda)} x \cdot e_1^\lambda(p) x \cdot e_2^\lambda(p), \quad Y_s, \quad O_1, \\ f_2(x, y) C_{1\lambda_1, 1\lambda_2}^{(2\lambda)} y \cdot e_1^\lambda(p) y \cdot e_2^\lambda(p), \quad Y_s, \quad O_1. \end{aligned} \quad (296)$$

The classification of these states are

(1s1d) are 56 – plet,

the $L = 2$ states of (1s1d) and (1p1p) are 70 – plet,

the $L = 1$ of (1p1p) are 20 – plet,

the $L = 0$ of (1p1p) are 70 – plet.

The complete wave functions of these states are constructed as

1. $L = 2$ 56-plet

Octet

$$\begin{aligned} B_{\alpha\beta\gamma,ijk}^{JM}(x, y)_l^m &= \epsilon_{i'j'k'} \sum_{\lambda, c} C_{2\lambda\frac{1}{2}c}^{JM} C_{1\lambda_1 1\lambda_2}^{2\lambda} \{x \cdot e^{\lambda_1}(p) x \cdot e^{\lambda_2}(p) \\ &+ \frac{4}{3} y \cdot e^{\lambda_1}(p) y \cdot e^{\lambda_2}(p)\} \{\Gamma_{\alpha\beta, \gamma}^{\frac{1}{2}}(x, y, p)_c (\epsilon_{ijm} \delta_{kl} + \epsilon_{ikm} \delta_{jl}) \\ &+ \Gamma_{\beta\gamma, \alpha}^{\frac{1}{2}}(x, y, p)_c (\epsilon_{jkm} \delta_{il} + \epsilon_{ikm} \delta_{jl})\}. \end{aligned} \quad (297)$$

Decuplet

$$B_{\alpha\beta\gamma,ijk}^{JM,lmn}(x, y) = \epsilon_{i'j'k'} d_{ijk}^{lmn} \sum_{\lambda_1, \lambda_2} C_{2\lambda\frac{3}{2}c}^{JM} C_{1\lambda_1, 1\lambda_2}^{2\lambda} \{x \cdot e^{\lambda_1}(p) x \cdot e^{\lambda_2}(p) + \frac{4}{3} y \cdot e^{\lambda_1}(p) y \cdot e^{\lambda_2}(p)\} \Gamma_{\alpha\beta\gamma}^{\frac{3}{2}}(x, y, p)_c. \quad (298)$$

2. $L = 0$ 56-plet

The wave functions can be obtained by replacing

$$\sum_{\lambda_1, \lambda_2} C_{2\lambda\frac{3}{2}c}^{JM} \{x \cdot e^{\lambda_1}(p) x \cdot e^{\lambda_2}(p) + \frac{4}{3} y \cdot e^{\lambda_1}(p) y \cdot e^{\lambda_2}(p)\}$$

of Eqs. (293,294) by

$$x^2 + \frac{4}{3}y^2 + \frac{1}{m^2} \{(p \cdot x)^2 + \frac{4}{3}(p \cdot y)^2\}.$$

These states are the radial excitations of the ground states of the 56-plet.

3. $L = 0$ 70-plet $S = \frac{1}{2}$ **Octet**

$$\begin{aligned} B_{\alpha\beta\gamma,ijk}^{\frac{1}{2}\lambda}(x, y)_l^m &= \frac{1}{2} \epsilon_{i'j'k'} (x \cdot y + \frac{1}{m^2} p \cdot x p \cdot y) \{ \Gamma_{\alpha\gamma, \beta}^{\frac{1}{2}}(x, y, p)_\lambda \epsilon_{ikm} \delta_{jl} \\ &+ \Gamma_{\gamma\beta, \alpha}^{\frac{1}{2}}(x, y, p)_\lambda \epsilon_{jkm} \delta_{il} \} + \frac{1}{8} \epsilon_{i'j'k'} \{ x^2 - \frac{4}{3} y^2 + \frac{1}{m^2} ((p \cdot x)^2 - \frac{4}{3} (p \cdot y)^2) \} \\ &\{ \Gamma_{\gamma\beta, \alpha}^{\frac{1}{2}}(x, y, p)_\lambda (\epsilon_{jim} \delta_{kl} + \epsilon_{kim} \delta_{jl}) + \Gamma_{\gamma\alpha, \beta}^{\frac{1}{2}}(x, y, p)_\lambda (\epsilon_{kjm} \delta_{il} + \epsilon_{ijm} \delta_{kl}) \}. \end{aligned} \quad (299)$$

$$S = \frac{3}{2} \text{ Octet}$$

$$B_{\alpha\beta\gamma,ijk}^{\frac{3}{2}\lambda}(x, y)_l^m = \frac{1}{2}\epsilon_{i'j'k'}\Gamma_{\gamma\beta\alpha}^{\frac{3}{2}}(x, y, p)_\lambda \left\{ (x \cdot y + \frac{1}{m^2}p \cdot xp \cdot y)\epsilon_{ijm}\delta_{kl} \right. \\ \left. + \frac{1}{4}[x^2 - \frac{4}{3}y^2 + \frac{1}{m^2}(p \cdot x)^2 - \frac{4}{3}\frac{1}{m^2}(p \cdot y)^2](\epsilon_{kjm}\delta_{il} + \epsilon_{kim}\delta_{jl}) \right\}. \quad (300)$$

$$S = \frac{1}{2} \text{ Decuplet}$$

$$B_{\alpha\beta\gamma,ijk}^{\frac{1}{2}\lambda,lmn}(x, y) = \epsilon_{i'j'k'}d_{ijk}^{lmn}(x \cdot y + \frac{1}{m^2}p \cdot xp \cdot y) \\ \{ \Gamma_{\gamma\beta,\alpha}^{\frac{1}{2}}(x, y, p)_\lambda + \Gamma_{\gamma\alpha,\beta}^{\frac{1}{2}}(x, y, p)_\lambda \}. \quad (301)$$

$$S = \frac{1}{2} \text{ Singlet}$$

$$B_{\alpha\beta\gamma}^{\frac{1}{2}\lambda}(x, y) = \epsilon_{i'j'k'}\epsilon_{ijk}(x \cdot y + \frac{1}{m^2}p \cdot xp \cdot y) \\ \{ \Gamma_{\beta\gamma,\alpha}^{\frac{1}{2}}(x, y, p)_\lambda + \Gamma_{\gamma\alpha,\beta}^{\frac{1}{2}}(x, y, p)_\lambda \} \\ + \frac{3}{8}\epsilon_{i'j'k'}\epsilon_{ijk} \{ x^2 - \frac{4}{3}y^2 + \frac{1}{m^2}(p \cdot x)^2 - \frac{4}{3}\frac{1}{m^2}(p \cdot y)^2 \} \Gamma_{\alpha\beta,\gamma}^{\frac{1}{2}}(x, y, p)_\lambda. \quad (302)$$

4. $L = 2$ 70-plet

$$S = \frac{1}{2} \text{ Octet}$$

$$B_{\alpha\beta\gamma,ijk}^{JM}(x, y)_l^m = \frac{1}{2}\epsilon_{i'j'k'} \sum_{\lambda_1, \lambda_2} C_{2\lambda\frac{1}{2}c}^{JM} C_{1\lambda_1, 1\lambda_2}^{2\lambda} \{ x \cdot e^{\lambda_1}(p) y \cdot e^{\lambda_2}(p) \}$$

$$\begin{aligned}
& (\Gamma_{\alpha\gamma,\beta}^{\frac{1}{2}}(x, y, p)_c \epsilon_{ikm} \delta_{jl} + \Gamma_{\gamma\beta,\alpha}^{\frac{1}{2}}(x, y, p)_c \epsilon_{jkm} \delta_{il}) \\
& + \frac{1}{4} [x \cdot e^{\lambda_1}(p) x \cdot e^{\lambda_2}(p) - \frac{4}{3} y \cdot e^{\lambda_1}(p) y \cdot e^{\lambda_2}(p)] \\
& (\Gamma_{\gamma\beta,\alpha}^{\frac{1}{2}}(x, y, p)_c \epsilon_{kjm} \delta_{il} + \Gamma_{\gamma\alpha,\beta}^{\frac{1}{2}}(x, y, p)_c \epsilon_{ijm} \delta_{kl}) \tag{303}
\end{aligned}$$

$S = \frac{3}{2}$ **Octet**

$$\begin{aligned}
B_{\alpha\beta\gamma,ijk}^{JM}(x, y)_l^m &= \frac{1}{2} \epsilon_{i'j'k'} \sum_{\lambda_1, \lambda_2} C_{2\lambda\frac{3}{2}c}^{JM} C_{1\lambda_1, 1\lambda_2}^{2\lambda} \Gamma_{\alpha\gamma\beta}^{\frac{3}{2}}(x, y, p)_c \\
& \{x \cdot e^{\lambda_1}(p) y \cdot e^{\lambda_2}(p) \epsilon_{ijm} \delta_{kl} + \frac{1}{4} [x \cdot e^{\lambda_1}(p) x \cdot e^{\lambda_2}(p) \\
& - \frac{4}{3} y \cdot e^{\lambda_1}(p) y \cdot e^{\lambda_2}(p)] [\Gamma_{\gamma\beta,\alpha}^{\frac{1}{2}}(x, y, p)_c + \Gamma_{\gamma\alpha,\beta}^{\frac{1}{2}}(x, y, p)_c]\}. \tag{304}
\end{aligned}$$

$S = \frac{1}{2}$ **Decuplet**

$$\begin{aligned}
B_{\alpha\beta\gamma,ijk}^{JM,lmn}(x, y) &= \frac{1}{2} \epsilon_{i'j'k'} d_{ijk}^{lmn} \sum_{\lambda_1, \lambda_2} C_{2\lambda\frac{1}{2}c}^{JM} C_{1\lambda_1, 1\lambda_2}^{2\lambda} \\
& \{x \cdot e^{\lambda_1}(p) y \cdot e^{\lambda_2}(p) \Gamma_{\gamma\beta,\alpha}^{\frac{1}{2}}(x, y, p)_c + \frac{1}{4} (x \cdot e^{\lambda_1}(p) x \cdot e^{\lambda_2}(p) \\
& - \frac{4}{3} y \cdot e^{\lambda_1}(p) y \cdot e^{\lambda_2}(p)) (\Gamma_{\gamma\beta,\alpha}^{\frac{1}{2}}(x, y, p)_c + \Gamma_{\gamma\alpha,\beta}^{\frac{1}{2}}(x, y, p)_c)\}. \tag{305}
\end{aligned}$$

$S = \frac{1}{2}$ **Singlet**

$$B_{\alpha\beta\gamma}^{JM}(x, y) = \frac{1}{2} \epsilon_{i'j'k'} \epsilon_{ijk} \sum_{\lambda_1, \lambda_2} C_{2\lambda\frac{1}{2}c}^{JM} C_{1\lambda_1, 1\lambda_2}^{2\lambda} x \cdot e^{\lambda_1}(p) y \cdot e^{\lambda_2}(p)$$

$$\begin{aligned}
& \{\Gamma_{\beta\gamma,\alpha}^{\frac{1}{2}}(x, y, p)_c + \Gamma_{\alpha\gamma,\beta}^{\frac{1}{2}}(x, y, p)_c\} \\
& + \frac{3}{8} \epsilon_{i'j'k'} \epsilon_{ijk} \sum_{\lambda_1, \lambda_2} C_{2\lambda\frac{1}{2}c}^{JM} C_{1\lambda_1, 1\lambda_2}^{2\lambda} \{x \cdot e^{\lambda_1}(p) x \cdot e^{\lambda_2}(p) \\
& - \frac{4}{3} y \cdot e^{\lambda_1}(p) y \cdot e^{\lambda_2}(p)\} \Gamma_{\alpha\beta,\gamma}^{\frac{1}{2}}(x, y, p)_c. \tag{306}
\end{aligned}$$

5. $L = 1$ 20-plet

$$S = \frac{1}{2} \text{ Octet}$$

$$\begin{aligned}
B_{\alpha\beta\gamma,ijk}^{JM}(x, y)_l^m &= \epsilon_{i'j'k'} \sum_{\lambda_1, \lambda_2} C_{1\lambda\frac{1}{2}c}^{JM} C_{1\lambda_1, 1\lambda_2}^{1\lambda} x \cdot e^{\lambda_1}(p) y \cdot e^{\lambda_2}(p) \\
& \{\Gamma_{\beta\gamma,\alpha}^{\frac{1}{2}}(x, y, p)_c \epsilon_{kim} \delta_{jl} + \Gamma_{\gamma\alpha,\beta}^{\frac{1}{2}}(x, y, p)_c \epsilon_{kjm} \delta_{il}\}. \tag{307}
\end{aligned}$$

$$S = \frac{3}{2} \text{ Singlet}$$

$$B_{\alpha\beta\gamma}^{JM}(x, y) = \epsilon_{i'j'k'} \epsilon_{ijk} \sum_{\lambda_1, \lambda_2} C_{1\lambda\frac{3}{2}c}^{JM} C_{1\lambda_1, 1\lambda_2}^{1\lambda} x \cdot e^{\lambda_1}(p) y \cdot e^{\lambda_2}(p) \Gamma_{\alpha\beta\gamma}^{\frac{3}{2}}(x, y, p)_c. \tag{308}$$

The $\Gamma_{\alpha\beta,\gamma}^{\frac{1}{2}}(x, y, p)_c$ and the $\Gamma_{\alpha\beta\gamma}^{\frac{3}{2}}(x, y, p)_c$ take the same expressions of Eq. (35) with different $f_{1,2}(x, y)$.

References

- [1] M. K. Jones, et. al., Phys. Rev. Lett. **84**, 1398 (2000); O. Gayou et. al., Phys. Rev. **C 64**, 038202 (2001); Phys. Rev. Lett. **88**, 092301 (2002), A. J. R. Puckett et al.,

- Phys. Rev. Lett. **104**, 242301 (2010).
- [2] A. J. R. Puckett, et. al., Phys. Rev. Lett. **104**, 24230 (2010).
- [3] B. D. Milbrath et. al., Phys. Rev. Lett., **80**, 452 (1998).
- [4] B. A. Li, Acta Physica Sinica (Chinese), **24** 21, (1975);
- [5] B. A. Li, Acta Physica Sinica(Chinese), **24**, 124 (1975). This paper has an English translation arXiv:hep-ph/0004142.
- [6] T. Z. Ruan and B. A. Li, Acta Physica Sinica (Chinese), **26**, 398 (1977).
- [7] J. M. Wu and B. A. Li, Acta Physica Sinica (Chinese), **26**, 443 (1977).
- [8] M. Gell-Mann, Phys. Letters **8**, 214 (1964); G. Zweig, CERN Reports No. TH 401, 1964 (unpublished).
- [9] O. W. Greenberg, Phys. Rev. Lett., **13**, 598 (1964).
- [10] M. Y. Han and Y. Nambu, Phys. Rev. **139**, B 1006, (1965).
- [11] Theoretical particle group, institute of atomic energy, acadia sinica, atomic energy (Chinese), **3**, 137 (1966). Elementary Particle Group (Beijing), Proceedings of Summer Symposium 1966.
- [12] Y. Y. Liu, Atomic Energy (Chinese), **3**, 232 (1966).

- [13] F. Gursey and L. A. Radicati, Phys. Rev. Lett. **13** 173 (1964); B. Sakita, Phys. Rev. **136**, B 1756 (1964).
- [14] (a) A. Kanazawa, Prog. Theor. Phys. **77** 1240 (1987); (b) B. A. Li, IL Nuovo Cimento, **A 107**, 59 (1994).
- [15] B. A. Li, Physica Energiae Fortis Et Physica Nuclearis, **3** 141 (1979).
- [16] J. C. Bernauer, et al., Phys. Rev. Lett. **105** 242001 (2010).
- [17] D. Borisyuk, Nucl. Phys. **A 843**, 59 (2010).
- [18] M. A. Belushkin, H. W. Hammer, and U. G. Meisner, Phys. Rev. **C 75**, 035202 (2007).
- [19] J. Arrington, K. d. Jager, and C. F. Perdrisat, J. Phys. Conf. Ser. **299**, 012002 (2011).
- [20] L. E. Price et al., *Phys. Rev.*, **D4** (1971), 45.
- [21] W. Bartel et al., *Nucl. Phys.*, **B58** (1973), 429.
- [22] S. Galster et al., Nucl. Phys. **B 32**, 221 (1971).
- [23] E. Melkonian et al., *Phys. Rev.*, **114**, 1571 (1959).
- [24] D. J. Hughes et al., *Phys. Rev.*, **90**, 497 (1966).
- [25] V. E. Krohn et al., *Phys. Rev.*, **148**, 1303 (1966).

- [26] R. Wilson, Proceedings (1971) International Symposium on Electron and Photon Interactions at High Energy 97.
- [27] M. R. Yearian and R. Hofstadter, Phys. Rev. **111**, 934 (1958).
- [28] C. B. Crawford et al., Phys. Rev. Lett. **98**, 052301 (2007); E. Geis et al., Phys. Rev. Lett. **101**, 042501 (2008).
- [29] G. Ron, et al., Phys. Rev. **C 84**, 055204 (2011).
- [30] X. Zhan et. al., Phys. Lett. **B 705**, 59 (2011).
- [31] see review articles by 1) C. F. Perdrisat, V. Punjabi, and M. Vanderhaeghen, Prog. Part. Nucl. Phys. **59**, 694 (2007), references therein; 2) Haiyan Gao, ECT* Workshop on Hard Meson and Photon Production, Oct 11-15, 2010, ECT*, 3) J. Arrington QCD Bound States Workshop, June 15-19, Argonne National Lab.
- [32] S. Platchkov et al., Nucl. Phys. **A 510**, 740 (1990).
- [33] S. Riordan et al., Phys. Rev. Lett. **105**, 262302 (2010).
- [34] G. Warren et al., Phys. Rev. Lett. **92**, 042301 (2004).
- [35] R. Madeay et al., Phys. Rev. Lett. **91**, 122002 (2003).
- [36] D. I. Glazier et al., arXiv: nucl-ex/0410026.

- [37] B. Plaster et al., Phys. Rev. **C 73**, 025205 (2006).
- [38] J. Golak et al., Phys. Rev. **C 63**, 034006 (2001).
- [39] M. Ostrick et al., Phys. Rev. Lett. **83**, 276 (1999).
- [40] J. Passchier et al., Phys. Rev. Lett. **82**, 4988 (1999).
- [41] R. Schiavilla and I. Sick, Phys. Rev. **C 64**, 041002(R), 2001.
- [42] H. Zhu et al., Phys. Rev. Lett. **87**, 08101 (2001).
- [43] J. Bermuth et al., Phys. Lett. **B 564**, 199 (2003).
- [44] N. Savvinov, AIP Conf. Proc. **675**, 630 (2003).
- [45] W. M. Alberioo et al., Phys. Rev. **C 79**, 065204 (2009).
- [46] J. Berlinger et al., Particle Data Group, Phys. Rev. **D86**, 1 (2012).
- [47] P. J. Mohr, B. N. Taylor, and D. B. Newell, Rev. of Modern Phys. **80**, 633 (2008).
- [48] G. Chew et al., *Phys. Rev.*, **106** (1957),
- [49] S. Stave et al., Phys. Rev. **C 78**, 025209 (2008).
- [50] T. Sato and T. S. H. Lee, Phys. Rev. **C 63**, 055201 (2001); S. S. Kamalov and S. N. Yang, Phys. Rev. Lett. **83**, 4494 (1999); T. A. Gail and T. R. Hemmert, Eur. Phys. J.

- A 28**, 91 (2006); V. Pascalutsa and M. Vanderhaeghen, Phys. Rev. Lett. **95**, 232001 (2005) and Phys. Rev. **D 73**, 034003 (2006); D. Drechsel et al., Nucl. Phys. **A 645**, 145 (1999); R. A. Amdt et al., Phys. Rev. **C 66**, 055213 (2002); S. S. Kamalov et al., Phys. Lett. **B 522**, 27 (2001).
- [51] M. Gourdin, Salin P. H., *Nuovo Cimento*, **27** (1963), 193; **28** (1963), 1294.
- [52] P. Pillantini et al., *Nucl. Phys.*, **B13** (1969), 320.
- [53] P. Noelle et al., *Nucl. Phys.*, **B26** (1971), 461.
- [54] R. A. Arndt, I. I. Strakovsky, and R. L. Workman, Phys. Rev. **C 56**, 577 (1997).
- [55] O. Hanstein, D. Drechsel, and L. Tiator, Phys. Lett. **385**, 45 (1996).
- [56] R. L. Walker, 4th International Symposium on Electron and Photon Interactions at High Energies (1969), 23.
- [57] G. Morpurgo, 14th International Conference on High-Energy Physics, Vienna (1968), 225.
- [58] R. A. Arndt, I. I. Strakovsky, and R. L. Workman, Phys. Rev. **C 56**, 577 (1997).
- [59] O. Hanstein, D. Drechsel, and L. Tiator, Phys. Lett., **B 385**, 45 (1996).
- [60] L. Durand et al., *Phys. Rev.*, **126** (1962), 1882.

- [61] K. Batjner et al., *Phys. Lett.*, **39B** (1972), 575.
- [62] W. Bartel et al., *Phys. Lett.*, **35B** (1971), 181.
- [63] V. V. Frolov et al., *Phys. Rev. Lett.* **82** 45 (1999).
- [64] M. Ungaro et al., *Phys. Rev. Lett.* **97** 112003 (2006).
- [65] A. N. Villano et al., *Phys Rev. C* **80** 035203 (2009), references therein.
- [66] C. Mertz et al., *Phys. Rev. Lett.* **86** 2963 (2001).
- [67] C. Kunz et al., *Phys. Lett. B* **564** 21 (2003).
- [68] N. E. Sparveris et al., *Phys. Rev. Lett.* **94** 022003 (2005).
- [69] N. E. Sparveris et al., *Phys. Lett. B* **651** 102 (2007).
- [70] J. J. Kelly et al., *Phys. Rev. C* **75** 025201 (2007); *Phys. Rev. Lett.* **95** 102001 (2005).
- [71] S. Stave et al., *Phys. Rev. C* **78** 025209 (2008).
- [72] I. G. Arznauryan et al., *Phys. Rev. C* **80** 055203 (2009).
- [73] K. Joo et al., *Phys. Rev. Lett.* **88**, 122001 (2002).
- [74] L. Tiator et al., *Nucl. Phys. A* **689**, 205c (2001).
- [75] M. M. Nirto, *Rev. Mod. Phys.* **40** 140 (1968).

- [76] J. M. Gaillard, Proc. of the XVI Intern. Conf. on High Energy Phys. p.175 (1972).
- [77] C. H. Llewellyn-Smith, Phys. Rep. **3C** 263 (1972).
- [78] V. Bernard, L. Elouadrhiri, and U. G. Meisner, J. Phys. **G 28**, R1 (2002), references therein.
- [79] A. Bodek et al., Eur. Phys. J. **C 53** 349 (2008).
- [80] M. A. Mann et al., Phys. Rev. Lett. **31** 844 (1973).
- [81] S. L. Adler and Y. Dothan, Phys. Rev. **151**, 1207 (1966).
- [82] L. Wolfenstein, in High Energy Physics and Nuclear Structure , ed. S. Devons (Plenum, New York, 1970) p.661.
- [83] P. Musset, 11th Conf. Intern. Sur les Particulaes Elementaries, Ax-en-Provence, (1973), p.23.
- [84] Y. Nakajima et al., Phys. Rev. **D 83**, 012005 (2011).
- [85] A. A. Aguilar-Arevalo et al., Phys. Rev. **D 81**, 092005 (2010).
- [86] V. Lyubushkin et al., Eur. Phys. J. **C 63**, 355 (2009), other experimental data can be found in this paper.
- [87] J. Dworkin et al., Phys. Rev. **D 41**, 780 (1990).

- [88] S. Y. Hsueh et al., Phys. Rev. **D 38**, 2056 (1988).
- [89] P. A. Schreiner et al., Nucl. Phys. **B 58**, 333 (1973).
- [90] G. M. Radecky et al., Phys. Rev. **D 25**, 1161 (1982).
- [91] J. Gasser, H. Leutwyler, and M. E. Sainio, Phys. Lett. **B 253** 252 (1991).
- [92] M. Knecht, hep-ph/9912443.
- [93] G. S. Li et al., arXiv:1206.7034 [hep-lat].
- [94] L. Alvarez-Ruso et al., arXiv:1304.0483 [hep-ph].
- [95] S. Choi et al., Phys. Rev. Lett. —bf 71, 3927 (1993).

Figure Captions

Fig. 1. Ratio of electric and magnetic form factors of proton.

Fig. 2. Ratio of electric and magnetic form factors of proton.

Fig. 3. Electric form factor of neutron.

Fig. 4. Electric form factor of neutron.

Fig. 5 The ratio $\frac{\mu_p G_E^p}{G_M^p}$.

Fig. 6 Charge form factor of neutron.

Fig. 7 Magnetic form factor of $p \rightarrow \Delta$.

Fig. 8(a) Magnetic form factor of $p \rightarrow \Delta$.

Fig. 8(b) Magnetic form factor of $p \rightarrow \Delta$ with a possible SU(6) symmetry breaking effect.

Fig. 9 Cross Section of virtual scalar photon.

Fig. 10 Axial-vector form factor of $p \rightarrow n$

Fig. 11 Cross Section of $\nu_\mu + n \rightarrow p + \mu^-$. E is the average neutrino energy.

Fig. 12 Cross Section of $\nu_\mu + n \rightarrow p + \mu^-$. E is the average neutrino energy.

Fig. 13 Cross Section of $\bar{\nu}_\mu + p \rightarrow n + \mu^+$. E is the average antineutrino energy.

Fig. 14 Cross Section of $\bar{\nu}_\mu + p \rightarrow \Lambda + \mu^+$.

Fig. 15 Cross Section of $\bar{\nu}_\mu + p \rightarrow \Sigma^0 + \mu^+$

Fig. 16 Cross Section of $\nu_\mu + p \rightarrow \Delta^{++} + \mu^-$.

Fig. 17 Differential cross Section of $\nu_\mu + n \rightarrow \Delta^{++} + \mu^-$, $\frac{d\sigma}{dq^2}$.

Fig. 18 Cross Section of $\nu_\mu + p \rightarrow \Delta^{++} + \mu^-$.

Fig. 19 Differential cross Section of $\nu_\mu + n \rightarrow \Delta^{++} + \mu^-$, $\frac{d\sigma}{dq^2}$.

Table 2: Form factors of weak interactions

process	b	f_V	f_T	f_S	g_A	g_P
$n \rightarrow p$	$\frac{1}{6}$					
$\Xi^- \rightarrow \Sigma^0$	$\frac{1}{6\sqrt{2}}$	$(5 - \frac{m_+}{m})a + (5 - \frac{m_+}{m'})a'$	$\mu[10 - (5 - \frac{1}{\mu m})a - (5 - \frac{1}{\mu m'})a']$	S	5A	-P
$\Xi^0 \rightarrow \Sigma^+$	$-\frac{1}{6}$	$+(5\zeta_- + \frac{\mu m_+ q^2}{mm'})aa'$	$+(5\zeta_+ - \frac{q^2}{mm'})aa'$			
$\Xi^- \rightarrow \Xi^0$	$-\frac{1}{6}$	$(1 - \frac{2m_+}{m})a + (1 - \frac{2m_+}{m'})a'$	$\mu[2 - (1 - \frac{2}{\mu m})a - (1 - \frac{2}{\mu m'})a']$	2S	A	-2P
$\Sigma^- \rightarrow n$	$\frac{1}{6}$	$+(\zeta_- + \frac{2\mu m_+ q^2}{mm'})aa'$	$+(\zeta_+ - \frac{2q^2}{mm'})aa'$			
$\Sigma^- \rightarrow \Sigma^0$	$-\frac{1}{6\sqrt{2}}$	$(4 + \frac{m_+}{m})a + (4 + \frac{m_+}{m'})a'$	$\mu[8 - (4 + \frac{1}{\mu m})a - (4 + \frac{1}{\mu m'})a']$	-S	4A	P
		$+(4\zeta_- - \frac{\mu m_+ q^2}{mm'})aa'$	$+(4\zeta_+ + \frac{q^2}{mm'})aa'$			
$\Sigma^+ \rightarrow \Lambda$	$\frac{1}{\sqrt{6}}$	$\frac{\mu' q^2}{2mm'}aa'$	$\mu[2 - (1 - \frac{1}{2\mu m})a - (1 - \frac{1}{2\mu m'})a']$	$\frac{S}{2}$	A	$-\frac{P}{2}$
$\Sigma^- \rightarrow \Lambda$	$\frac{1}{\sqrt{6}}$		$+\frac{aa'm_+^2}{mm'}]$			
$\Lambda \rightarrow p$	$-\frac{3}{2\sqrt{6}}$	$a + a' + aa'\zeta_-$	$\mu[2 - (a + a' - aa'\zeta_+)]$	0	A	0
$\Xi^- \rightarrow \Lambda$	$\frac{1}{2\sqrt{6}}$	$(1 + \frac{m_+}{m})a + (1 + \frac{m_+}{m'})a'$	$\mu[2 - (1 + \frac{1}{\mu m})a - (1 + \frac{1}{\mu m'})a']$	-S	A	P
		$+(\zeta_- - \frac{\mu m_+ q^2}{mm'})aa'$	$+(\zeta_+ + \frac{q^2}{mm'})aa'$			

where $\mu = \frac{\kappa}{2m_p}$, $\mu' = 1 + \mu m_+$, $\zeta_{\pm} = \frac{q^2 + m_{\pm}^2}{2mm'}$, $S = \frac{\mu' m_-}{mm'}aa'$, $A = \lambda(a + a' + aa'\zeta_-)$, $P = \lambda(\frac{a}{m} + \frac{a'}{m'} - \frac{aa'm_+}{mm'})$

Table 3: Theoretical values of R and $\frac{G_A}{G_V}$

Process	BR(theory)	BR(exp.)	$\frac{G_A}{G_V}(th)$	$\frac{G_A}{G_V}(exp)$
$n \rightarrow pe^- \bar{\nu}$	$0.892 \times 10^3 s$	$(.8801 \pm 0.0011) \times 10^3 s$	input	1.25
$\Sigma^+ \rightarrow \Lambda e^+ \nu$	1.92×10^{-5}	$(2.0 \pm 0.5) \times 10^{-5}$	0(here is $\frac{G_V}{G_A}$)	
$\Sigma^- \rightarrow \Lambda e^- \bar{\nu}$	0.59×10^{-4}	$(0.573 \pm 0.027) \times 10^{-4}$	0(here is $\frac{G_V}{G_A}$)	$0.01 \pm 0.10(\frac{G_V}{G_A})$
$\Sigma^- \rightarrow \Sigma^0 e^- \bar{\nu}$	1.43×10^{-10}		0.50	
$\Xi^- \rightarrow \Xi^0 e^- \bar{\nu}$	2.32×10^{-10}	$< 2.3 \times 10^{-3}$	-0.25	
$\Lambda \rightarrow pe^- \bar{\nu}$	8.79×10^{-4}	$(8.32 \pm 0.14) \times 10^{-4}$	0.75	0.718 ± 0.015
$\Lambda \rightarrow p\mu^- \bar{\nu}$	1.51×10^{-4}	$(1.57 \pm 0.35) \times 10^{-4}$	0.75	0.718 ± 0.015
$\Sigma^- \rightarrow ne^- \bar{\nu}$	1.01×10^{-3}	$(1.017 \pm 0.034) \times 10^{-3}$	-0.25	$-(0.34 \pm 0.017)$
$\Sigma^- \rightarrow n\mu^- \bar{\nu}$	0.48×10^{-3}	$(0.45 \pm 0.04) \times 10^{-3}$	-0.25	
$\Xi^- \rightarrow \Lambda e^- \bar{\nu}$	0.52×10^{-3}	$(0.563 \pm 0.031) \times 10^{-3}$	0.25	0.25 ± 0.05
$\Xi^- \rightarrow \Lambda\mu^- \bar{\nu}$	0.15×10^{-3}	$(0.35^{+0.35}_{-0.22}) \times 10^{-4}$	0.25	
$\Xi^- \rightarrow \Sigma^0 e^- \bar{\nu}$	0.42×10^{-4}	$(0.87 \pm 0.17) \times 10^{-4}$	0.92	
$\Xi^- \rightarrow \Sigma^0 \mu^- \bar{\nu}$	0.54×10^{-6}	$< 0.8 \times 10^{-3}$	0.92	
$\Xi^0 \rightarrow \Sigma^+ e^- \bar{\nu}$	2.5×10^{-4}	$(2.53 \pm 0.08) \times 10^{-4}$	1.24	
$\Xi^0 \rightarrow \Sigma^+ \mu^- \bar{\nu}$	0.22×10^{-5}	$< (4.6^{+1.8}_{-1.4}) \times 10^{-6}$	1.24	

Table 4: Theoretical values of coefficients

process	$\alpha_{e\nu}$	α_e	α_ν	α_B
$\Sigma^+ \rightarrow \Lambda$	-0.40	-0.70	0.68	0.06
$\Sigma^- \rightarrow \Lambda$	-0.40	-0.70	0.68	0.06
$\Sigma^- \rightarrow \Sigma^0$	0.43	0.28	0.85	-0.71
$\Xi^- \rightarrow \Xi^0$	0.789	-0.52	-0.31	0.53
$\Lambda \rightarrow p$	0.0058	0.031	0.97	-0.61
$\Sigma^- \rightarrow n$	0.56	-0.58	-0.46	0.45
$\Xi^- \rightarrow \Lambda$	0.63	0.26	0.50	-0.50
$\Xi^- \rightarrow \Sigma^0$	-0.35	-0.39	0.92	-0.30
$\Xi^0 \rightarrow \Sigma^+$	-0.20	-0.17	0.99	-0.48

Table 5: Experimental values of coefficients of $\Lambda \rightarrow pe^- \bar{\nu}$

Lab	$\alpha_{e\nu}$	α_e	α_ν	α_p
Argonne	-0.08 ± 0.10	0.09 ± 0.11	0.75 ± 0.11	-0.55 ± 0.11
CERN	-0.07 ± 0.09	0.15 ± 0.09	0.89 ± 0.08	-0.52 ± 0.08

Table 6: Density matrix elements

	ρ_{33}	ρ_{3-1}	ρ_{31}
Experimental value [85]	0.58 ± 0.09	-0.24 ± 0.11	-0.18 ± 0.11
Experimental value [86]	0.661 ± 0.036	-0.088 ± 0.042	-0.107 ± 0.040
Theoretical value	0.95	-0.01	-0.26